

**MANIPULATION OF GASIFICATION COAL FEED IN
ORDER TO INCREASE THE ASH FUSION
TEMPERATURE OF THE COAL TO OPERATE THE
GASIFIERS AT HIGHER TEMPERATURES**

JC VAN DYK

AUGUST 2006

TO HIM WHO DESERVES ALL HONOUR

**AND MY WIFE MARIKÉ, SON JEAN-PIERRE AND PARENTS,
PA FRIK AND MA JOEY**

**MANIPULATION OF GASIFICATION COAL FEED IN ORDER TO
INCREASE THE ASH FUSION TEMPERATURE OF THE COAL
TO OPERATE THE GASIFIERS AT HIGHER TEMPERATURES**

A Thesis submitted to the Potchefstroom UNIVERSITY OF NORTH-WEST, in
fulfillment of the requirements for the degree PhD (Chemical Engineering)

By

Johannes Chrisstoffel van Dyk

B.Sc (Chem)(PU for CHE)(1993)

Hons. B.Sc (Chem)(PU for CHE)(1994)

M.Sc. (Eng)(WITS)(1999)

School of Chemical- and Mineral Engineering
North-West University
Potchefstroom
South-Africa

Promoter: Prof. FB Waanders

August 2006

ACKNOWLEDGEMENTS

I would like to thank the following people and organizations for their help and support throughout this study:

To HIM who deserves all honour.

My wife, MARIKÉ, and parents for all the encouragement and support.

PROF. FB WAANDERS for his input and guidance as supervisor.

MR. J BUNT for his assistance, support, patience and input as line-manager throughout the study.

MR. E BAILY for proofreading of this thesis.

MR. JH SLAGHUIS for his inputs to the summary and synopsis.

SASOL TECHNOLOGY R&D for funding this research project.

DR. CF REINECKE and DR. JHP van Heerden for their continuous interest and support during this study.

DR. A SOBECKIE and DR. S MELZER for HT-XRD analysis.

DR. C VAN ALPHEN for inputs on the CCSEM analysis.

Coal and Minerals Technology for all routine coal analysis.

COLLEAGUES:

JH Slaghuis and A Ooms for their valuable technical inputs.

B Ashton for his assistance in the work and preparation of the coal samples.

DECLARATION

I, the undersigned, declare that the work contained in this thesis is my own original study and has not previously been submitted at any university for a degree.



JC van Dyk

15/9/2006

Date

INDEX

SYNOPSIS		I
OPSOMMING		III
LIST OF ABBREVIATIONS		V
LIST OF FIGURES		VI
LIST OF TABLES		VIII
CHAPTER 1: BACKGROUND AND LITERATURE REVIEW		1
1	HYPOTHESIS AND STUDY OBJECTIVE	1
1.1	<i>Background</i>	1
1.2	<i>Operational opportunity</i>	1
1.3	<i>Proposed solution to address the operational opportunity</i>	2
1.4	<i>Confirming the hypothesis and opportunity</i>	3
2	SASOL-LURGI FIXED BED DRY BOTTOM (FBDB) GASIFICATION	4
2.1	<i>The gasification vessel</i>	5
2.2	<i>Process description</i>	7
2.3	<i>Advantages and disadvantages</i>	10
3	COAL	11
3.1	<i>Coal definition and formation</i>	12
3.2	<i>Rank of coal</i>	13
3.3	<i>Composition (types) of coal macerals</i>	14
3.4	<i>Coal structure</i>	15
4	ASH FUSION PROPERTIES (AFT) AND MINERAL MATTER	16
4.1	<i>Ash fusion temperature (AFT)</i>	17
4.2	<i>Mineral matter</i>	19
4.3	<i>Specific (most abundant) mineral species in coal</i>	23

5	REVIEW OF PREVIOUS WORK DONE ON ASH FUSION CHARACTERISTICS OF COAL, SLAGGING AND MINERAL CHARACTERISTICS	25
5.1	Summary of previous research and findings	25
5.2	Shortcomings and summary of published work and analyses techniques	30
6	SUMMARY	34
CHAPTER 2: EXPERIMENTAL PROCEDURES, ANALYSES AND STUDY METHODOLOGY		35
1	INTRODUCTION	35
2	GENERAL COAL AND ASH ANALYSIS	36
3	COAL ASH AND COAL ASH CHARACTERISATION TECHNIQUES CONDUCTED AND UTILIZED IN THIS STUDY	38
3.1	Ash fusion temperature (AFT)	38
3.2	Ash composition	39
3.3	Scanning electron microscopy	39
3.4	Morphology analysis	41
4	EFFECT OF SILICA (SiO_2), ALUMINA (Al_2O_3) AND TITANIA (TiO_2) ON ASH FUSION TEMPERATURE	41
4.1	Dense medium separation of coal	42
4.2	Chemical fractionation of coal	42
5	HIGH TEMPERATURE X-RAY DIFFRACTION (HT-XRD) ANALYSES - FORMULATING A MECHANISM FOR MANIPULATED COAL FEED AND HIGHER ASH FUSION TEMPERATURE	44
6	TOOLS USED FOR QUANTIFYING EXPERIMENTAL RESULTS AND MECHANISM FOR INCREASING ASH FUSION TEMPERATURE	45
6.1	FactSage modelling	45
6.2	Viscosity modelling	47

CHAPTER 3: RESULTS AND DISCUSSIONS	49
1 INTRODUCTION	49
2 GENERAL COAL AND COAL ASH CHARACTERISTICS	49
2.1 <i>Proximate analyses</i>	49
2.2 <i>Ultimate analysis and calorific value</i>	50
2.3 <i>Maceral analysis and rank</i>	51
3 OTHER COAL AND COAL ASH CHARACTERISTICS	52
3.1 <i>Ash fusion temperature (AFT)</i>	52
3.2 <i>Ash composition</i>	53
3.3 <i>Computer-controlled scanning electron microscopy (CCSEM)</i>	54
3.4 <i>Morphology analysis</i>	54
4 EFFECT OF SILICA (SiO₂), ALUMINA (Al₂O₃) AND TITANIA (TiO₂) AS PURE COMPOUNDS ON THE AFT	56
4.1 <i>Discussion of results by means of 3-component phase diagrams</i>	59
4.1.1 <i>Al₂O₃-SiO₂-TiO₂</i>	59
4.1.2 <i>Al₂O₃-SiO₂-Fe₂O₃</i>	61
4.1.3 <i>Al₂O₃-SiO₂-CaO</i>	63
4.1.4 <i>Al₂O₃- SiO₂-Na₂O</i>	64
4.2 <i>Effect of silica (SiO₂), alumina (Al₂O₃) and titania (TiO₂)-containing substances (i.e. kaolinite and siltstone) on the AFT</i>	65
4.3 <i>Other experimental findings on manipulating the mineral composition of a coal blend versus ash fusion temperature with statistical evaluations as support of the mechanism for increasing the AFT</i>	67
4.3.1 <i>Effect of dense medium separation of coal on mineral composition and ash fusion properties</i>	67
4.3.2 <i>The statistical evaluation of the effect of leaching (chemical fractionation) of coal on AFT</i>	70
5 HT-XRD	74
5.1 <i>Mineral decomposition of base case coal sample</i>	74
5.2 <i>Mineral decomposition of manipulated base case coal sample with Al₂O₃ addition</i>	80

CHAPTER 4: FACTSAGE MODEL DEVELOPMENT AND OTHER TOOLS USED FOR	85
QUANTIFYING EXPERIMENTAL RESULTS	
4.1	85
<i>FactSage modelling</i>	
4.1.1	85
<i>FactSage model development and inputs for base case model</i>	
4.1.1.1	89
<i>Drying and devolitalization zone</i>	
4.1.1.2	90
<i>Gasification zone</i>	
4.1.1.3	90
<i>Combustion zone</i>	
4.1.2	91
<i>FactSage modelling results</i>	
4.1.2.1	93
<i>Drying and devolutilization zone</i>	
4.1.2.2	95
<i>Gasification zone</i>	
4.1.2.3	98
<i>Combustion zone</i>	
4.2	100
<i>Viscosity and sintering modelling</i>	
4.2.1	101
<i>Viscosity modelling of mineral matter compositions obtained by dense</i>	
<i>medium separation of coal</i>	
4.2.2	104
<i>Viscosity modelling of base case mineral matter compositions with</i>	
<i>added mineral matter from the roof and the floor of the coal seam</i>	
CONCLUSIONS	108
APPENDIX A	112
APPENDIX B	121
APPENDIX C	126
REFERENCES	138

SYNOPSIS

Coal is a crucial feedstock for South Africa's unique synfuels and petrochemicals industry and used by Sasol as a feedstock to produce synthesis gas via the **Sasol-Lurgi Fixed Bed Dry Bottom (FBDB)** gasification process. The ash fusion temperature (AFT) gives detail information on the suitability of a coal source for gasification purposes, and specifically to the extent ash agglomeration or clinkering is likely to occur within the gasifier. Ash clinkering inside the gasifier can cause channel burning and unstable operation.

Sasol-Lurgi FBDB gasifiers are currently operated with the philosophy of adding an excess of steam to the process to control the H_2/CO ratio of the syngas produced, but indirectly also to control the maximum gasifier temperature below the AFT of the coal. An opportunity exists to increase the AFT of the coal fed to the gasifiers by adding AFT increasing minerals to the coal blend before it is fed into the gasification process. For the aim of this study a typical Highveld Nr. 4 coal seam was investigated, as being used by the gasification operations in Secunda.

In the **drying and devolatilization zone** no slag formation in the coal was observed. Based on HT-XRD analysis the predominant phases in the untreated coal sample were quartz, muscovite, calcite, dolomite, hematite, anhydrite, rutile and kaolinite. Kaolinite started to decompose to metakaolinite at $\pm 450^\circ\text{C}$ with the formation of amongst others mullite at a temperature of 850°C to 1000°C . Mullite formation can also take place if free Al_2O_3 is present in the coal that can react with free SiO_2 . However, free Al_2O_3 is normally not present in coal and the presence of the alumina-silicate (Al_2SiO_5) is formed as an intermediate phase due to the decomposition of kaolinite. From 500°C to 900°C , the carbonates, calcite and dolomite, started to decompose with the formation of lime and periclase. The feldspar ($CaAl_2Si_2O_8$) observed, formed as a reaction product between the SiO_2 , Al_2O_3 and Ca-containing species present in the coal.

In the **gasification zone** slag-liquid formed at a temperature from 1000°C . The formation of anhydrite ($CaSO_4$) took place after the formation of calcite. At 1000°C anorthite, initially present as feldspar ($CaAl_2Si_2O_8$) and gehlenite ($Ca_2Al_2SiO_7$) became stable, due to partial melting of the low AFT mineral phases. Anorthite and gehlenite were formed as products from anhydrite, alumina and silica at temperatures around 900°C to 1100°C . Mullite decomposed at temperatures $>1100^\circ\text{C}$, while quartz and anorthite were observed up to 1350°C . Above 1350°C the whole mineral phase

assemblage in the coal sample was molten. When comparing the base case sample with the Al_2O_3 -manipulated sample, it was clear that the mullite is one mineral that showed a significant difference in formation and mechanistic behaviours.

In the **combustion zone** the decrease in the slag-liquid content confirmed the cooling and actual mineral formation and crystallization within the gasifier combustion zone. The representative coal ash, as it was produced after gasification, showed evidence of crystallization from the melt phase and formed due to the interaction of specific mineral species to produce a molten phase that had the correct chemistry to crystallize again.

Mullite formation can also take place when free Al_2O_3 in the coal is available that can react with free SiO_2 , also present in the coal. With the addition of $\gamma\text{-Al}_2\text{O}_3$, the free SiO_2 in the coal can react with the $\gamma\text{-Al}_2\text{O}_3$ to form mullite ($\text{Al}_6\text{O}_5(\text{SiO}_4)_2$) directly. The Al_2O_3 in the reactive form acts as a network former where SiO_2 can be reacted on, to form mullite. The main conclusion of the addition of $\gamma\text{-Al}_2\text{O}_3$ to the blend is that the slag-liquid content decreased with addition, only when the temperature was greater than 1100°C , which is of importance in the operating region where the proposed higher gasifier temperature of more than 1250°C , is aimed for.

Another observation from the AFT results was that the AFT was definitely non-additive (not a linear weighted calculated average) and not the weighted average AFT as was expected for the other coal properties such as the ash content, for example. The ash slagging behaviour is a non-additive property of individual coal sources in the blend and therefore difficult to predict. Viscosity modelling can be another tool for predicting slag mineral behaviour and used as a predicting tool, as has been done in this study. A higher viscosity for all relative density fractions were observed for all temperature ranges in comparison with the results obtained from the AFT analysis.

In general it can be concluded that the unique opportunity that exists to increase the AFT, was tested, proven and mechanistically outlined in this study on the coal source fed to the Sasol-Lurgi FBDB gasifiers. The AFT can be increased to $>1350^\circ\text{C}$ by adding AFT increasing minerals or species, for example Al_2O_3 or other mineral species, to the coal blend before it is fed into the gasification process. By increasing the AFT, the direct effect will be that steam consumption can be decreased, which in turn will improve carbon utilization.

OPSOMMING

Steenkool is 'n noodsaaklike voerstroom vir Suid-Afrika se unieke sintesegas and petrochemiese nywerheid. Sasol gebruik die voerstroom om sintese gas te produseer met behulp van die **Sasol-Lurgi vaste bed nie-slakkende vergassingsproses (FBDB)**. Die assmelttemperatuur is 'n steenkool eienskap wat spesifieke inligting rondom die geskiktheid van die steenkoolbron vir vergassing verskaf, en spesifiek die mate van klinkering wat kan plaasvind binne die vergasser. Asklinkering binne die vergasser kan tot kanaalvorming en onstabiele bedryf lei.

Sasol-Lurgi vergassers word met suurstof en 'n beheerde oormaat stoom bedryf. Die oormaat stoom word benodig om die chemiese ewewig te stuur om 'n sintesegas met 'n H_2/CO verhouding van 1.7 tot 2.0 te verkry. Die oormaat stoom het as bykomende funksie die doel om die klinkering van die asvormende minerale te onderdruk. 'n Verlaging van die H_2/CO verhouding is soms wenslik en kan verkry word deur die oormaat stoom te verminder. Dit het egter tot gevolg dat ernstige slakvorming mag plaasvind en die vergasserintegriteit in gevaar stel. 'n Unieke geleentheid is geïdentifiseer waarby die byvoeging van die geselekteerde minerale die assmeltpunt van 'n gegewe steenkool sinvol verhoog om sodoende die slakvorming te onderdruk. Vir die doel van hierdie studie is 'n tipiese Hoëveld nommer 4 laag steenkool ondersoek soos gebruik in die Sasol-Lurgi vergassers te Secunda.

In die **droging- en ontvlugtingsone** word geen slakvorming waargeneem nie. Volgens HT-XRD analises is die mees prominente minerale in die oorspronklike steenkool kwarts, muskovieet, kalsiet, dolomiet, hematiet, rutiel and kaoliniet. Kaoliniet ontbind by ongeveer $550^{\circ}C$ na meta-kaoliniet met die vorming van onder andere mulliet vanaf $850^{\circ}C$ tot $1000^{\circ}C$. Mulliet vorming kan ook plaasvind indien vry $\gamma-Al_2O_3$ in die steenkool teenwoordig is wat met die vry SiO_2 in die steenkool kan reageer. Vry Al_2O_3 is normaalweg nie in steenkool teenwoordig nie en die teenwoordigheid of die vorming van sillimaniet (Al_2SiO_5) in the steenkool tydens ontbinding van kaoliniet, is slegs 'n intermediêre fase. Die Al_2O_3 tree op as netwerkvormer waarop die SiO_2 kan reageer om mulliet te vorm. Die gevolg van die reaksie met die byvoeging van $\gamma-Al_2O_3$ by die die steenkool mengsel, is dat slakvorming afneem by temperature $>1100^{\circ}C$, wat ook die temperatuurgebied is waar die vergassers bedryf word. Die karbonate, kalsiet en dolomiet ontbind tussen $500^{\circ}C$ en $900^{\circ}C$ met die vorming van periklaas en kalk. Sillimaniet (Al_2SiO_5) as intermediêre fase vorm waarskynlik as gevolg van die ontbinding van kaoliniet wat in die oorspronklike steenkool

teenwoordig is. Waargenome feldspaat kan as 'n produk van die interaksie tussen inherente SiO_2 , Al_2O_3 en Ca-bevattende komponente beskou word.

In die **vergassingsone** begin slakvorming by 'n temperatuur van ongeveer 1000°C plaasvind. Die vorming van kalsiumsulfaat (CaSO_4) vind plaas na die ontbinding van kalsiet. By 'n temperatuur van ongeveer 1000°C vorm anortiet wat as stabiele produk uit die slak begin kristalliseer. Anortiet en gehleniet ($\text{Ca}_2\text{Al}_2\text{SiO}_7$) vorm as produkte van die smelting van anhidriet, alumina and silika by temperature tussen 900°C en 1100°C . Mulliet ontbind of vorm deel van die slak (smelt proses) vanaf 1200°C . Kwarts en anortiet word waargeneem by temperature so hoog as 1350°C . Indien die oorspronklike steenkool vergelyk word met die steenkool waar vry $\gamma\text{-Al}_2\text{O}_3$ bygevoeg is, is dit duidelik dat mulliet een van die minerale is wat betekenisvol toeneem en 'n duidelike rol in die meganisme van 'n verhoogde assmeltemperatuur speel.

In die **verbrandingsone** is die maksimum vergassingstemperatuur waargeneem met die meeste slakvorming. Dit is ook in hierdie sone waar die as afkoel tot in die asbed. Kristallisasie van die slak is waargeneem. Die verteenwoordigende steenkoolas, soos deur produksie-ergassers geproduseer, het ook bewyse van kristallisasie van minerale uit die slak getoon.

Die resultate toon aan dat die assmeltemperatuur nie-additief (nie-liniêr) is en dat 'n teoretiese, geweegde gemiddelde waarde tussen twee bronne, nie bereken kan word nie; anders as vir die absolute asinhoud van die steenkool. Die assmelteienskappe van steenkoolmengsel is dus moeilik om te voorspel.

Modellering van die viskositeit is 'n alternatiewe hulpmiddel wat gebruik kan word om slagvorming van 'n mineraal samestelling te voorspel. Goeie korrelasies met eksperimentele resultate is in hierdie studie verkry.

Ter opsomming kan dit beklemtoon word dat 'n unieke geleentheid om die assmeltemperatuur te verhoog, in hierdie studie bewys en getoets is. Die meganisme vir die mineraal-transformasies tydens Sasol-Lurgi vaste bed vergassing is bespreek. Die assmeltemperatuur van die steenkool kan tot $>1350^\circ\text{C}$ verhoog word deur die byvoeging van assmeltemperatuur verhogende minerale soos byvoorbeeld Al_2O_3 of soortgelyke mineraal-bevattende-komponente voordat dit na die vergassers gestuur word. Die effek van verhoogde assmeltemperatuur van die steenkool, sal direk 'n besparende effek op die stoomverbruik tot gevolg hê, wat op sy beurt sal lei tot beter koolstof doeltreffendheid.

LIST OF ABBREVIATIONS

AFT	ash fusion temperature
ANF	atomic number frequency
ASTM	American Society for Testing and Materials
BSE	back scattered electron
CCSEM	computer controlled scanning electron microscopy
CMT	Coal and Mineral Technologies
DGC	Dakota Gasification Company
EDX	energy dispersive X-ray
EMPA	electron microprobe analysis
FBC	Fluidised Bed Combustion
FBDB	Fixed Bed Dry Bottom
FBG	Fixed Bed Gasification
FT	Fischer-Tropsch
HT	hemispherical temperature
HT-XRD	high temperature X-ray diffraction
IDT	initial deformation temperature
IEA	International Energy Agency
IGCC	Integrated Gasification Combined Cycle
ISO	International Organization for Standardization
P	pressure
R&D	Research and Development
RD	relative density
SABS	South African Bureau of Standards
SCS	Sasol Coal Supply
SEM	scanning electron microscopy
SI	Sasol Infrachem
SNG	Substitute Natural Gas
SSF	Sasol Synfuels
ST	softening temperature
T	temperature
UK	United Kingdom
USA	United States of America
XRD	X-ray diffractometry

LIST OF FIGURES

CHAPTER 1: BACKGROUND AND LITERATURE REVIEW

FIGURE	TITLE	PAGE
1.1	A SIMPLIFIED REPRESENTATION OF THE SASOL-LURGI FBDB GASIFICATION SYSTEM [COLLET, 2002]	6
1.2	MAJOR DIMENSIONS OF GASIFIERS CURRENTLY OPERATED BY SASOL	7
1.3	MOVING OR FIXED BED GASIFIER	8
1.4	MINERAL MATTER TRANSFORMATIONS OF DIFFERENT MINERAL MATTER ASSOCIATIONS [COUCH, 1994]	21

CHAPTER 2: EXPERIMENTAL PROCEDURES, ANALYSIS AND STUDY METHODOLOGIES

FIGURE	TITLE	PAGE
2.1	ASH MELTING TEMPERATURE PREDICTION CURVE [MICROBEAM TECHNOLOGIES, 2003]	36
2.2	CHANGES IN CONE SHAPE DURING ASH FLOW TRANSFORMATION [CARPENTER, 2002 AND SLEGEIR, ET. AL., 1988] (ASTM D1857)	38
2.3	TYPICAL CCSEM SET-UP	40

CHAPTER 3: RESULTS AND DISCUSSIONS

FIGURE	TITLE	PAGE
3.1	HISTOGRAM OF RANK OF THE COAL INVESTIGATED	52
3.2	MINERAL VARIATIONS IN COAL STRUCTURE [IMAGE TAKEN BY M LAUMB, MTI]	55
3.3	INCREASING MASS % IN SI AND AL ABUNDANCE IN DIFFERENT SIZE FRACTIONS	55
3.4	EFFECT OF INDIVIDUAL COMPOUNDS ON AFT	57
3.5	CORRELATION TRENDS AS PUBLISHED BY VASSILEV ET. AL. [1995]	58
3.6	SLAG-LIQUIDUS SURFACE AND PHASE RELATIONS IN THE $Al_2O_3-SiO_2-TiO_2$ SYSTEM	60
3.7	LIQUIDUS SURFACE AND PHASE RELATIONS IN THE $Al_2O_3-Fe_2O_3-SiO_2$ SYSTEM	61
3.8	LIQUIDUS SURFACE AND PHASE RELATIONS IN THE $Al_2O_3-Fe_2O_3-SiO_2$ SYSTEM	62
3.9	LIQUIDUS SURFACE AND PHASE RELATIONS IN THE $Al_2O_3-CAO-SiO_2$ SYSTEM	63
3.10	LIQUIDUS SURFACE AND PHASE RELATIONS IN THE $Al_2O_3-NA_2O-SiO_2$ SYSTEM	65
3.11	EFFECT OF INDIVIDUAL MINERAL PHASES ON AFT	66
3.12	DENSE MEDIUM CURVE	68
3.13	EFFECT OF DENSE MEDIUM SEPARATION (DESTONING) ON AFT FOR INDIVIDUAL DENSE MEDIUM FRACTIONS	68
3.14	SiO_2 , Al_2O_3 , TiO AND CAO PERCENTAGE VERSUS THE AFT OF THE DENSE MEDIUM FRACTIONS	69
3.15	Si/Al RATIO VERSUS ASH FUSION TEMPERATURE	69
3.16	INTEGRAL INTENSITIES OF IDENTIFIED PHASES AS A FUNCTION OF TEMPERATURE	75
3.17	DECOMPOSITION OF KAOLINITE AND FORMATION OF MULLITE AS FUNCTION OF TEMPERATURE	76
3.18	DECOMPOSITION OF CALCITE AND DOLOMITE AS FUNCTION OF TEMPERATURE	77
3.19	INTEGRAL INTENSITIES OF SPECIES (RUTILE, ANHYDRITE, ANORTHITE, DOLOMITE AND CALCITE) AS FUNCTION OF TEMPERATURE	77

3.20	INTEGRAL INTENSITIES OF SPECIES GEHLENITE, HEMATITE, LIME AND QUARTZ AS FUNCTION OF TEMPERATURE	78
3.21	DECOMPOSITION OF CALCITE AND DOLOMITE AS FUNCTION OF TEMPERATURE	78
3.22	FORMATION OF ANORTHITE AS FUNCTION OF TEMPERATURE	79
3.23	DECOMPOSITION OF MULLITE AS FUNCTION OF TEMPERATURE	79
3.24	CRYSTALLINE MATERIAL (DECOMPOSITION OF MINERAL MATTER AND SLAG FORMATION AS FUNCTION OF TEMPERATURE)	80
3.25	DECOMPOSITION OF CALCITE AND DOLOMITE AS FUNCTION OF TEMPERATURE	81
3.26	FORMATION AND DECOMPOSITION OF ANHYDRITE AS FUNCTION OF TEMPERATURE	82
3.27	FORMATION OF ANORTHITE AS FUNCTION OF TEMPERATURE	82
3.28	FORMATION OF GEHLENITE AS FUNCTION OF TEMPERATURE	83
3.29	FORMATION OF MULLITE AS FUNCTION OF TEMPERATURE	84

CHAPTER 4: FACTSAGE MODEL DEVELOPMENT AND OTHER TOOLS USED FOR QUANTIFYING EXPERIMENTAL RESULTS

FIGURE	TITLE	PAGE
4.1	TYPICAL ZONES IN SASOL-LURGI GASIFICATION PROCESS	88
4.2	GAS AND SOLIDS FLOW IN DRYING AND PYROLISYS ZONE	90
4.3	MODELLING RESULTS OF MINERAL MATTER IN DRYING AND DEVOLITILIZATION ZONE RESULTS OF BASE CASE COAL	93
4.4	SILLIMANITE FORMATION IN DRYING AND DEVOLITILIZATION ZONE WITH Al_2O_3 ADDITION	94
4.5	SiO_2 TRENDS AND SILLIMANITE FORMATION IN DRYING AND DEVOLITILIZATION ZONE WITH Al_2O_3 ADDITION	95
4.6	MODELLING RESULTS OF MINERAL MATTER IN GASIFICATION ZONE OF BASE CASE COAL	96
4.7	CHANGES IN SLAG-LIQUID FORMATION WITH Al_2O_3 ADDITION	97
4.8	FORMATION OF MULLITE IN GASIFICATION ZONE	98
4.9	COMBUSTION ZONE OF BASE CASE COAL	99
4.10	PREDICTED VISCOSITIES AT DIFFERENT TEMPERATURES FOR EACH INDIVIDUAL DENSE MEDIUM FRACTION	101
4.11	PREDICTED VISCOSITIES AT 1300°C FOR EACH INDIVIDUAL DENSE MEDIUM FRACTION	102
4.12	ASH FLOW TEMPERATURES FOR EACH INDIVIDUAL DENSE MEDIUM FRACTION	103
4.13	SiO_2 , Al_2O_3 , TiO and CaO VERSUS VISCOSITY AT 1300°C OF ALL DENSE MEDIUM FRACTIONS	103
4.14	VISCOSITY PREDICTIONS AT DIFFERENT TEMPERATURES WITH THE ADDITION OF ROOF	105
4.15	VISCOSITY PREDICTIONS AT DIFFERENT TEMPERATURES WITH THE ADDITION OF FLOOR MATERIAL TO THE COAL BLEND	106
4.16	SINTERING GROWTH BY VISUAL OBSERVATION	107

LIST OF TABLES

CHAPTER 1: BACKGROUND AND LITERATURE REVIEW

TABLE	TITLE	PAGE
1.1	SASOL MINING (PTY) LTD. PRODUCTION HIGHLIGHTS [SASOL ANNUAL REPORT, 2002]	12
1.2	CHARACTERISTICS OF THE MACERAL GROUPS [FALCON AND SNYMAN, 1986]	15

CHAPTER 3: RESULTS AND DISCUSSIONS

TABLE	TITLE	PAGE
3.1	PROXIMATE ANALYSIS (AIR DRIED BASIS)	50
3.2	ULTIMATE ANALYSIS (DRY ASH FREE BASIS)	50
3.3	MACERAL ANALYSIS AND RANK	51
3.4	AFT (OXIDISING CONDITIONS)	53
3.5	ASH COMPOSITION ANALYSIS (MASS %) OF SOUTH AFRICAN COAL BLEND USED IN THIS STUDY	53
3.6	MINERAL COMPOSITION MASS % [VAN ALPHEN, 2004]	54
3.7	AVERAGE ELEMENTAL COMPOSITION OF COAL (MASS %) OF SPECIFIC PREPARED PARTICLE SIZE FRACTIONS	54
3.8	AFT OF BLENDS WITH ADDITIVE (Al ₂ O ₃ , TiO ₂ and SiO ₂) ADDITION (°C)	56
3.9	OPTICAL BASICITY VALUES [Allibert <i>et. al.</i> 1995]	59
3.10	ASH COMPOSITION (MASS %) OF COAL USED IN THIS STUDY	61
3.11	ASH COMPOSITION NORMALISED TO THREE-COMPONENT SYSTEMS	61
3.12	AVERAGE PROPERTIES OF ROOF AND FLOOR OF THE TOTAL COAL SEAM [VAN DYK AND KEYSER, 2002]	65
3.13	AFT OF BLEND RATIOS BETWEEN SCS COAL AND KAOLINITE, ROOF AND FLOOR (°C)	66
3.14	SUMMARY OF MODEL STATISTICS FOR THE AFT	71
3.15	CORRELATION COEFFICIENTS (r) BETWEEN MINERAL RATIOS AND AFT	73

CHAPTER 4: FACTSAGE MODEL DEVELOPMENT AND OTHER TOOLS USED FOR QUANTIFYING EXPERIMENTAL RESULTS

TABLE	TITLE	PAGE
4.1	MOISTURE, FIXED CARBON, VOLATILE MATTER AND ASH FLOW	86
4.2	COMPOSITION OF VOLATILE MATTER	86
4.3	CARBON, HYDROGEN, NITROGEN, SULPHUR AND OXYGEN (DRY ASH FREE BASIS) FLOW OF SOUTH AFRICAN COAL BLEND USED IN THIS STUDY	87
4.4	MINERAL COMPOSITION MASS FLOW OF SOUTH AFRICAN COAL BLEND USED IN THIS STUDY	87
4.5	TABULATED GAS FLOW FROM ZONES IN SASOL-LURGI GASIFIER (DATA FROM ASPEN THERMODYNAMIC MODEL)	88
4.6	SUMMARY OF INPUT REACTANTS INTO FACTSAGE DEVOLATILIZATION AND DRYING ZONE	89
4.7	GAS FLOW FROM GASIFICATION ZONE	89
4.8	SUMMARY OF INPUT REACTANTS INTO FACTSAGE DEVOLATILIZATION ZONE	92
4.9	MINERAL MATTER OUTPUT FROM DRYING AND DEVOLATILIZATION ZONE WITH Al ₂ O ₃ ADDITION AT 690°C	92
4.10	MINERAL MATTER OUTPUT FROM GASIFICATION ZONE WITH Al ₂ O ₃ ADDITION AT 1200°C	96
4.11	MINERAL MATTER OUTPUT FROM COMBUSTION ZONE WITH Al ₂ O ₃ ADDITION AT 344°C	100
4.12	AVERAGE PROPERTIES OF THE ROOF AND FLOOR OF A COAL SEAM	105

CHAPTER 1

BACKGROUND AND LITERATURE REVIEW

1 HYPOTHESIS AND STUDY OBJECTIVE

The hypothesis for this study relates to a method of increasing the ash fusion temperature of a coal blend (decreasing the amount of slag propensity), which will then allow operating a fixed bed dry bottom gasifier at higher temperatures.

1.1 Background

Sasol has been operating the **Sasol-Lurgi Fixed Bed Dry Bottom (FBDB)** coal gasification process for more than 50 years, and with 80 units in operation remains the world's largest commercial user of this technology. A detail discussion on the Sasol-Lurgi gasification technology is given in **Section 2** of this chapter. Coal is a crucial feedstock for South Africa's unique synfuels and petrochemicals industry and it is used by Sasol as a feedstock to produce synthesis gas (CO and H₂) via the Sasol-Lurgi FBDB gasification process. The Sasol plants located in Secunda (South Africa) gasify >30 million tons of bituminous coal to synthesis gas per year, which is converted to fuels and chemicals via the Fischer-Tropsch (FT) process. South Africa, as well as many other countries in the world, will for many years to come rely on its abundant coal resources for energy and petrochemical products.

The Sasol-Lurgi FBDB gasifiers use a low-rank inertinite-rich coal having properties that may vary significantly from mine to mine. New coal sources and areas under exploration for utilization in Sasol-Lurgi FBDB gasification are characterized in detail and the results compared with historical data to determine the suitability of these new coal sources for gasification purposes. Coals from the different sources used by Sasol vary substantially in terms of chemical and physical properties and these properties directly impact on the gasifier behaviour. A background on coal in general and specific coal properties, affecting gasifier behaviour are given in **Section 3** of this chapter.

1.2 Operational opportunity

Sasol-Lurgi FBDB gasifiers are currently operated with the philosophy of adding an excess of steam to the process. For a given coal source, the maximum efficiency is determined by the

coal-to-oxygen fed ratio [Yoon *et. al.*, 1978]. The reason for this being primarily to control the H₂/CO ratio of the syngas produced, but indirectly also to:

- (1) hold the maximum gasifier temperature below the average AFT of the coal,
- (2) control the gasifier raw gas outlet temperature i.e. lower the temperature to below the limit where the gasifiers have to cut back on load, and
- (3) as an easy way of operating the gasifier in a general stable operating mode.

Another means of controlling the gasifier stability and temperature inside the gasifier can be achieved by varying the oxygen load into the gasifier. However, when the oxygen load is decreased, this directly relates to a cut-back in gas production. Thus, the preferred way in operating the gasifier and controlling temperatures, is by varying the steam consumption. Despite the fact that the desired gasifier operating mode and stability can be achieved by varying the steam consumption, this also has a direct effect on the carbon utilization:



An opportunity exists, and will be shown in this study, to increase the average AFT of the coal fed to the Sasol-Lurgi FBDB gasifiers by adding AFT increasing minerals or species, for example kaolinite, to the coal blend before it is fed into the gasification process. By increasing the AFT, the direct effect will be that steam consumption can be decreased, which in turn will improve carbon utilization (less CO₂ production) in the gasification process .

The possible advantages of this type of technology or process manipulation can be listed as the following:

- Less cut-backs in gasification and gasifier trips occurring due to ash sintering and higher gas outlet temperatures
- A decrease in steam consumption during gasification will be obtained
- A lower H₂/CO ratio and less CO₂ production from gasification will result
- Lower gas liquor production will occur, which could lead to easier tar separation and treatment and would result in lower gas liquor treatment costs
- Less CO₂ to be routed to Rectisol, reducing the load on Rectisol
- Less CO₂ will be in the Rectisol off-gas, so that the H₂S concentration in the feed to the sulphur removal plant would be higher, resulting in more efficient sulphur removal and lower sulphur emissions.

1.3 Proposed solution to address the operational opportunity

It is well known to add additives, e.g. calcium compounds[Vassilev *et. al.*, 1995,

Slegeir, 1988, Seggiani, 1999 and Alpern *et. al.* 1984], to carbonaceous material being gasified in a slagging gasifier to decrease the ash fusion temperature. However, in the case of fixed bed dry bottom gasifiers such as the Sasol-Lurgi FBDB gasifier, the slagging of ash is undesirable as it leads to unstable operation or inoperability of the gasifier [Zevenhoven-Onderwater *et. al.*, 2001]. A fixed bed dry bottom gasifier must thus be operated in a temperature region such that the maximum gasifier temperature is below the ash fusion temperature of the carbonaceous material, which is being gasified. Conventionally, this is achieved by decreasing the oxygen load into the gasifier or by operating the gasifier with an excess of steam as gasification or moderating agent. Decreasing the oxygen load into the gasifier is undesirable as it results in a direct reduction in synthesis gas production.

The aim is thus to add an ash fusion temperature (AFT) increasing agent such as kaolinite ($\text{Al}_2\text{Si}_2\text{O}_5(\text{OH})_4$), alumina (Al_2O_3), silica (SiO_2) or titania (TiO_2) [Seggiani, 1999, Vassilev *et. al.*, 1995 and Slegeir, 1988]. A detail literature discussion with relevant R&D work done on this topic and shortcomings are given in **Section 5** of this chapter. While not wishing to be bound by theory, it is believed that some of the observed effects can be explained by considering the reactive chemical species. For example, mullite is a high temperature melting mineral [Alpern, *et. al.*, 1984] and its formation is believed to cause the AFT of the ash mixture to increase, resulting in the formation of less slag (liquid) – or more viscous liquid.

The main objective of this study was to confirm a method for increasing the AFT of a coal blend (decreasing the amount of slag propensity), which will then allow operating a fixed bed dry bottom gasifier at higher temperatures.

1.4 Confirming the hypothesis and opportunity

The standard AFT test was originally developed to indicate the likely clinker forming characteristics of ash from lump coal in stoker-fired furnaces [Reifenstein *et. al.*, 1999]. Today the main objective is to ensure that the coal ash has characteristics that minimize slagging. However, applicability of the test results to reliably predict the behaviour of coal ashed in real combustion processes has been questioned [Reifenstein *et. al.*, 1999]. The well documented shortcomings of the standard technique for estimating the AFT of coal ash are its subjective nature and poor accuracy [Collet, 2002]. Literature in support of this hypothesis on this topic are given in **Section 5** of this chapter. There are tests and measurements that attempt to predict slagging properties, for example AFT, oxide analyses, etc., but have proven to

produce results that are of doubtful accuracy [Wall *et. al.*, 1996]. The AFT tests are not really measurements, but are rather observations [Wall *et. al.*, 1996]. The AFT test, however, is still today a widely used method of assessing propensity of coal ash to slag, although some shortcomings and concerns also exist. These are well documented shortcomings and relate to the uncertainties as predictive tools of plant performance, and the reproducibility of AFT measurements [Wall *et. al.*, 1996].

Based on the shortcomings summarised herewith, the secondary objective of this study was also to understand the chemistry and interpret mineral matter transformations during Sasol-Lurgi FBDB Gasification by means of high temperature X-ray diffraction (HT-XRD), in combination with FactSage modelling. Normal AFT analyses give an average flow property and do not indicate exactly at what temperature the first melt/slag is occurring. Operating experience indicates that even when the gasifiers are operated at temperatures above the fusion temperature, as given by AFT analysis, a percentage of slag is formed. This could probably be an improved way to interpret flow properties of mineral matter in coal and assist in quantifying slag formation in gasifier operation at temperatures not reflected by AFT analyses.

2 SASOL-LURGI FIXED BED DRY BOTTOM (FBDB) GASIFICATION

In this study a focus on the application of the **Sasol-Lurgi Fixed Bed Dry Bottom (FBDB)** coal gasification process and background related to this technology is conducted. Sasol-Lurgi FBDB gasification and the process also called moving bed gasification will be explained based on the literature available.

The conversion of coal into a combustible gas is as old as the 18th and 19th century [Schilling, *et. al.*, 1979], whilst coal gasification is a broad term used to describe the conversion of coal to gas [Nowacki, 1981]. Gasification is thus the conversion of coal into a combustible gas that can be classified by pyrolysis and heterogeneous reactions [Schilling, *et. al.*, 1979, Nowacki, 1981 and Slaghuis, 1993], or in other words a process that produces mixtures of hydrogen and carbon monoxide (synthesis gas or syngas) from carbon-based feedstocks such as coal [Nowacki, 1981 and Utilis Energy, 2005]. Coal gasification entails the mixing of coal with a reactive gas, steam and oxygen or air to produce gaseous, combustible products [Schilling, *et. al.*, 1979, Nowacki, 1981 and Slaghuis, 1989]. Gasification is a fairly simple and commercially proven process for the conversion of solid and liquid carbonaceous feedstocks to synthesis gas. In the past, gasification was viewed by many as a “dirty” technology

with great associated adverse environmental impacts [US Dept of Energy, 2002 and Slaghuis, 1993]. However, gasification is the most environmentally friendly alternative to produce electricity and fuels [US Dept of Energy, 2002]. The technology is ideally suited to treat wastes and by-products from other processes, as well as natural or renewable feedstocks like biomass, agricultural and municipal waste. The increasing concerns over environmental issues are viewed as strong drivers for the future growth of gasification technology, despite the fact that a solid by-product is produced which has to be disposed of in an environmentally acceptable manner [Slaghuis, 1993]. Gasification produces valuable synthesis gas, consisting mainly of H₂ and CO, due to the stoichiometric shortage of oxygen and the presence of steam [Schilling, *et. al.*, 1979, Nowacki, 1981 and Slaghuis, 1993].

2.1 *The gasification vessel*

The first full scale Lurgi coal gasification plant was constructed at Hirsch-felde, Germany, in 1936 [Nowacki, 1981]. The Sasol-Lurgi process is a medium temperature and pressure process, suitable for a large variety of coal feedstock. The Sasol-Lurgi gasifier is designed to work under pressures of up to about 3 MPa [Schilling, *et. al.*, 1979, Nowacki, 1981 and Slaghuis, 1993]. It consists of a double-walled, water-cooled steel vessel with no refractory lining. Coal as primary feedstock is gasified at a typical pressure of 3 MPa in the presence of steam and oxygen (as gasification agents) to produce a gas suitable for a variety of applications ranging from [Nowacki, 1981 and Slaghuis, 1993]:

- (1) production of fuels through the Fischer-Tropsch process;
- (2) the production of town gas, typically employed in urban and industrial heating networks;
- (3) the production of Substitute Natural Gas (SNG) used to supplement low natural gas supplies;
- (4) the generation of electricity by means of an Integrated Gasification Combined Cycle (IGCC).

At Sasol's Secunda operations, the synthetic gas produced from coal is processed by means of a high temperature Fischer-Tropsch (FT) process utilizing the Sasol Advanced Synthol proprietary technology, to produce fuel in the petrol and diesel range for automotive use, as well as chemicals.

These gasifiers are sometimes also referred to as 'fixed bed' gasifiers, although 'moving bed' is probably more correct since the coal bed moves downwards under

gravity [Slaghuis, 1993]. Two modes of operation are possible, i.e. (1) the ash can be removed in a dry state, or (2) as a molten slag [Schilling, *et. al.*, 1979 and Nowacki, 1981]. The Sasol-Lurgi FBDB gasifiers are commercially proven for pressurised application, and these gasifiers are known to be very reliable and tolerant to changes in feedstock quality [Slaghuis, 1993 and Collot, 2002]. The Sasol-Lurgi gasifier technology produces approximately 28% of the total amount of synthesis gas produced worldwide [SFA Pacific report, 2000]. Figure 1.1 shows a schematic presentation of a typical Sasol-Lurgi FBDB gasifier.

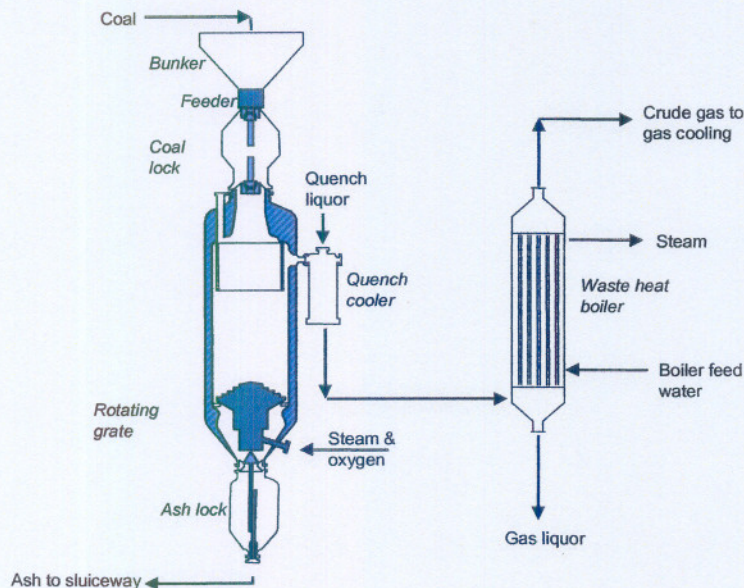


FIGURE 1.1 A SIMPLIFIED REPRESENTATION OF THE SASOL-LURGI FBDB GASIFICATION SYSTEM[COLLET, 2002]

At both Sasolburg and Secunda locations, all synthesis gas is currently produced from coal using the Sasol-Lurgi FBDB gasifiers. A high ash content (20% to 35%) and high AFT coal ($>1250^{\circ}\text{C}$) is used to produce a high H_2/CO syngas to satisfy the high demand for hydrogen in the FT synthesis.

Sasol One (located in Sasolburg) was originally equipped with 10 gasifiers each having an internal diameter of 3,66 m (called the Mark III gasifiers). Three gasifiers of similar design were added in 1966. In 1978 an additional 3 gasifiers with an internal diameter of 4 meters (called Mark IV gasifiers) (scaled up 55% above original design), were installed and 1 gasifier with a 5 meter diameter (called Mark V) (114% scaled up of original) in 1980 (Figure 1.2) [Sasol-Lurgi, 2005].

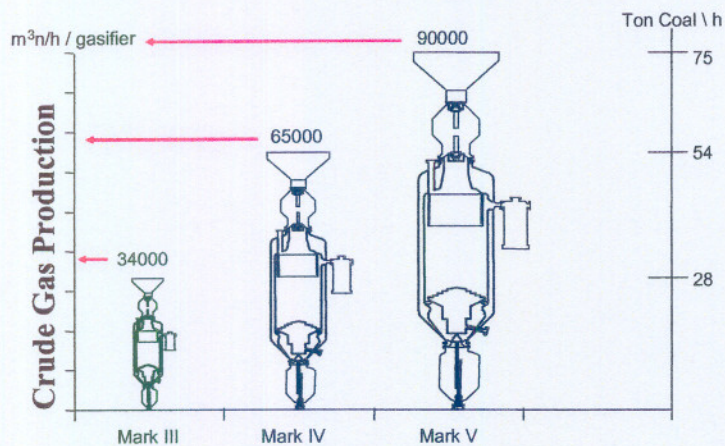


FIGURE 1.2 MAJOR DIMENSIONS OF GASIFIERS CURRENTLY OPERATED BY SASOL

The original gasifiers built in Germany before and during World War II had a diameter of 2.5m. Later models, installed around the world, had diameters of up to 3.7 m and an experimental model installed at the Sasolburg plant had a diameter of almost 5 m [Slaghuis, 1993]. Sasol currently operates 83 Mark IV gasifiers of which Sasol Two and Three located in Secunda each have 40 units. These units can truly be seen as the “work horses” of syngas production from coal at Sasol. The demand for synthesis gas at Sasol has increased steadily over the years, resulting in a continuous pressure to increase the production rates of individual units.

From a bunker, screened coal enters the gasifier via a lock hopper system. The coal bed rests on a rotating grate installed at the bottom of the gasifier. The grate is fitted with a number of scrapers or ploughs which aid in removing the ash from the vessel into an ash lock hopper. The rotational speed of the grate can be varied to control the ash removal and ash bed height [Schilling, *et. al.*, 1979, Nowacki, 1981 and Slaghuis, 1993]. The solid ash is removed batch-wise from the gasifier and quenched with water.

2.2 Process description

The processes are all linked together in an overall process scheme. The most important achievement of Sasol in this field was that: (1) gas from coal is produced on a mega scale and (2) continuous improvement on the output of the plants is rendering high mechanical availability of equipment. This could only be achieved by technical break-throughs in each of the component plants in the overall flow scheme.

Within the gasifier bed, different reaction zones (Figure 1.3) are distinguishable from the top to bottom [Schilling, *et. al.*, 1979, Nowacki, 1981 and Slaghuis, 1993], namely:

- (1) the drying zone where moisture is released,
- (2) the devolatilization zone where pyrolysis takes place,
- (3) the reduction zone where mainly the endothermic reactions occur,
- (4) the exothermic oxidation or combustion zone,
- (5) the ash bed at the bottom.

Due to the counter-current mode of operation, hot ash exchanges heat with the cold incoming agent (steam and oxygen or air), while at the same time hot raw gas exchanges heat with the cold incoming coal [Schilling, *et. al.*, 1979 and Nowacki, 1981]. This heat exchange mode results in the ash and raw gas leaving the gasifier at relatively low temperatures when compared to other types of gasifiers, which improves the thermal efficiency and lowers the steam consumption.

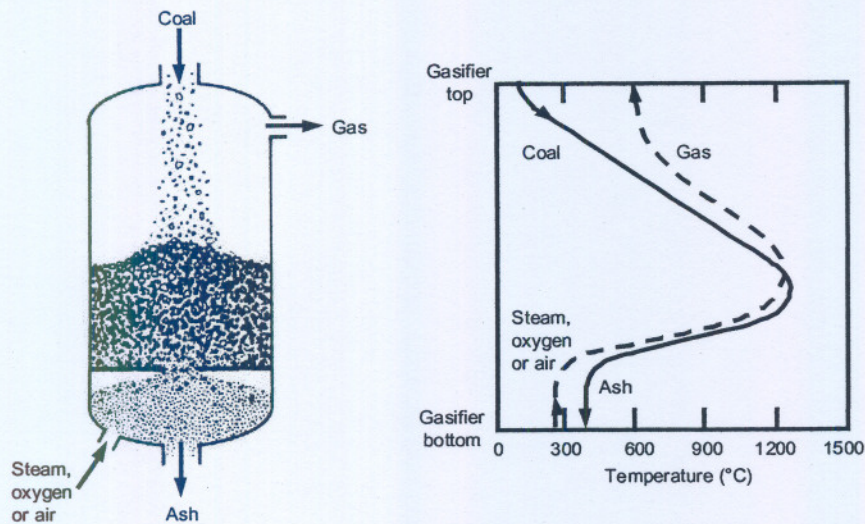


FIGURE 1.3 MOVING OR FIXED BED GASIFIER

The chemistry of gasification is extremely complex. The topic is widely covered in the open literature [Schilling, *et. al.*, 1979, Nowacki, 1981, Howard, *et. al.*, 1981 and Slaghuis, 1993], and a complete review will not be given here. The most important reactions relevant to the gasification process are similar to those of gas reforming, and the processes of gasification and reforming therefore show a lot of similarities. Both take place at relatively high temperature (approximately 1000°C or more), which is a result of the exothermic combustion (oxidation) reactions which are required to drive the endothermic reduction reactions. In the drying zone; the coal loses all of its moisture; and this drying process is an endothermic reaction. The temperature of the exit gas will be highly affected by the moisture content present in the feed coal. When the dried coal reaches a temperature of about 350-400°C it starts to devolatilize with the production of gases, oils and tars [Nowacki, 1981 and Slaghuis, 1993]. In the pyrolysis zone the coal is heated in an inert atmosphere to a temperature of 700°C.

The coal undergoes pyrolysis or destructive distillation due to the action of heat and the decomposition could be described as follows:



where C = carbon, H = hydrogen, m = number of C-atoms, n = number of H-atoms

Pyrolysis has been defined as "the decomposition of organic substances by heat" [Jucks and Sandhoff, 1980 and Slaghuis, 1993]. Thermal decomposition is the transformation of a substance into another substance, or into other substances through the severance of chemical linkages under the influence of heat [Jucks and Sandhoff, 1980, Schilling, *et. al.*, 1979 and Nowacki, 1981]. The basic gasification reactions are the following:

Oxidation:



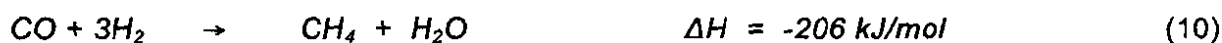
Reduction:



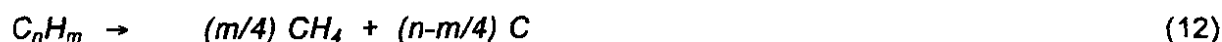
Water-gas shift:



Methane formation:



Cracking:



Hydrogenation:



In addition to the reactions above, the coal goes through the stages of drying and pyrolysis as soon as it is exposed to heat. Pyrolysis reaction chemistry is complex, and involves free radical reaction mechanisms in addition to cracking and hydrogenation reactions [Howard *et. al.*, 1981, Schilling, *et. al.*, 1979, Nowacki, 1981 and Slaghuis, 1993]. In most gasification processes the pyrolysis reactions are not of much importance since the pyrolysis products are in any event decomposed, but in the Sasol-Lurgi FBDB gasification processes (which is the technology of choice for the Sasol process), pyrolysis products like: tars, pitches, phenols, etc. are valuable

by-products from the gasification process. The important process parameters affecting pyrolysis product yields are: the coal petrographic composition, particle size, heating rate, final temperature, pressure, and the composition of the gaseous atmosphere within which pyrolysis occurs. The net heat of the pyrolysis reaction can be positive, negative, or thermally neutral, depending on the maceral and mineral composition of the coal [Howard *et. al.*, 1981 and Slaghuis, 1993].

In almost all gasifiers the water-gas shift reaction proceeds fast to very near chemical equilibrium conditions [Schilling, *et. al.*, 1979, Nowacki, 1981 and Slaghuis, 1993]. It is fairly easy to calculate approximate raw gas compositions for most gasifiers from general thermodynamic principles. The effect of the gasifier choice and operating conditions is essential on the H₂/CO ratio of the synthesis gas. This issue will be discussed further in the next section. The water-gas shift reaction is however only slightly exothermic, and therefore the H₂/CO ratio has a very small effect on the heating value of the synthesis gas [Slaghuis, 1993].

2.3 Advantages and disadvantages

The Sasol-Lurgi FBDB gasification process is a suitable process for the conversion of low-grade high ash content coal types with high AFT to high value products. Such coals are abundant in many countries, including China and India. As these countries develop, energy demand growth will require that the low-grade coal resources be exploited.

The ability of fixed bed gasifiers to handle a variety of different feedstocks is seen as a significant advantage. Other distinct characteristics (advantages) of fixed bed dry bottom gasifiers are the following [Nowacki, 1981, Slaghuis, 1993, Yoon *et. al.*, 1978 and Collot, 2002]:

- The gasifiers uses lump coal and limited grinding is required. Coal used for fixed bed gasification is mined, crushed down to <100mm and screened at a bottom size of 5-8mm.
- Coal with a high ash content can be gasified without severe losses in thermal efficiency, since the ash is not extracted in the molten state.
- High "cold gas" thermal efficiency is achieved through counter-current operation, which allows the gas and solid product streams to exit at relatively low temperatures.
- Low oxidant requirements due to the high thermal efficiency.
- Valuable co-products like tars, pitches, oils and chemicals are produced.

- A H₂/CO ratio of 1.7 to 2.0 is produced directly which is suitable for FT synthesis without the need for additional water-gas shift conversion to adjust the H₂/CO ratio, and this is a cost advantage.
- Large fuel inventory provides safety, reliability, stability.

Some disadvantages are the following [Nowacki, 1981, Slaghuis, 1993 and Collet, 2002]:

- The operating temperature has to be controlled below the ash fusion temperature of the coal. This is also then a specific issue that will be addressed in this study.
- The gasifier is sensitive to fine coal <6 mm.
- Coal dust tends to be entrained in the raw gas which causes downstream clean-up problems.
- The gasifier has a high steam demand. A large excess of steam is needed to control the temperature of the fire bed in the combustion zone.
- Due to the high coal inventory in the gasifier the unit responds relatively slowly to changes in operating conditions. The time needed to start a gasifier from cold may take up to 12 hours.
- Commercial operation with caking coal is less certain.
- Internal moving parts with higher degree of mechanical complexity.

3 COAL

With the basic principles of fixed bed gasification introduced, it is necessary to understand coal and coal properties in more detail and also specifically elucidate the role of mineral properties of coal during gasification. Much has been written about the origin of coal and its various maceral and mineral constituents and will be discussed in this section.

Sasol Mining (Pty) Ltd. is responsible for coal mining in the Sasolburg and Secunda regions and supplies coal to Sasol's synthetic fuels and chemical plants. The division operates regional operations comprising the Sigma Colliery and Wonderwater strip mining operations at Sasolburg; and the Secunda Collieries, which consist of six underground operations. During the 2002 financial year, the company supplied 45.7 million tons of saleable coal from the 51.6 million tons of coal extracted to the operations of Sasol Synfuels (SSF) at Secunda and Sasol Infrachem (SCI) at Sasolburg (Table 1.1) [Sasol Annual Report, 2002].

TABLE 1.1 SASOL MINING (PTY) LTD. PRODUCTION HIGHLIGHTS [SASOL ANNUAL REPORT, 2002]

Production (millions of tons)	2001	2002
Total production	51.3	51.6
Sigma Colliery including Wonderwater	5.4	5.9
Secunda Collieries:		
Bosjesspruit Colliery	7.3	7.3
Brandspruit Colliery	8.5	8.3
Middelbult Colliery	8.2	8.1
Twistdraai Colliery	5.5	5.2
Twistdraai Export Colliery	7.4	8.1
Syferfontein (underground and strip) Colliery	9.0	8.7
Saleable production from all mines	49.5	49.5
International sales	3.6	3.5

3.1 Coal definition and formation

From literature the following definitions for coal can be highlighted:

Dr. Marie Stopes, in 1919, distinguished four rock types called lithotypes:

Vitrain (Bright, black, usually brittle, frequently with fissures)

Clarain (Semi-bright, black, very finely stratified)

Durain (Dull, black or grey-black, hard rough surface)

Fusain (Silky lustre, black, fibrous, soft, quite friable) [Grainger and Gibson, 1981].

Other references classified coal as a heterogeneous substance, but fixed carbon, volatile matter, moisture and mineral matter can be easily distinguished [Dakic *et. al.*, 1989]. Coal is composed of a whole family of substances, covering a range of rank with a black or brownish-black colour in reflected light. Its surface may be dull or bright in certain bands. Coal consists of a complex mixture of organic substances containing carbon, hydrogen and oxygen, with smaller amounts of nitrogen, sulphur and trace elements [Grainger and Gibson, 1981]. Coal is not a uniform mixture of C, H, N, S, O and other elements; and also not a uniform polyaromatic substance. Neavel (1981) described coal as analogous to a fruitcake being formed out of a mixture of diverse ingredients, and then baked to a product that is heterogeneous. Oxygen is the predominant functional group in coal, but sulphur and nitrogen also exist in the coal. The concentrations of these elements may be lower than the oxygen functional groups [Ayat, 1987]. The lack of experimental evidence relative to the functional groups and the complex structure of coal, complicate the task of trying to imply the structures of hetero-atom functionalities [Attar and Hendrickson, 1982].

Coals are macromolecular solids. It is not a polymer in the sense that it contains a repeating unit, but it does have properties of synthetic cross linked macromolecular networks [Green, 1987]. The following properties of coal provide evidence for the

cross linked macromolecular model of coals:

- The insoluble component of coals will absorb solvents and swell.
- Coals are visco-elastic and deform when subjected to stress [Green, 1987]

Coals were formed by the breakdown of plant remains; the residues of plant life may be seen in thin sections, which can be examined microscopically by transmitted light. Remains of plants and trees can be found in coal seams [Grainger and Gibson, 1981]. "Coal is a fossil or an organic sedimentary rock, formed mainly by the action of temperature and pressure on plant debris and always has associated with it various amounts of moisture and minerals." [Grainger and Gibson, 1981].

The principal initiating requirements for coal formation are a swampy or marshy environment, climatic conditions favourable for rapid plant growth, with enough depth of water to exclude or severely restrict oxygen supply during the breakdown of the original plant material when it dies and falls into the water [Grainger and Gibson, 1981]. During the early stage of peat accumulation the formation of the macerals is dependent on a number of factors including: type of plant community, climatic controls, ecological conditions, the acidity (pH) and the redox or Eh value [Falcon and Snyman, 1986]. The differing degrees of pressure and heat over different periods of time in the geochemical stage, which act on the peat-like deposits, are responsible for the difference in coalification, referred to as the "rank" of the coal [Grainger and Gibson, 1981]. More discussion in terms of coal rank is given in **Section 3.1.3** of this chapter.

Coal is fundamentally composed of the fossilised remains of plant debris, which have undergone progressive physical and chemical alteration through geological time. The proportions of the organic constituents which are formed during biochemical degradation at the peat stage (and which impart to a coal its organic matter composition or TYPE); and the process of maturation or metamorphosis (or RANK of a coal) are therefore independent of one another. Grade refers to the mineral matter composition [Grainger and Gibson, 1981 and Falcon and Snyman, 1986].

3.2 Rank of coal

Rank is the degree of metamorphosis to which coal has been subjected to after the time of burial [Grainger and Gibson, 1981 and Falcon and Snyman, 1986]. This results in the transformation of the original peat swamp through the progressive stages of brown coal (lignite), sub-bituminous and bituminous coals to anthracites

and the meta-anthracites. The level to which a coal has reached in this coalification series is termed its rank [Falcon and Snyman, 1986]. The rank of coal can be measured because the reflectance of the vitrinite present increases with increasing rank [Grainger and Gibson, 1981].

Rank refers to the degree of maturity or metamorphism or coalification achieved by a coal through the processes of time, temperature, and pressure as a result of depth of burial or proximity to heat following peat accumulation. The progressive change from peat into coal passes through a number of stages, i.e.

Peat → lignite → bituminous → semi-anthracite → anthracite → graphite [Falcon, 1988].

3.3 Composition (types) of coal macerals

Macerals are organic substances derived from plant tissues and cell contents that were variably subjected to decay, incorporated into sedimentary strata, and then altered physically and chemically by natural (geological) processes [Neavel, 1981]. The extent of the decomposition and differences in the plant material during the biochemical stage account for the different petrographic components or macerals [Grainger and Gibson, 1981 and Borrego *et. al.*, 1997]. Falcon and Snyman (1986) stated that macerals are entities, which formed from different plant-derived tissues.

Each of the materials recognised as belonging to a specific maceral class has physical and chemical properties that depend upon its composition in the peat swamp (**Table 1.2**), and the effects of subsequent metamorphic alteration [Neavel, 1981]. For applications in coal utilisation it is often sufficient to group the macerals together under the headings: vitrinite, exinite (or liptinite) and inertinite [Grainger and Gibson, 1981]. In South African coals a fourth maceral group i.e. reactive semi-fusinite has been identified [Falcon and Snyman, 1986]. The distinction of the group macerals is based on reflectance. These group macerals are termed vitrinite, exinite and inertinite [Falcon and Snyman, 1986].

The different components (macerals) in coal can be distinguished by optical examination. Coal petrology is the study of these components [Grainger and Gibson, *et. al.*, 1981 and Given *et. al.*, 1960]. Macerals may be distinguished from one another on the basis of morphology, relief, size, shape, colour, reflectance and, sometimes origin [Falcon and Snyman, 1986]. Their names are descriptive, and conventionally end in "inite". Each maceral has a distinct set of physical, chemical

and technological properties for a given rank [Falcon and Snyman, 1986].

The most widespread method of microscopic examination of coal is the use of reflected light on polished surfaces under oil immersion to enhance reflectivity differences. This method of coal petrology is the study of the microscopic organic and inorganic constituents in coal [Falcon and Snyman, 1986]. The advantage of petrographic analysis lies in the ability to separate two variables, namely the rank and the maceral composition [Grainger and Gibson, 1981]. It is possible to predict the technological behaviour of a coal from its petrographic composition [Falcon and Snyman, 1986].

TABLE 1.2 CHARACTERISTICS OF THE MACERAL GROUPS [FALCON AND SNYMAN, 1986]

MACERAL GROUP	PLANT ORIGIN	REFLECTANCE		
		Description	% Reflected light (Rank)	Characteristic element
Vitrinite	Woody trunks, branches, stems,	Dark to medium grey	0.5-1.1	Intermediate hydrogen content
	stalks, bark, leaf tissue	Pale grey	1.6-2.0	
		White	2.0-10.0	
Exinite	Cuticles, spores, resin, bodies,	Black-brown to dark grey	0.00-1.1	Hydrogen-rich
	algae accumulating in	Pale grey	-1.1-1.6	
	sub-aquatic conditions	Pale grey to white shadows	-1.6-10.0	
Inertinite	As for vitrinite, but fusinitized in	Medium grey	0.7-1.6	Hydrogen poor
	aerobic oxidising conditions	Pale grey to white and yellow-white	-1.6-10.0	

3.4 Coal structure

A discussion of the three main maceral groups is given below:

- **Vitrinite** is a group of microscopically recognisable constituents, which formed from cell-wall material and the cell fillings of the woody tissue of plants [Falcon and Snyman, 1986]. Vitrinites show very homogeneous properties at any given rank [Borrego *et. al.*, 1997]. The physical and chemical properties of the vitrinite materials in a specific coal were conditioned largely by the magnitude of temperature and pressure to which they were subjected to after burial [Neavel, 1981]. Vitrinite is the major component of most coals. It generally

occurs in bands and is usually uniform in appearance sometimes showing cell structure [Given, 1964].

- **Inertinite** represents a group of macerals derived from plant material that has been strongly altered and degraded in oxidising conditions in the peat stage of coal formation [Falcon and Snyman, 1986]. Initially, the term 'inert' coined to group those macerals that remained unfused during carbonisation, could be misleading when applied to combustion, since the interest here is placed on the ability of a coal to burn efficiently rather than to develop a highly porous structure [Borrego *et. al.*, 1997]. The fact that vitrinites show very homogeneous properties at any given rank and that these properties vary with rank in a quite regular and predictable way, points to the inertinites as being responsible for any anomalous behaviour of coals during combustion [Borrego *et. al.*, 1997]. Inertinite has a low volatile matter content, does not soften or swell on combustion and gives a dense, less reactive char. Inertinite shows characteristic fibrous, cellular structure [Given, 1964]. The term inertinite is used to simplify the nomenclature of coal petrology by combining, (in a single term), the macerals: micrinite, semi-fusinite, fusinite and sclerotinite [Francis, 1961].
- The term **exinite** was originally used to describe the chemically resistant exines of spores in coal [Falcon and Snyman, 1986]. Exinite has a lower density and higher volatile content, compared to the vitrinite, whereas; the inertinite has a higher density and lower volatile content than that of vitrinite [Grainger and Gibson, 1981]. As a result of liptinites high volatile matter and hydrogen contents as well as its low aromaticity, the presence of moderate amounts of liptinite is regarded as a positive feature that favours the onset of a stable flame [Borrego *et. al.*, 1997]. Exinite consists of the remains of plant spores, pollen and cuticles with characteristic shape [Given, 1964]. The exinite group comprises the macerals: sporinite, cutinite, suberinite, resinite, alginite and liptodetrinite. Exinites are distinguished from vitrinite by a higher hydrogen content in coals with a low rank [Stach *et. al.*, 1982].

4 ASH FUSION PROPERTIES (AFT) AND MINERAL MATTER

With this basic understanding of coal it is furthermore important to review the physico-chemical behaviour of the coal with particular relevance to coal gasification and the mineral matter content in the coal. The principles of AFT properties, and mineral matter transformations occurring during fixed-bed gasification will be discussed, prior to focussing on the subject of increasing the AFT and feedstock manipulation.

The AFT behaviour during gasification and mineral matter reactions, will be discussed in detail, because it is essential for the work and the objective of this thesis, but it must be noted that other properties may affect gasifier performance and stability as well.

4.1 Ash fusion temperature (AFT)

Ash clinkering inside the gasifier can cause channel burning, pressure drop problems and unstable gasifier operation. Seggiani [1999] also stated that although ash fusibility is not the only factor that must be considered when choosing a coal for a given application, it is one of the most traditional parameters used to predict ash behaviour and to know whether slagging and ash-deposit problems will be encountered.

As already mentioned, the AFT consists of four temperatures, which reflect the stages of the "flow" process [Carpenter, 2002 and Slegeir *et. al.*, 1988]. The ideal gasifier operation is to operate at a temperature above the initial deformation temperature (IDT) in order to obtain enough agglomeration to improve bed permeability, but to operate below the AFT to prevent excessive clinkering. Secunda and Sasolburg coal sources currently used for gasification typically have an AFT > 1300°C and an IDT of >1250°C [SABS, 1999], but successful gasification in Sasol-Lurgi gasifiers is not limited to this temperature range.

Although the standard AFT test is currently used as the only predictive tool for measuring the AFT of coal, Alpern (1984) has shown that this may not represent the actual fusion temperature of certain minerals and mineral phases. Various authors, such as Seggiani (1999) and Alpern *et. al.* (1984), have reported and expressed the fusibility of the ash as function of the content of the eight principal oxides frequently found in coal ash, i.e. SiO₂, Al₂O₃, TiO₂, Fe₂O₃, CaO, MgO, Na₂O and K₂O. The acid/base ratio is the most frequently used parameter for correlating ash fusibility with its composition. Slegeir *et. al.* (1988) highlighted the fact that coal ash fusibility characteristics are difficult to determine precisely, partly because coal ash contains many components and does not have a sharp melting point like a pure compound. Correlations between AFT data and ash composition indicates that, although the regression approaches are more complicated, in many cases they are no more accurate than the approaches based on the acid-base formalism. Correlations are thus not obtained with single elements, but as an interaction between different ash forming elements [Seggiani, 1999 and Alpern *et. al.*, 1984].

Ash management, according to Baxter (2003) is and will always be a major design and operational issue for low-grade fuel (coal, biomass, waste, etc.) gasification and combustion. Despite its undisputed importance, effective means of controlling and anticipating ash deposition remain discussed and highly researched. The following three major factors contribute to this difficulty and to the current uncertainty in predicting ash deposition and slagging [Baxter, 2003]:

- Inorganic material in low-grade fuels is almost always classified in terms of elemental or oxide composition only, while the behavior of inorganic material depends strongly on its mineralogy.
- Most indices and analyses developed to describe ash deposition behavior are based on fuel analyses, whereas ash deposits often form selectively.
- Ash deposition depends strongly on plant design and operation conditions.

From experience within Sasol and personal discussions, visual investigation of actual ash produced from a fixed bed gasifier, it is clear that the coarse and fine ash is sometimes extracted from the gasifier with the important middle fraction being absent. This can possibly be explained by the fact that some minerals already slag and clinker at low temperatures. A detail description of the AFT test and advantages/disadvantages are given in Chapter 2.

The AFT of coals and coal blends is one of the parameters currently widely used in coal marketing and utilization to assess coal quality, coal ash fusibility and flow characteristics, and to predict the flow behavior of the coal ash in power generation reactors, as well as gasifiers [Jak, 2002]. It is therefore important to be able to predict AFT's to assist in a number of technical issues such as: coal blending and fluxing, optimization and maximization of the use of coal resources. Research on AFT's provides a better understanding of the meaning of this test and the correlations between the AFT values and actual behavior of the coal ash in industrial processes [Jak, 2002]. There have been a number of studies [Jak, 2002, Seggiani, 1999 and Alpern *et. al.* 1984] on the prediction of AFT's from the coal ash compositions, such as empirical and statistical correlations between coal ash compositions and AFT's derived using regression analysis [Jak, 2002].

As in the case of fixed bed gasifiers, slags are formed during coal combustion or gasification as a result of partial melting and reaction of the mineral matter. Predicting the outcome of these complex chemical reactions has long been a problem and is still worldwide a high priority study [Jak *et. al.*, 1998]. The same concept and problem was addressed that form deposits due to slagging on the heat adsorbing surfaces causing significant reduction in thermal efficiency, but so is the problem of relevance to fixed bed gasification [Kalmanovitch and Williamson, 1986]. The study involved an investigation of the crystallization of coal ash

melts and the effect this has on the formation and growth of the troublesome deposits [Kalmanovitch and Williamson, 1986].

4.2 Mineral matter

There is a general agreement in the literature that clays, sulphides, carbonates and quartz are the most common minerals in coal [Alpern, et. al., 1983]. However, the abundance in percentage of mineral matter is very variable from one basin to the other. The most abundant minerals in South African coals are clays, carbonates, sulphides, quartz and glauconite [Falcon and Snyman, 1986 and Van Alphen 2004].

Mineral particles can be observed in coal sections and form a major portion of the ash [Grainger and Gibson, 1981]. The forms in which minerals occur in coal fall into two major categories: the first includes the intrinsic inorganic matter, which was present in the original living plant tissue; the second category includes the extrinsic or introduced forms of mineral matter [Falcon and Snyman, 1986]. Intrinsic inorganic matter is trapped in coal in the form of sub-microscopic mineral grains and as organo-metallic complexes. The extrinsic mineral may be primary or syngenetic, and arise from the accumulation of the minerals at the time of peat accumulation by means of wind and water or precipitation from saturated solutions in situ [Falcon and Snyman, 1986].

The inorganic constituents of coal may be considered in two forms. The first form consists of inorganic constituents in the coal forming plants, while the second class consists of inorganic constituents added to the coal-forming deposit after the death of plants. These two classes are sometimes called "inherent" and "adventitious" [Francis, 1961].

The inorganic matter in coal can be classified into three groups:

- inorganic matter from the original plants;
- inorganic - organic complexes and minerals which formed during the first stage of the coalification process; or which were introduced by water or wind into the coal deposits as they were forming;
- minerals deposited during the second phase of the coalification of the coal, by ascending or descending solutions in cracks [Stach *et. al.*, 1982].

The term ash is commonly misused and misunderstood. Normally ash is regarded as a product of coal combustion. Specifically, there is no ash in coal. Ash is formed as

the inorganic material in the fuel decomposes, oxidizes, melts and reacts during combustion or gasification. Much of the inorganic material in low-rank coal is atomically dispersed or otherwise associated with the organic fraction of coal [Baxter, 2003]. Coal has a significant inorganic material content, varying from less than 3-4 wt%, to more than 40 wt% [Seggiani, 1999]. Extensive literature exists regarding the thermal transformations of isolated minerals unrelated to coal [Alpern *et. al.*, 1984], but minerals in coal are seldom isolated. The matrix is often organic, but can have also mixtures of different minerals [Alpern *et. al.*, 1984]. There is a general agreement in literature that clays, sulphides, carbonates and quartz are the most common minerals found in coals [Alpern *et. al.*, 1984].

The mineral matter present in coal may be classified in the form of two major groups [Tomeczek and Palugniok, 2002]:

- Extraneous minerals: particles containing over 90 wt% of mineral matter, and can be separated from the organic matter as a result of prior-to-combustion crushing.
- Inherent minerals: closely associated with organic coal particles, which cannot be separated prior to combustion. The content of the inherent minerals is usually below 10 wt% in the organic particles.
- The simplified mechanism of mineral matter liberation of the different mineral associations is given in Figure 1.4 [Couch, 1994].

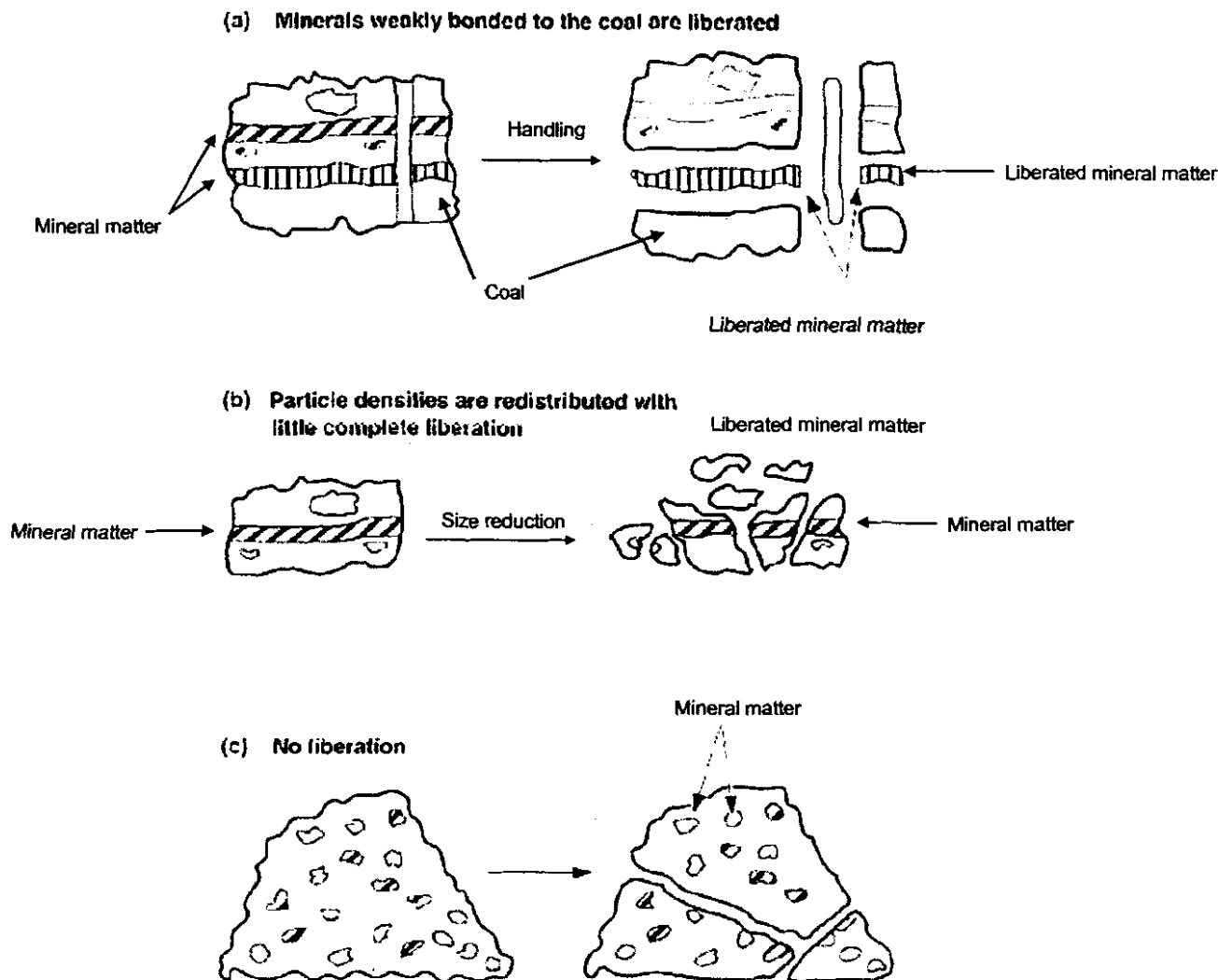


FIGURE 1.4 MINERAL MATTER LIBERATIONS OF DIFFERENT MINERAL MATTER ASSOCIATIONS [COUCH, 1994]

The material described as “mineral matter” in coal encompasses dissolved salts in the pore water and inorganic elements associated with the organic compounds, as well as discrete crystalline and non-crystalline mineral particles [Ward, 2002]. From a genetic point of view, the mineral matter in coal, like the organic matter, is a product of the processes associated with the peat accumulation and rank advance, as well as changes in subsurface fluids and other aspects of sediment diagenesis [Ward, 2002]

Apart from artefacts produced by oxidation of the organic matter in the course of low-temperature ashing, or by drying out of coals with high moisture contents, the minerals occurring in coal may form by a range of different processes. These include the input of fragmental sediments into the original peat-forming environment by epiclastic and pyroclastic processes, accumulation of skeletal particles and other biogenic components within the peat deposit, and precipitation of material from solution in the peat swamp or in the pores of the peat bed [Ward, 2002]. It also

includes precipitation of minerals in pores, cleats and other fractures of the coal by post-coalification processes. Non-mineral inorganics, which are also part of the mineral matter, may be concentrated in different parts of low-rank, water-filled coal seams by post-depositional ion migration effects [Ward, 2002].

Some of the mineral matter in coal represents material washed or blown as detrital fragments into the accumulating peat deposit. This includes components from river water and flood inputs, airborne dust, etc., introduced by epiclastic processes and volcanic debris introduced to the peat from pyroclastic activity [Ward, 2002].

Many of the minerals in coal, or at least in modern-day peat deposits, result directly from biological activity in the peat swamp. These include skeletal fragments from diatoms, molluscs and other organisms, minerals formed within living plant tissues (phytoliths) and possibly minerals deposited in the peat swamp as faecal pellets [Ward, 2002].

Minerals formed by crystallization in place (i.e. authigenic minerals), either within the peat deposit at or shortly after its formation (primary or syngenetic precipitates), or in the cleats and fractures of the coal after compaction and probably rank advance (secondary or epigenetic precipitates), are a very common component of coal seams. Primary precipitates include siderite nodules, microcrystalline pyrite framboids, and a range of cell and pore infillings (typically kaolinite, quartz, phosphate minerals and pyrite). Cleat infillings can include calcite, dolomite, ankerite and siderite, as well as pyrite, marcasite, apatite, illite and chlorite [Ward, 2002].

A number of different minerals, including sulphides, carbonates, quartz and clay components are found as post-depositional fracture infillings in coal seams. Most of the infillings are quite persistent, following the different cleat fractures within the coal [Ward, 2002].

Particularly in lower-rank coals (sub-bituminous coals and lignites), a significant part of the inorganic matter may be represented as elements associated with the organic constituents. This is specifically of importance on South African coal sources. Such occurrences include inorganic components dissolved in the pore water of the coal, elements held in exchangeable relationships with particular organic compounds (i.e. carboxylates) and inorganic elements forming chelates and the organometallic complexes within the organic matter. [Ward, 2002].

4.3 Specific (most abundant) mineral species in coal

The most common minerals present in the South African coals, which have relevance to this thesis, are also the main mineral groups in other coals sources [Vassilev and Vassileva, 1996 and Van Alphen, 2004], making the literature in the global arena relevant to this study. The most common minerals in coal, with a brief discussion on each and possible changes that occur during thermal changes are given below:

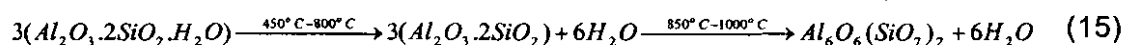
- **Quartz (SiO_2)** does not change below $573^\circ C$, but only inverts from α to β -quartz [Deer *et. al.*, 1966], which is a structural change and volume change and it is unlikely that quartz influences the thermal fragmentation of coal up to $850^\circ C$.
- Differential thermal analysis and dehydration experiments are widely used for the characterisation and identification of kaolinite (**clays**) ($Al_2Si_2O_5(OH)_4$). The dehydration of clay minerals proceeds in a number of stages [Deer *et. al.*, 1966]. Some of its adsorbed water (surface and interlayer) is lost on heating to $110^\circ C$ as with any other mineral, but the remainder comes off gradually and is not completely expelled up to about $400^\circ C$. For kaolinite, little or no surface adsorbed water is present; and most of the dehydration (loss of OH) takes place between $400^\circ C$ and $525^\circ C$ [Deer *et. al.*, 1966]. All clay minerals decompose at approximately $400^\circ C$ [Deer *et. al.*, 1966]. The maximum rate of decomposition occurs at $570^\circ C$. The decomposition continues over a temperature range of $300^\circ C$; complete at about $750^\circ C$ [Slaghuis, 1989].



When kaolinite minerals are heated so that all water molecules and OH ions are driven off (a stage which is almost reached by about $650^\circ C$, and is complete by $800^\circ C$), the product is called meta-kaolinite.

In agreement with the transformations as summarized by Deer *et. al.* (1966), Alpern *et. al.* (1984) summarized the thermal transformations as follows:

- loss of adsorbed water (endothermic) at $50^\circ C$ to $150^\circ C$,
- loss of H_2O (endothermic)
- lattice destruction at $850^\circ C$ to $1000^\circ C$.



- The temperature of transformation of **pyrite** (FeS_2) depends very much on the reducing or oxidizing conditions [Alpern *et. al.*, 1984]. Slaghuis [1989] stated that decomposition starts at 480°C and reaches a maximum at 540°C after which it slows down up to 580°C. With further heating the decomposition rate increases again to reach a maximum at about 640°C. Some pyrite samples in coal start decomposing at about 450-500°C, whereas other samples of pyrite only start decomposing at 650°C. This might be explained by possible trace elements in the pyrite structure or the particle size distribution of the pyrite structures. A simplified reaction showing the decomposition of pyrite is



Under oxidizing conditions SO_3 or SO_2 gases form, resulting in a final residue of hematite following a transition sulphatic phase [Alpern *et. al.*, 1984]. Under reducing conditions the gas evolved is mainly H_2S and the residue is pyrrhotite [Alpern *et. al.*, 1984].

- **Sulphates** ($CaSO_4$) are not very abundant in coals and are generally represented by gypsum, which is always destroyed and underestimated by nearly all thermic methods of ash content measurements [Alpern *et. al.*, 1984]. Under reducing conditions the following transformation occurs:



- In general (oxidizing and neutral atmosphere) there is a loss of CO_2 from **carbonates** and a residue of oxides (CaO , MgO , FeO) at temperatures from 710°C depending on the associated matrix [Alpern *et. al.*, 1984]. Slaghuis [1989] reported that the onset of decomposition of $CaCO_3$, for example in a CO_2 atmosphere was found to be at 945°C with reaction extended over a 70°C span. The maximum rate of decomposition for calcite was found to be 970°C, but strongly depends on the heating rate of the experimental procedure.
- The dehydration of **illites** ($K_2Al_4(Si_6Al_2O_{20})(OH)_4$) proceeds in a number of stages. Most of the water adsorbed on the surface of particles, and the small amount which may be inter-layered with illite sheets comes off rapidly below 110°C, and the remainder more slowly between 110°C and 350°C. Water formed by expulsion of $(OH)^-$ ions come off rapidly at first between 350°C and 600°C. Differential thermal analysis curves of illite show three endothermic

peaks:

- between 100-200°C representing loss of loosely held water,
- at 550-650°C corresponding to loss of (OH)⁻,
- at 850-950°C corresponding to disruption of the remaining structure of inherent moisture [Deer *et. al.*, 1966].

5 REVIEW OF PREVIOUS WORK DONE ON ASH FUSION CHARACTERISTICS OF COAL, SLAGGING AND MINERAL CHARACTERISTICS

As was mentioned initially, the study of understanding mineral matter changes during gasification and AFT are of great significance. A discussion on the prior work conducted in this area and quantification methods and tools used in the study of mineral matter and AFT changes will be outlined in this section.

5.1 Summary of previous research and findings

Extensive studies have been conducted to relate the AFT to chemical composition of the coal ash (see **Section 5.1** and **5.2** with detail references), and some relationships have been established to predict the flow behaviour of the ash. Surprisingly, the most important dependence of the AFT from coal and ash minerals, and their behaviour during heating has not been explored in full detail as yet, although research has been conducted for some time on this specific topic. For example, the work of Vassilev *et. al.* (1995) and Kamer *et. al.* (1994) can be used as an example to highlight the matter:

- Results indicate that despite correlation trends, a reliable explanation and prediction of the AFT only from the total chemical composition is inadequate. [Vassilev *et. al.*, 1995].
- Kamer *et. al.* [1994] stated that severe fouling can be controlled, but it demands a thorough understanding of how minor changes in the chemical and physical properties of coal and ash and operating conditions can cause hardened deposits.

The coal ash fusibility properties are difficult to determine accurately, but are valuable to the clean, reliable and efficient utilization of coal [Collet, 2002]. The fusibility characteristic of a coal ash depends largely on the mineral phases present in the coal, and are also related to their chemical composition [Sakorafa *et. al.*, 1996]. A number of groups have described correlations between the ash composition and the AFT's [Slegeir, 1988], which will be discussed and summarized in this section. According to

[Slegeir, 1988] no single correlation seems "ideal" for the various types of coal of interest, as well as for the specific application for example in the case of Sasol-Lurgi FBDB gasification. Coal ash fusibility characteristics are difficult to determine precisely, because AFT tests use a sample of high temperature ash, which has destroyed the minerals present in the original coal. A rather simple method to express the fusibility characteristics of coal ash is the ASTM AFT test (Chapter 2) [Slegeir, 1988]. A number of workers [Seggiani, 1999 and Alpern *et. al.* 1984] have reported correlations between AFT data and ash composition; one is based on regression analysis and employs multiple variables, while the other is based on what is termed here as the acid-base formalism where all the components are considered as oxides. According to Seggiani [1999] and Slegeir [1988] the acid-base ratio is the most frequently used parameter for correlating ash fusibility.

$$\% \text{ Base components} = \% \text{ Na}_2\text{O} + \% \text{ K}_2\text{O} + \% \text{ CaO} + \% \text{ MgO} + \% \text{ Fe}_2\text{O}_3 \quad (18)$$

$$\% \text{ Acid components} = \% \text{ SiO}_2 + \% \text{ Al}_2\text{O}_3 + \% \text{ TiO}_2 \quad (19)$$

$$\text{Acidity} = (\text{SiO}_2 + \text{Al}_2\text{O}_3) / (\text{Fe}_2\text{O}_3 + \text{CaO} + \text{MgO} + \text{Na}_2\text{O} + \text{K}_2\text{O}) \quad (20)$$

The coal AFT alone was not sufficient to be able to satisfactorily distinguish between the good (non-slugging) versus poor (slugging) performing coals [Carpenter, 2002]. Further investigation revealed that the iron levels in the coal ash, and several indices such as base to acid ratio, slugging factor and iron loading can provide a base for distinguishing the coals that cause slugging and those that did not. However, the split between successful and unsuccessful coal types was found to be specific to a certain plant and cannot be generalised for all operations and performances. By incorporating the ash chemistry into the evaluation and reviewing past experience, techniques were found to better quantify coal characteristics with plant operating experience. The following commonly used expressions were found to be useful in segregating the successful and unsuccessful coals [Hatt and EPRI Report, 1980]:

$$\text{From loading, lb. iron / Mbtu} = (\% \text{ Fe}_2\text{O}_3 * (\% \text{ Ash} / 100)) / ((\text{Btu/lb.} / 100)) \quad (21)$$

*Slugging index, Rs = dry % S * B / A, where*

$$B / A = (\% \text{ Fe}_2\text{O}_3 + \% \text{ CaO} + \% \text{ MgO} + \% \text{ K}_2\text{O} + \% \text{ Na}_2\text{O}) / (\% \text{ SiO}_2 + \% \text{ Al}_2\text{O}_3 + \% \text{ TiO}_2) \quad (22)$$

$$\text{Silica index} = 100 * (\% \text{ SiO}_2 / (\% \text{ SiO}_2 + \% \text{ Fe}_2\text{O}_3 + \% \text{ CaO} + \% \text{ MgO}))$$

(23)

An index based on CCSEM results was also developed and is given as [Biggs and Lindsay, 1996]:

$$\text{Index} = \text{Sum of all minerals}[\text{mass fraction} * (\text{CaO} + \text{Fe}_2\text{O}_3 * (1 - 0.5 * (\text{Fe}_2\text{O}_3 / (\text{Fe}_2\text{O}_3 + \text{Al}_2\text{O}_3 + \text{SiO}_2))) \quad (24)$$

Apart from the above indices, work in the UK [Gibb, 1996] had focussed on developing suitable slagging indices based on either chemical composition or some physical parameter, e.g. AFT or viscosity. When a UK study was initiated [Gibb, 1996] authors around the world were increasingly recognising that slagging indices based on bulk ash composition had limitations and that any improvement would require a knowledge of the composition and distribution of the minerals in the coal. The complexity of the slagging process of the coal minerals means that many factors beyond those already mentioned must be taken into account in determining the risk of slagging in an individual process [Gibb, 1996].

Coal and ash based indices are often used to predict slagging and fouling behaviour of coals, but these are rarely accurate [Juniper, 1996]. The reality is that there is a need to use better techniques in describing the ash characteristics. A new index which has been previously proposed for some southern-hemisphere coal sources (being simply the Fe_2O_3 plus CaO contents) was shown to be a reasonable indicator of the slagging potential [Juniper, 1996]. The T_{250} temperature is a commonly used index and is the estimated ash temperature corresponding to an ash viscosity of 250 poise, but did not appear to be appropriate for Australian coals. In the same study it was found that there were some coals having IDT's less than 1150°C , which did not produce molten deposits at reasonable high gas temperatures, and there were others with an IDT $>1300^\circ\text{C}$ which were shown to have poor characteristics in this region [Juniper, 1996]. Gupta *et. al.* (1998) have also shown that the IDT does not represent formation of the first liquid phases indicating the doubtfulness of using just one indicator.

Alkali components play a major role in deposit formation and bed agglomeration in FBC (Fluidised Bed Combustion) and FBG (Fixed Bed Gasification) [Zevenhoven-Onderwater *et. al.*, 2001]. Deposit formation in the flue gas channel is dependent on the release of alkali components from the fuel during combustion or gasification. Alkali components can react with the bed material as present in the thermal

conversion system, forming a coated layer on the surface [Zevenhoven-Onderwater *et. al.*, 2001], and in order to provide a better understanding of the processes taking place in agglomeration of bed material, a better understanding of the chemistry behind the processes is needed. SEM analysis of agglomerates can partly achieve this [Zevenhoven-Onderwater *et. al.*, 2001].

Knowledge of the mineral matter in coal, as opposed simply to the elemental composition of the coal ash, is important in the understanding of the inorganic chemistry associated with slag / ash formation [Ward and Taylor, 1996]. It is also important in understanding the aspects of materials handling, boiler erosion, ash formation and slagging behaviour in coal processes, etc. [Ward *et. al.*, 2001].

An interesting finding, that is contradictory to other published results, is that clays can react with sodium to form products that melt at significantly higher temperatures than sodium silicates or sulphates. The products formed, are sodium aluminosilicates such as nepheline, $\text{Na}_2\text{O} \cdot \text{Al}_2\text{O}_3 \cdot 2\text{SiO}_2$ [Ross *et. al.*, 2003], which is only possible if no free SiO_2 is present. The higher AFT is related to an increased content of silica-containing minerals [Vassilev *et. al.*, 1995]. Normally sodium acts as a fluxing agent, taken into account the correlations published in literature [Seggiani, 1999 and Alpern *et. al.* 1984].

Coal ash is an extremely complex mixture of crystalline, partially crystalline and glassy phases [Gray, 1987 and Jak and Hayes, 2005]. One of the relative successful techniques used in predicting the AFT is with the aid of equilibrium phase diagrams of the major mineral oxide species. It is assumed by various authors that coal ash can be regarded as a four component system ($\text{SiO}_2 - \text{Al}_2\text{O}_3 - \text{Fe}_2\text{O}_3 - \text{CaO}$), and expresses the composition of the ash by means of sections through a triangular prism at various percentages of lime which yield ternary diagrams with SiO_2 , Al_2O_3 and Fe_2O_3 as vertices for different lime levels [Gray, 1987 and Jak and Hayes, 2005].

The major coal ash components are SiO_2 , Al_2O_3 , CaO and 'FeO' [Kondratiev and Jak, 2001]. As per normal ash composition analyses the total Fe and is reported as Fe_2O_3 , but for modelling purposes expressed as 'FeO'. Analysis of phase equilibrium (properties of the liquid and solid phases) is an essential first stage in the selection of a fluxing regime. [Kondratiev and Jak, 2001]. Coal ashes have very complex compositions and their $\text{SiO}_2/\text{Al}_2\text{O}_3$ ratio can vary over a broad range. Another common feature is the fact that the viscosity depends strongly on the $\text{SiO}_2/\text{Al}_2\text{O}_3$ ratio only in the ranges of the conditions where proportions of solids are different

[Kondratiev and Jak, 2001]. Another way to achieve 'target' coal ash slag flow characteristics is to use coal blending which could be a more cost efficient strategy [Kondratiev and Jak, 2001], because less additives can be used. It was concluded that the viscosity model which has been developed for the CaO-FeO- Al₂O₃-SiO₂ system in equilibrium with iron adequately describes experimental viscosities from a complete range of compositions and a wide range of temperatures applicable to coal gasifiers. It was assumed by Watt *et. al.* [1969] and Kondratiev and Jak [2001] that the viscosity of a coal ash slag was determined primarily by the oxides SiO₂, Al₂O₃, CaO, MgO and 'FeO'. A study by Jak (2001) was done on Australian coal sources under oxidizing and reducing conditions with similar findings.

Scanning electron microscopy and electron microprobe analysis (SEM/EMPA) provide researchers with the analytical tools necessary to truly understand deposit formation mechanisms [Kamer, *et. al.*, 1994 and Skorupska, Carpenter, 1993 and Van Alphen, 2004]. It is used to characterise the phase-mineralogy and chemical composition, together with microstructural observations [Vassilev and Vassileva, 1996]. This technique exposes the size, shape and chemistry of the individual ash particles formed when coal burns. In a study completed with this technique it was, for example, shown that the deposits were dominated by calcium aluminosilicates derived by reaction between ionically dispersed calcium and clay minerals [Kamer, *et. al.*, 1994].

Statistically significant numbers of inorganic particles, either individual mineral grains in coal or crystalline and glassy particles in ash are automatically located, measured and chemically analysed to determine their size, shape and compositional category [Kamer, *et. al.*, 1994 and Skorupska and Carpenter, 1993]. By studying the inorganic constituents in coal and its subsequent char, fly ash and ash deposits, CCSEM can follow the changes in the size, chemistry and shape of the mineral grains through the various stages of combustion [Skorupska and Carpenter, 1993]. Van Alphen (2004) also developed a method for analyzing specifically South African ash and was used on the coal samples studied.

Advantages of the CCSEM technique include characteristics such as repeatability, and automization, as well as being carried out directly on coal [Carpenter, 2002]. CCSEM has been found to be a powerful technique for quantitative analysis, but has its limitations as well [Carpenter, 2002], complex data interpretation, one compound can only be assigned to one class, etc. It is believed that the CCSEM technique is a significant advance on the more conventional methods of coal mineral analysis, such

as SEM and EMPA described by ASTM and other standards [Skorupska and Carpenter, 1993].

5.2 Shortcomings and summary of published work and analyses techniques

The investigations by most authors, as referred to in **Section 5.1**, show that a number of mineral and organic matter transformations, which occur during low-temperature ashing, can cause misleading results. Although the acid-base ratio is the most frequently used parameter for correlating ash fusibility, it is less effective when applied to a large number of samples from various sources having a wide range of compositions. It also permits the effect of adding extraneous minerals such as CaO, which changes the ash fusibility that will be predicted [Seggiani, 1999]. Ash slagging behaviour is a non-additive property of the pure coals and hence difficult to predict. Coal ash tendency to slag is related to its bulk chemistry and AFT [Seggiani, 1999 and Alpern *et. al.* 1984]. Practice has shown that the behaviour of blends does not always comply with the expected weighed average value of parameters from the pure coals comprising the blend. Interaction between the coals has to be suspected as the main reason behind the observed deviations; and agglomeration of solids or ash slagging is considered one of them. A point of interest is that experimental evidence shows that the slag performance of blended coals can be worse than that of the performance of the individual coals [Goni *et. al.*, 2003]. Although Tomeczek and Palugniok [2002] published one of many mechanisms of mineral transformations in coal, they indicated that the mechanism of specifically fine ash is still not completely understood.

The temperature at which the minerals become sticky is defined as the temperature where the amount of liquid in the material is high enough for the mixture to stick onto a metal surface, and the fusion temperature is defined as the temperature where the amount of liquid and viscosity are high enough for the mixture to flow down a vertical surface [Backman *et. al.*, 1995]. The difference between the temperature of the first appearance of a melt and the temperature of complete flow varies strongly depending on the composition [Backman *et. al.* 1995]. Scrutiny of the standards and of equipment used to measure the AFT shows ample scope for improvement in the experimental technique and in accuracy [Gray, 1987]. The present results show that routine AFT testing is an insufficient method to characterise the AFT properties of a given coal, and new approaches and methods are required [Vassilev *et. al.*, 1995].

The well documented shortcomings of the standard technique for estimating the AFT of coal ash are its subjective nature and poor accuracy (reproducibility) [Collet, 2002]. A number of tests and analytical techniques are used to evaluate the potential of coals to foul and slag in furnaces. There are tests and measurements that attempt to predict slagging properties, for example AFT, oxide analyses, etc., but have proven to produce results that are of doubtful accuracy [Wall *et. al.*, 1996]. The AFT tests are not really measurements, but are rather observations [Wall *et. al.*, 1996]. The AFT test is still today the most accepted method of assessing propensity of coal ash to slag, although some shortcomings and concerns also exist there. These are well documented shortcomings and relate to the uncertainties as predictive tools of plant performance, and the reproducibility of AFT measurements [Wall *et. al.*, 1996]. The standard AFT test was originally developed to indicate the likely clinker forming characteristics of ash from lump coal in stoker-fired furnaces. Today it is primarily intended to ensure that the coal ash has characteristics that minimize slagging. However, applicability of the test results to reliably predict the behaviour of coal ashed in real combustion processes has been questioned [Reifenstein *et. al.*, 1999]. As a result of this, several alternative methods of characterizing coal ash behaviour have been developed [Reifenstein *et. al.*, 1999].

As already indicated, a number of bench-scale empirical indices for evaluating the slagging and fouling propensity of a coal have been derived [Carpenter, 2002]. [Skorupska and Carpenter, 1993] They are generally based on the chemical analysis or the physical tests on laboratory prepared ash. The advantages of using indices based on chemical composition [Carpenter, 2002] are as follows:

- Widely employed
- Analysis procedures are standardised
- Results are generally repeatable and reproducible
- Relatively inexpensive.

However, the level of confidence in these indices remains low. It frequently gives misleading results and reliability is often poor. The main concern reported by the International Energy Agency (IEA) [Carpenter, 2002] are the following:

- Derived from experience with a limited range of coal sources and unlikely to be applicable to other coal sources
- Based on the properties of laboratory prepared ash samples which are produced under oxidation conditions that are different from those occurring in pf-fired boilers
- Minerals that impart the properties to coal ash, not the oxides

- Reflect the average composition of the coal bed
- Provide misleading estimates where the assumption of linear relationships are questioned
- Calibrated in boilers under baseline conditions that may or may not be occurring in boilers today.

Given the shortcomings of the empirical indices, it seem likely that using better analytical data about the mineral matter in coal and with a better understanding of transformation mechanisms, the prospects for prediction will improve [Carpenter 2002].

X-ray diffractometry (XRD) is a long-established and definitive tool for mineral identification. It has been applied to the study of minerals in coal for many years, based mainly on residues isolated by low-temperature oxygen-plasma ashing and similar techniques [Ward and Taylor, 2001]. The full profile of an XRD pattern provides considerably more information for mineral quantification than the integrated intensities of particular diffractogram peaks. A Rietveld formula was developed to give the proportion of a single mineral at any point in the scan, with information on how to refine the relevant crystal structure and instrumental parameters. Ward and Taylor, 2001, Yan *et. al.*, 2002, Erickson *et. al.*, 1995 and Russell *et. al.*, 2002 have reported that XRD of raw coal samples, without an ashing process to concentrate the mineral matter, can also be used to evaluate the minerals in the coals. Comparisons are presented between the results of quantitative X-ray diffractometry using the Rietveld-based method on low-temperature ash and normative calculations from chemical analysis of high temperature ash for a series of coals [Ward and Taylor, 1996].

CCSEM provides more information about the mineral matter in coal than the current tests [Carpenter, 2002], although the other tests, for example AFT, and indices derived from ash composition analyses, will also be used in a supportive way. A mathematical model of ash formation during high-rank pulverised coal combustion has also been developed which is based on the CCSEM characterisation of minerals in pulverised coals [Yan *et. al.*, 2002]. Currently CCSEM is a widely used and applied method for determining the size, association, composition and abundance of minerals in coal [Galbreath *et. al.*, 1996] and the value of CCSEM for quantifying the mineral matter distribution in the coals has been demonstrated by Gibb [1996].

Studies have been undertaken to provide an insight into the effects of mineral matter

distributions in coal on the nature of slags formed during combustion [Russell *et. al.*, 2002]. An interesting finding was that it was reported that the medium density fraction which contained mostly included mineral matter, produced the densest vitreous slag in comparison with the cases where the mineral matter was excluded. It was further concluded that the coals with more excluded minerals produced a reduced slagging propensity [Russell *et. al.*, 2002].

Ash fusion temperature (AFT) is one property that specifically gives more information on the suitability of a coal source for combustion or gasification purposes albeit its shortcomings. Therefore the chemistry and mineral interactions have to be understood in order to determine the suitability for fixed bed gasification purposes with regards to ash fusion properties. Various authors [Seggiani, 1999 and Alpern, *et. al.*, 1984] have expressed the fusibility of coal ash as a function of the content of the principal oxides frequently found in coal ash, i.e. SiO_2 , Al_2O_3 , TiO_2 , Fe_2O_3 , CaO , MgO , Na_2O and K_2O . The acid/base ratio is the most frequently used parameter for correlating ash fusibility with its composition. However, coal ash fusibility characteristics are difficult to determine precisely, partly because coal ash contains many components with different chemical behaviours [Slegeir, *et. al.*, 1988] and may vary from coal source to coal source. As already mentioned and indicated, one property that specifically gives more information on the suitability of a coal source for gasification purposes is the AFT. Conventional AFT analyses (SABS/ISO methods) are currently used to predict slagging properties from mineral matter transformations of coal sources. Normal AFT analysis gives an average flow property but does not indicate exactly at what temperature the first melt/sinter occurs due to specific mineral matter transformations. Operating experience indicates that even when the gasifiers are operated at temperatures below the AFT, as given by an AFT analysis, a percentage of slag (clinker) is formed. Leaching and chemical speciation will also result in different mineral compositions with different AFT properties [Govender, A., 2005]

FactSage modelling provides the opportunity to calculate and manipulate phase diagrams, but has been established mainly in the field of complex chemical equilibrium and process simulation. For example, with FactSage it is possible to access both Fact (slag, matte, salt, ceramic and aqueous) and alloy databases, import and export streams and mixtures and also import ChemSage data files. Another advantage of FactSage is that it can also handle carbon reactions together with the minerals whilst varying the gas composition and atmosphere.

In the present a method is proposed to increase the AFT of a coal blend (decreasing the amount of slag propensity), which will then result in operating a fixed bed dry bottom gasifier at higher temperatures. The opportunity exists and it will be proven in this study, to increase the average AFT of the coal fed to the Sasol-Lurgi FBDB gasifiers by adding AFT increasing minerals or species to the coal blend before it is fed into the gasification process can be beneficial. By increasing the AFT, the direct effect will be that steam consumption can be decreased and in turn will improve carbon utilization. The aim is to add an ash fusion temperature increasing agent such as kaolinite ($\text{Al}_2\text{Si}_2\text{O}_5(\text{OH})_4$), alumina (Al_2O_3), silica (SiO_2) or titania (TiO_2) and to propose a method for increasing the ash fusion temperature of a coal blend (decreasing the amount of slag propensity), which will then result in operating a FBDB gasifier at higher temperatures. Based on shortcomings, the secondary aim of this study was also to understand the chemistry and interpret mineral matter transformation occurring during Sasol-Lurgi FBDB Gasification by means of high temperature X-ray diffraction (HT-XRD), in combination with FactSage modelling. Normal AFT analyses give an average flow property and do not indicate exactly at what temperature the first melt/slag occurs. Operating experience indicates that even when the gasifiers are operated at temperatures above the fusion temperature as given by AFT analysis, a low percentage of slag is formed. This could probably be an improved way to interpret flow properties of mineral matter in coal and assist in quantifying slag formation in gasifier operation at temperatures not reflected by AFT analyses.

CHAPTER 2

EXPERIMENTAL PROCEDURES, ANALYSIS AND STUDY METHODOLOGIES

1 INTRODUCTION

As already indicated and discussed in *Chapter 1*, the opportunity exists to increase the AFT of the coal feed to the Sasol-Lurgi FBDB gasifier to $>1350^{\circ}\text{C}$ (from the current $\pm 1300^{\circ}\text{C}$) by adding some additive to the coal blend. The standard approach for slagging gasifiers is normally to lower the AFT.

Preliminary indications where some advantages can be obtained at gasification and downstream units associated with gasification (Phenosolvan, Rectisol and sulphur units) which will specifically result from an increase in ash fusion temperature are the following:

- Less cut-backs in gasification and gasifier trips due to ash sintering and higher gas outlet temperatures
- Decrease in steam consumption during gasification
- Lower H_2/CO ratio, less CO_2 from gasification
- Lower gas liquor production, which could lead to easier tar separation and treatment and would result in lower gas liquor treatment costs
- Less CO_2 to Rectisol, reducing the load on Rectisol
- Less CO_2 in Rectisol off-gas, so that the H_2S concentration in the feed to the sulphur removal plant would be higher, resulting in more efficient sulphur removal and lower sulphur emissions.

Work done by an independent R&D institution [Microbeam Technologies, USA] on Sasol's coal blend as pre-work towards this study indicated that the ash composition (oxide elemental composition) has an acceptable fit to the ash melting prediction curve (Figure 2.1).

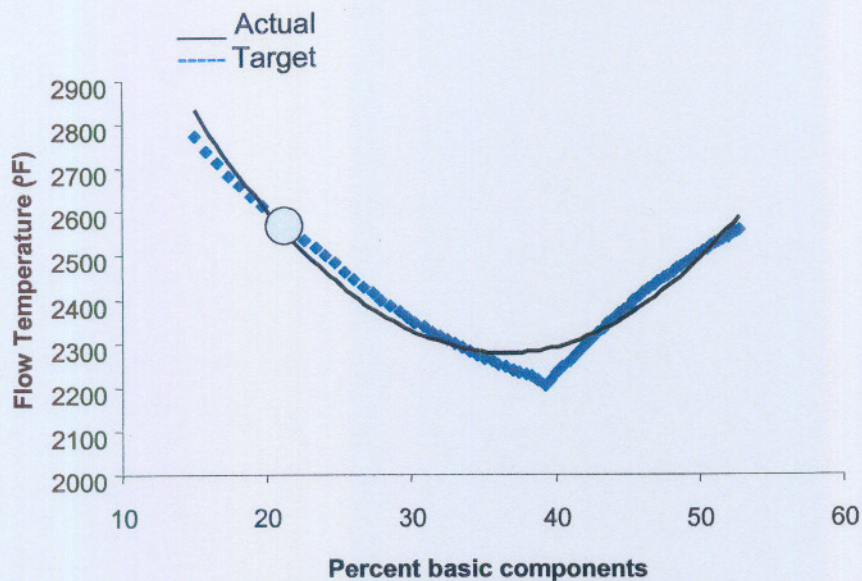


FIGURE 2.1 ASH MELTING TEMPERATURE PREDITION CURVE [MICROBEAM TECHNOLOGIES, 2003]

This trend, shown in Figure 2.1, was developed for northern hemisphere coal sources and was only used as a guideline for further work on Sasol's coal sources. However, from these results it is clear that the amount of basic components have to be decreased in order to have an increasing effect on the AFT. Basic components are defined as the sum of oxides Ca, Mg, Fe, K and Na as given by an ash composition analyses. Kaolinite, for example, is a common clay mineral with high concentrations of Si and Al that can react with other elements, i.e. sodium to form products that melt at significantly higher temperatures [Ross, *et. al.*, 2003]. A provisional patent by Van Dyk and Coertzen, Sasol Technology, has been filed on this idea and attached in Appendix A.

Based on this idea an in-depth study is needed in (1) determining if this principle of increasing ash melting temperatures can be applied on Sasol's coal sources and (2) understanding and explaining the mechanism of the chemistry taking place.

2 GENERAL COAL AND COAL ASH ANALYSIS

The coal samples used for this study represent a coal blend of 6 different coal sources as it is fed into the gasification process at Sasol. The blend consists of 6 different sources from coal mines in the Mpumalanga area in South Africa, which are properly blended on a stacker-reclaimer before it is fed to the gasification process. A detail discussion on the blend, preparation and feeding of the coal to gasification will not be given, as it will not be of relevance for this study.

It is also important to confirm if the most relevant characteristics of the coal used for

this study are representative of the coal used for gasification currently. This is in order to confirm that the bulk sample used for this study is relevant and a representation of the coal currently used for the gasification process. The following tests were conducted to confirm the representativeness in comparison with the base case data available.

All routine analysis, for example proximate, ultimate and other analysis, are outsourced to a respected coal routine test laboratory in South Africa who conduct analysis for most South-African coal mines and coal research institutions. Coal and Minerals Technology (CMT) is the laboratory that Sasol uses for this type of analysis [Visser, 2004].

Sample preparation was done by CMT according to method *SABS 0135 Part II*. The following standard analyses were conducted on the coal sample:

- Proximate analysis (*SABS 924, ISO 1171 and ISO 562*)
 - Ash (*SABS 924 and ISO 1171*)
 - Moisture (*SABS 924 and ISO 1171*)
 - Volatiles (*ISO 562*)
 - Fixed carbon (by difference)
- Ultimate analysis
 - Total sulphur (*ASTM D4239*)
 - Carbon, hydrogen and nitrogen (*ASTM D5373*)
- Ash fusion temperature (*ASTM D1857*)
- Ash constituent analysis (*ASTM D3682*)
- Calorific value (*ISO 1928*)
- Maceral analysis and rank (*ISO Standard 7404 – 2 - 1985, ISO Standard 7404 - 3, 1994, Steyn & Smith for South African coals*)

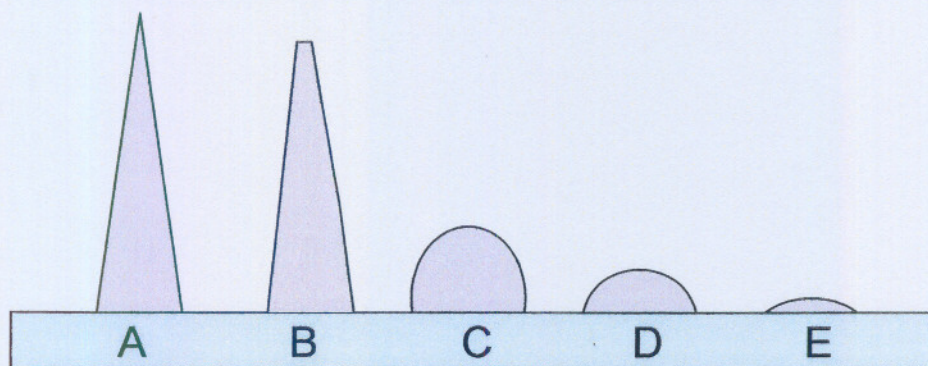
The procedures used by CMT for characterizing purposes are given in brackets.

As these analyses are not used as a decision making tool, but as an overall direction given indicator, they will not be discussed in more detail. Characteristics of the sample used in this study, as well as the variation and average characteristics of the coal sources used during previous base case tests will be compared.

3 COAL ASH AND ASH CHARACTERISATION TECHNIQUES CONDUCTED AND UTILIZED IN THIS STUDY

3.1 Ash fusion temperature (AFT)

In AFT analyses the softening and flow (melting or slagging) behaviour of ash as it is heated through the temperature ranges to a specified temperature are measured [Carpenter, 2002], which in this study is 1600°C under oxidising conditions. A cone of ash is prepared by the standard ashing procedure as used for a proximate analysis and then heated at a controlled rate in an oxidising atmosphere to simulate the gasification environment in the ash bed [Carpenter, 2002]. The four temperatures at which the melting process proceeds are illustrated in Figure 2.2:



- (A) Original cone before heating
- (B) Initial deformation temperature where first rounding of cone tip is taking place (IDT)
- (C) Softening or sphere temperature where the cone height = cone width (ST)
- (D) Hemispherical temperature where cone height = $\frac{1}{2}$ cone width (HT)
- (E) Fluid or flow temperature where cone height = 1.6mm (FT)

FIGURE 2.2 CHANGES OF CONE SHAPE DURING ASH FLOW TRANSFORMATION [CARPENTER, 2002 AND SLEGEIR, ET. AL., 1988] (ASTM D1857)

Although AFT tests are widely employed, they do not always predict the AFT behaviour accurately. Two ashes which have similar fusion characteristics can have significant different melting behaviours [Carpenter, 2002]. Advantages of the AFT test include:

- Widely employed
- Standardised
- Inexpensive
- Capable of automation

Concerns against the standard AFT test are the following [Carpenter, 2002]:

- Subjective - based on observations rather than measurements
- Poor reproducibility. The correlations and approach described by Slegeir,

et.al. [1988] routinely provide results that are comparable to the ASTM reproducibility limits, but that mean deviations for the average and expert systems of about 100°F (38°C) are attainable.

- The IDT is not the temperature at which melting begins.
- AFT's are measured over short periods, whereas deposits typically accumulated for hours are formed during cooling

3.2 Ash composition

The compositional determination of the mineral matter was done by analysing the chemical composition of the coal ash. These analyses are commonly based on atomic absorption spectroscopy inductively coupled plasma-atomic emission spectroscopy or X-ray techniques [Carpenter, 2002 and ASTM D3682, 2002].

Methods such as the atomic absorption spectroscopy technique require the sample to be in solution. Before dissolution, the coal samples are usually ashed. Ashing enriches the element abundances and the composition of ash tends to be more homogeneous than that of coal [Carpenter, 2002]. The basis of atomic absorption spectroscopy is the reaction of a plasma containing free (dissociated) atoms of the element to be determined. Atoms in the ground state can absorb radiation at discrete wave-lengths to create atoms in an excited state. A beam of light at the desired wave-length is passed through the plasma. The amount of energy absorbed is directly proportional to the number of atoms present [Carpenter, 2002].

As this is done as standard analysis in routine laboratories, it will not be discussed in further detail. The ash composition analyses were done by Coal and Mineral Technologies (CMT) [Visser, 2004].

3.3 Scanning electron microscopy

As computer controlled scanning electron microscopy (CCSEM) analysis is a highly specialised technique that requires expensive instrumentation and detailed understanding, which was acquired during the experimental phase of this study, the analysis was out-sourced and conducted by Van Alphen [2004].

A typical set-up of a CCSEM is given in Figure 2.3 [Skorupska and Carpenter, 1993].

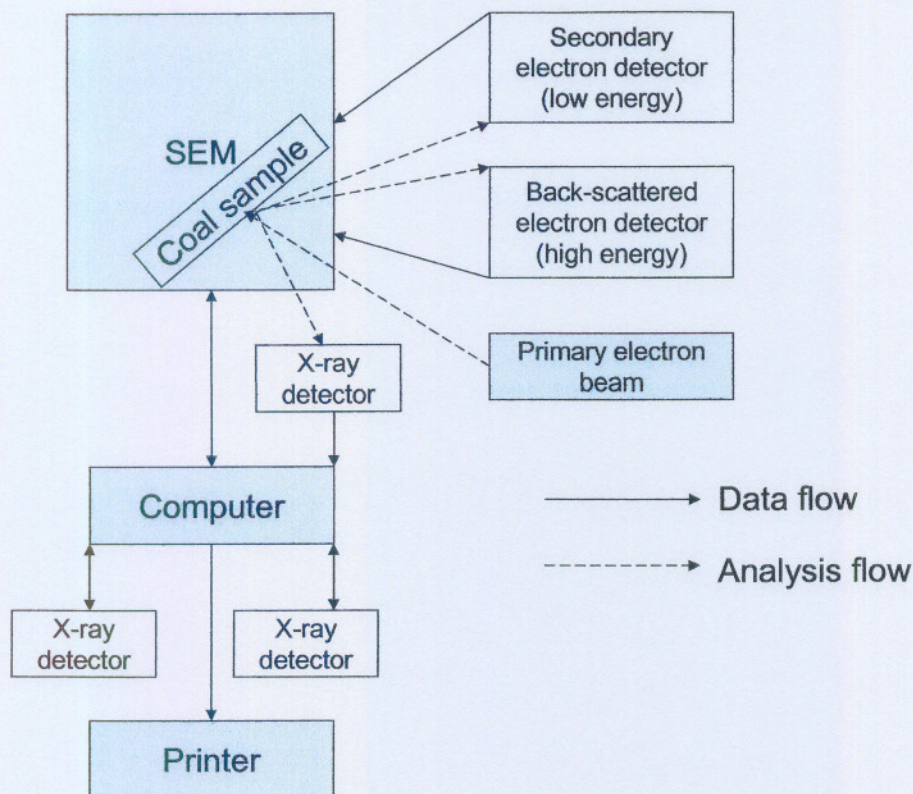


FIGURE 2.3 TYPICAL CCSEM SET-UP

CCSEM has been found to be a powerful technique for quantitative analysis, but has limitations [Carpenter, 2002], such as complex data interpretation, one compound can only be assigned to one class, it cannot detect inorganic constituents in grains $<1\mu\text{m}$ and small samples. The main concern of the exercise with the bias that may originate from using different of equipment, software and operating conditions. It was, however, found that [Skorupska and Carpenter, 1993]:

- the reproduceability was better than 0.2 relative standard deviation;
- the type of minerals had no effect on reproduceability;
- errors arising from counting statistics were the major source of bias;
- reproducibility needed improvement for clay mineral groups;

Advantages of the CCSEM technique include characteristics such as reproduceability, and automization, as well that it can also be carried out directly on coal [Carpenter, 2002]. It is believed that the CCSEM technique is a significant advance on the more conventional methods of coal mineral analysis, such as SEM and EMPA described by ASTM and other standards [Skorupska and Carpenter, 1993].

3.4 Morphology analysis

Morphological analysis is used to determine the microstructural features in coal, ash and slag samples. Representative portions of the sample are placed in rubber molds and covered with epoxy resin. Each sample is polished to 1-micron grit and coated with carbon. The carbon coating was used to provide a conductive surface on the sample for improved SEM imaging. Morphological analysis consists of obtaining images and chemical analysis of selected features of ash or deposit samples. Backscattered scanning electron micrographs, which show compositional differences based on atomic number, are taken of selected regions. Energy-dispersive x-ray analysis is performed on points and areas within the regions [Microbeam, 2003].

Scanning electron microscopy point count (SEMPC) is used to determine the abundance of phases in the ash and slag. The chemical compositions of the points are matched to known phases and the abundance of each phase is then determined quantitatively. Based on these results, the abundance of liquid phases is determined. The chemical composition of the liquid phases in the deposit is used to calculate the viscosity distribution as a function of temperature. This information can be used to determine the temperature and atmospheres present when the deposit formed [Microbeam, 2003].

4 EFFECT OF SILICA, ALUMINA AND TITANIA AS PURE COMPOUNDS ON ASH FUSION TEMPERATURE

With the specific aim of this study to increase the AFT, and from literature results presented in **Chapter 1**, experimental AFT determination on blends are necessary for this study to evaluate and determine the experimental effect of silica (SiO_2), alumina (Al_2O_3) and titania (TiO_2) as individual pure compounds on the AFT before the mechanistic path can be addressed and studied.

Blends with the SCS coal sample and pure compounds SiO_2 , Al_2O_3 and TiO_2 were prepared with additions of pure compounds from 0 mass % to 10 mass %. The AFT of the different blends were then determined and results statistically evaluated.

The purpose of this part of the investigation, to determine the effect of SiO_2 , Al_2O_3 and TiO_2 on the AFT, was to evaluate the impact of the additions on dense medium separation (destoning) and leaching on coal properties such as ash composition and ash fusion properties. The results were then statistically evaluated.

4.1 Dense medium separation of coal

Since the fixed bed gasifier technology which Sasol uses requires a coarse coal, the coal for gasification purposes cannot be ground to fully liberate or remove unwanted constituents as stated in **Section 4.2, Chapter 1**. The question then remains as to what extent the AFT can be manipulated with dense medium separation of the original coal source, and what the impact of washing on AFT and ash composition will be. The original experimental procedure for this work was developed by Baxter [2003] and used in the present study.

Dense medium separation was thus investigated to evaluate the impact of destoning at different relative densities on coal properties such as the ash composition and AFT as another way (above destoning and leaching) to change the overall composition in order to obtain insight to the effect of the oxides Si, Al and Ti on the AFT. A typical Secunda ROM coal blend (SCS) was used and coal washing was performed according to the ISO 7936 standard, which uses a -25mm+0.5mm size fraction prepared by crushing and screening steps. The samples were washed at relative densities from 1.4 to 2.1 with increments of 0.1 (ISO 7936).

Dense medium separation was conducted by CMT as already referred to.

4.2 Chemical fractionation of coal

Baxter [2003] proposed that the combination of standardized analyses and chemical fractionation tests represents a necessary and sufficient analysis of coals for predicting inorganic behavior [Baxter, 2003 and Van Dyk, *et. al.*, 2005]. Baxter [2003] then further presented the technique for determining mineral species-specific descriptions of all the inorganic material in coal. This technique was originally developed by *Miller and Given* [Baxter, 2003 and Van Dyk, *et. al.*, 2005] and uses selective extraction of elements, based on solubility, which reflects their association in the fuel.

Three coal samples were selected for the study, namely

- (1) SCS blend which consisted of 6 different coal samples,
- (2) an individual coal source with a high caking propensity, and
- (3) an individual coal source with a medium caking propensity.

The experimental procedure was conducted on each sample. Representative samples from the different feed streams were sampled as a belt cut on the 3 streams. The 3 streams contained material with a particle size distribution ranging from 0 to 100mm. The three samples were then individually prepared to a representative, workable mass sample of particle size <1mm (*SABS 0135 Part II*).

As part of the preparation the sample was crushed to <150µm in order to be completely permeated by the leaching agents (water, ammonium acetate, hydrochloric acid and nitric acid). Each sample was then homogenized by the coning-and-quartering technique before representative sub-samples were taken from the original sample.

The experimental procedure for the leaching process consisted of three successive extractions. The first was by water only and was intended to remove water-soluble elements such as sodium. The second extraction process used ammonium acetate to remove elements such as sodium, calcium and magnesium that are ion exchangeable. In the third extraction process acid (HCl or HNO₃) was used to remove acid soluble species such as alkaline earth sulfates, carbonates, etc. The residual material typically consisted of silicates, oxides and sulfides. The experimental procedure for each leaching process was used in the chemical fractionation procedure and was divided into 4 steps i.e. sample preparation, analysis of the unleached materials, analysis of the sample after each of the three leaching steps; and characterization of the inorganics in the solid samples from each of the four stages of the procedure [Baxter, 2003].

One 20g sample was used for leaching. The weights of the total sample before and after water washing were noted. From this information and the initial dry weight of the sample (taking into account the total moisture of the sample), the change in the dry weight induced by washing can be calculated. The leaching process for each leaching agent was as follows:

- 3 ml of leaching agent per gram of coal was added
- Mixture was stirred for 24 hours at room temperature
- After mixing it was filtered and rinsed with 100ml distilled H₂O
- Total weight of sample was determined

All coal samples and leachates were then submitted for chemical analysis i.e. ash composition and inorganic elemental analysis.

5 HIGH TEMPERATURE X-RAY DIFFRACTION (HT-XRD) ANALYSES - FORMULATING A MECHANISM FOR MANIPULATED COAL FEED AND HIGHER ASH FLOW TEMPERATURE

The HT-XRD analyses were conducted by Corus R&D, The Netherlands [Melzer, 2004], as well as Sasol Technology R&D [Sobiecki, 2004].

The HT-XRD technique is a new advanced analytical technique for characterising mineral matter transformations in coal and the investigation into this technique started with Corus R&D. Corus R&D assisted in standardising and setting up the technique at Sasol Technology R&D, and this is the reason why two analytical laboratories were used for characterisation purposes. The base sample was first analysed by Corus R&D where-after the results also served as a bench-mark for further work and development at Sasol Technology. A similar base case coal sample was submitted to Corus and Sasol Technology. The pre-preparation of the samples differ slightly between the two laboratories due to set-up and product analysis done on the equipment. The main difference is that Corus started with the original coal sample, where as Sasol Technology started with a sample ashed to 500°C. The product spectra from 500°C onwards as needed and studied in this thesis are the important transition areas which will be compared and evaluated. Results on the base sample from both laboratories will be compared for reference purposes.

In summary the sample preparation and HT-XRD analyses were conducted as follows: Firstly a representative sample with particle size distribution of -1mm of the SCS coal blend was ashed at 500°C in a normal furnace under ambient conditions for a period of 12 hours. The sample was then submitted for HT-XRD and finely milled to -10µm with a McCrone micronising mill. The high temperature transformations of the SCS coal sample, as well as the manipulated SCS coal samples, were investigated under a nitrogen (N₂) atmosphere from 500°C to 1400°C in 100°C intervals. A XPert PRO X-ray diffraction system equipped with a HTK2000 Anton Paar high temperature camera and the X'Celerator detector was used. The pre-ashed sample was directly scanned on a platinum strip.

A summary of the experimental parameters used during the HT-XRD analysis were as follows [Sobiecki, 2004]:

Goniometer:	PW3050/60 (θ / θ configuration)
X-ray detector:	X'Celerator (Solid State, RTMS)
X-ray tube:	Cobalt target, ceramic, LFF-type; $\lambda_{Co K\alpha} = 1.7889 \text{ \AA}$
HT Camera:	HTK2000 (Anton Paar)
Heating strip:	Platinum (1mm thick)
Heating range:	500 – 1400 °C (scanning every 100 °C)

Ramp rate:	10 °C min ⁻¹
Cooling medium:	water pumped at the constant 25 °C
Duration of <i>in situ</i> scans:	10 x 1hr30min
Scanning:	Continuous
Carrier gas:	Nitrogen (99.9999%)
Gas flow:	50 ml min ⁻¹
Voltage:	40 kV
Amperage:	40 mA
Prog. Divergence Slit:	1.0°
Anti-scatter Slit:	2.0°
Scan from:	5° 2θ
Scan to:	140° 2θ
Soller slits:	0.04°

All the scans at the different temperatures were evaluated and the net peak areas of intensity calculated in order to determine the concentration levels.

6 TOOLS USED FOR QUANTIFYING EXPERIMENTAL RESULTS AND MECHANISM FOR INCREASING ASH FUSION TEMPERATURE

Viscosity and sintering are two of the properties available for predicting slagging behaviour of coal sources already published and studied in the past. This study will also include FactSage as modelling software package for the development of a model to predict the mineral- and slagging behaviour of specific mineral phases during gasification.

6.1 FACTSAGE modelling



GTT Technologies are the developers and databases administrators of thermodynamic software and packages, such as FactSage. FactSage is the fusion of two well-known software packages in the computational thermochemistry – Fact-Win and ChemSage. The Fact development started in the late 70's and is today the biggest thermochemical package and database available. FactSage is not only in a position to calculate and manipulate phase diagrams, but has been established mainly in the field of complex chemical equilibrium and process simulation. Another advantage of FactSage is that it can also take carbon reactions with the minerals into account and that the gas composition and atmosphere can be varied.

The specific value to Sasol in this study will be that these thermochemistry models can be used to analyse equilibrium conditions for reactions occurring between

inorganic and/or organic materials, as well as the mineral formation and slag formation. The database will assist in understanding, as well as predicting, what can and will happen with specific coal and mineral sources inside the gasification process. For example, the areas in which thermochemistry are used today:

- In industry to help understand and improve extraction and manufacturing processes.
- In basic R&D to confirm experimental work by doing the needed work and reduce the amount of experimental work.
- To improve energy efficiency.
- To optimise yields.

FactSage package runs on a PC operating system under Microsoft Windows® and consists of a series of information, database, calculation and manipulation modules that enable one to access and manipulate pure substances and solution databases. FACTSAGE is a 32-bit application written with a blend of Visual-Basic (45%), Delphi (20%), C++ (10%) and Fortran-90 (25%). Information can be obtained at www.factsage.com. With the various modules one can perform a wide variety of thermochemical calculations and generate tables, graphs and figures. FACT is the facility for the analysis of chemical thermodynamics and started in 1976. FACTSAGE 5.2 was used for modelling work in this study. The FACT solution database contains critically evaluated thermodynamic data for the system containing SiO₂, CaO, Al₂O₃, etc [Bale, *et. al.*, 2002].

The most used modules for this study were the Equilib and Phase Diagram modules. The following is a short description of the two modules as published by Bale, *et. al.* [2002]:

- The Equilib module is the Gibbs energy minimization workhorse of FACTSAGE. It calculates the concentrations of mineralogical coal species (phases) when specific elements or compounds react or partially react to reach a state of chemical equilibrium. A detail description in step-by-step format will be given in the results (Chapter 5 section 4).
- The Phase Diagram module is a generalized module that permits one to calculate, plot and edit unary, binary, ternary and multi component phase diagram sections where the axes can be various combinations of T, P, V composition, activity chemical potential, etc. The resulting phase diagram is automatically plotted by the Figure module.

Various authors, and a study by the University of Queensland [Jak and Hayes, 2005]

focussed on the relationship between ash fusion temperature and FACT liquidus calculations. It has been demonstrated that the application of FACT computer software and database for the prediction of ash fusion temperature, as well as for blending strategies is successful [Jak and Hayes, 2005].

A new model simulating the gasification process was developed during this PhD study using the FactSage thermochemical software package.

6.2 Viscosity modelling

From a major UK collaborative research program [Gibb, 1996] to address all aspects of slagging it was found that the key to the behaviour of ash deposits lies in understanding the consolidation by a viscous flow mechanism and the effect of the main fluxing agents on viscosity. Ash slagging behaviour of a blended coal is a non-additive property of the pure coals and hence difficult to predict. This explains why viscosity modelling of the total ash blend is an important tool in describing the ash properties and slagging tendency at specific temperatures.

The tendency of coal ash to slag is related to its bulk mineralogy and the AFT. AFT is a result of slagging and melting. Practice has shown that the behaviour of blends does not always comply with the expected weighted average value of parameters from the pure coals comprising the blend [Goni, *et. al.*, 2003]. Interaction between the coals has to be suspected as the main reason behind the observed deviations with agglomeration of solids or ash slagging, this is considered one such characteristic. Experimental evidence shows that the slag performance of blended coals can be worse or better than the performance of the individual coals [Goni, *et. al.*, 2003], which is the reason why viscosity modelling also has to be investigated.

The model used in this study to determine viscosities is that of Kalmanovitch or the so-called "modified Urbain model" [Kalmanovitch and Frank, 1988]. The model is based on the following calculations:

Step 1: Determine the mole fraction of all components based on the chemical oxide composition. Fe_2O_3 is converted to equivalent FeO.

Step 2: Calculate M where
 $M = CaO + MgO + Na_2O + K_2O + FeO + 2TiO_2$ *mole fractions*

Step 3: Calculate alpha where

$$\text{Alpha} = M / (M + \text{Al}_2\text{O}_3) \text{ mole fractions}$$

Step 4: Calculate B where

$$B = BO + (B1 \cdot \text{SiO}_2) + (B2 \cdot (\text{SiO}_2)^2) + (B3 \cdot (\text{SiO}_2)^3)$$

$$BO = 13.8 + 39.9355 \cdot \text{alpha} - 44.049 \cdot (\text{alpha})^2$$

$$B1 = 30.481 - 117.1505 \cdot \text{alpha} + 129.9978 \cdot (\text{alpha})^2$$

$$B2 = -40.9429 + 234.0486 \cdot \text{alpha} - 300.04 \cdot (\text{alpha})^2$$

$$B3 = 60.7619 - 153.9276 \cdot \text{alpha} + 211.1616 \cdot (\text{alpha})^2$$

Step 5: $\ln[A] = -(0.2812 \cdot B + 11.8279)$

Step 6: Calculate the natural log of the viscosity at a given temperature T in degrees K

$$\ln[\text{viscosity}] = \ln[A] + \ln[T] + (1000 \cdot B/T)$$

One conclusion from the model was that the modified Urbain model can predict both viscosities of bulk coal ash melts as well as simple oxide glasses, with specific emphasis on CaO-MgO-Al₂O₃-SiO₂ systems. Furthermore SEMPC together with viscosity modelling is the preferred way to study ash-related materials [Kalmanovitch and Frank, 1988 and Laumb, *et. al.*]. The real advantage of SEMPC is that it does not rely on the bulk composition, but is capable of determining the chemical composition and relative amount of phases actually responsible for the ash behaviour [Kalmanovitch and Frank, 1988]. It has also been published that the Kalmanovitch models work the best for coals high in SiO₂ and lower in Fe, [Laumb, *et. al.*, 2004] which is appropriate for the coal sources used in this study.

CHAPTER 3

RESULTS AND DISCUSSION

1 INTRODUCTION

As already indicated, the coal samples used for this study represents the coal blend as it is fed into the gasification process at Sasol. This blend consists of 6 different sources from coal mines in the Mpumalange area in South Africa, which are properly blended on a stacker-reclaimer before it is fed to the gasification process.

As discussed and mentioned in *Chapter 1* and *2*, the objectives of this study were to increase the AFT of the coal blend and to understand the mechanism involve with the changes during the gasification process. However, in order to fully understand how coal properties and specifically how mineral properties influence the AFT, it is necessary to have a detail understanding of the coal source that is used, as well as what pre-work has been conducted as direction indicators for this study. Some pre-work, as it will be discussed in this chapter, will give insight and alignment to the mechanistic and modelling that will follow and how to approach the problem in formulating a mechanism for AFT manipulation.

2 GENERAL COAL AND COAL ASH CHARACTERISTICS

It is firstly necessary to confirm if the general characteristics of the coal used for this study are comparable with the characteristics of the coal used for gasification.

2.1 Proximate analyses

From the proximate analysis (Table 3.1) the moisture, fixed carbon, volatiles and ash content are given. The fixed carbon content is normally calculated by difference. The ash content gives an indication of the amount of inorganic material in the coal from a source and includes mineral matter in-situ in the coal structure, as well as out-of-seam inorganic contamination. The ash yield is commonly used as an indicator of the quality of a coal as it provides an indication of the amount of incombustible or non-gasifiable coal material. The ash also has a significant impact on the performance of gasifier and combustion plants [Carpenter, 2002]. In the standard tests the ash content is the mass of the residue remaining after ashing. The measurement of the ash content is used by Sasol Mining and other similar industries

as an operating tool to prepare blends with an ash content within the agreed limits and with a relatively small variation in ash content over time.

TABLE 3.1 PROXIMATE ANALYSIS (AIR DRIED BASIS)

COMPOSITION	Result of coal sample used in this study (mass %)	Coal characteristic as used during previous base case tests (1998-2003)	
		Average (mass %)	Variation (minimum and maximum) (mass %)
Moisture	5.0	4.3	2.7-5.5
Fixed Carbon	46.3	46.5	39.3-51.6
Volatiles	22.9	22.7	17.0-28.6
Ash	25.8	26.5	22.2-31.6

The important variable, ash content, of the sample used in this study (25.8%) is almost the same as the average of that of the coal used for gasification the past 5 years. It can be seen that the values of the moisture content and volatile matter of the sample used in this study also fall in the data range of the previous base case tests.

2.2 *Ultimate analysis and calorific value*

An ultimate analysis gives the total amount of the principal chemical elements present in coal, namely carbon (C), hydrogen (H), nitrogen (N) and oxygen(O), calculated by difference (Table 3.2).

TABLE 3.2 ULTIMATE ANALYSIS (DRY ASH FREE BASIS)

ELEMENT	Result of coal sample used in this study (mass %)	Coal characteristic as used during previous base case tests (1998-2003)	
		Average (mass %)	Variation (minimum and maximum) (mass %)
Carbon	78.8	78.8	75.0-82.9
Hydrogen	4.1	3.7	2.2-4.2
Nitrogen	2.1	1.7	0.9-2.0
Sulphur	2.0	1.5	1.0-2.0
Heating value (MJ/kg)	20.8	21.1	19.5-22.6

The heating value, or also called the calorific value or specific energy, is according to Carpenter [2002], the single most important parameter in the evaluation of coals for combustion or other applications. It is also used as benchmark of coal quality and its economic value. Table 3.2 indicates that the elemental analysis and heating value of the coal under investigation are comparable with the coal currently used for gasification.

2.3 Maceral analysis and rank

In the procedure for maceral analysis the group types under a reflecting light microscope using an oil immersion technique are identified. The macerals are distinguished by their relative reflectance, colour, size and morphology and the proportions are determined by a point count procedure. The volume percent of vitrinite, liptinite and inertinite is recorded where the sum of the macerals is 100% [Carpenter, 2002]. The standard procedure for determining the rank (reflectance of vitrinite) measures the amount of reflected light from a specific area of well-polished vitrinite under oil immersion using a photomultiplier or similar device. This is compared with light reflected under identical conditions from a number of standards of known reflectance. The measurement is carried out in monochromatic light. The mean maximum or mean random vitrinite reflectance, as a percent (%), is reported [Carpenter, 2002].

The maceral analyses and rank determination were done by VM du Cann from CMT, South Africa [Du Cann, 2004] and given in Table 3.3 and Figure 3.1. A petrographic block of the sample was prepared in accordance with the *ISO Standard 7404 - 2, 1985* and then examined under the microscope. A maceral analysis to determine the petrographic composition of the coal was carried out. The group maceral analysis was carried out in accordance with the *ISO Standard 7404 - 3, 1994*.

TABLE 3.3 MACERAL ANALYSIS AND RANK

MACERALS	Results of coal sample used in this study (mass %)	Coal characteristic as used during previous base case tests (1998-2003)	
		Average (mass %)	Variation (minimum and maximum) (mass %)
Vitrinite	20.0	19.7	16.0-23.0
Exinite	3.0	3.7	3.0-5.0
Total inertinites	60.0	59.8	54.0-67.0
Visible minerals	17.0	16.8	15.0-19.0
Rank (RoV)	0.68	0.6	0.6-0.7

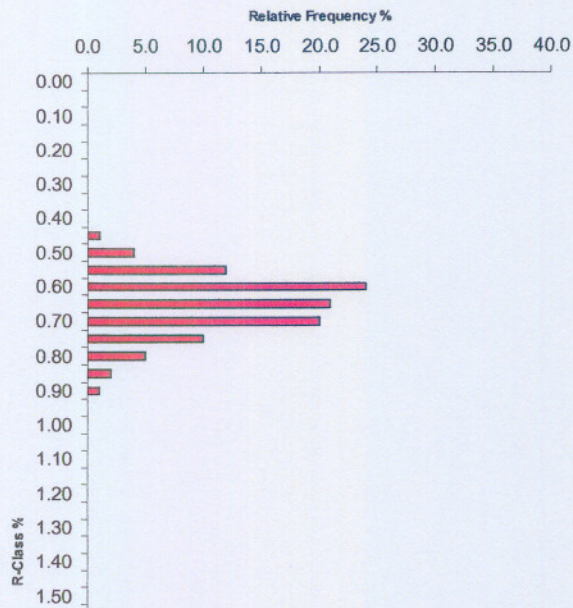


FIGURE 3.1 HISTOGRAM OF THE RANK OF THE COAL INVESTIGATED

According to the standard coal properties, i.e. ash content, volatile content, carbon content and maceral composition, it can be concluded that the coal sample used for this was representative and comparable with the coal currently used for gasification purposes.

3 OTHER COAL AND COAL ASH CHARACTERISTICS

3.1 Ash fusion temperature (AFT)

The results on the AFT will be highlighted throughout the thesis as this forms a crucial part of the understanding of the results and the AFT. These temperatures can be measured under either oxidizing or reducing conditions (or both), with the difference between the oxidizing and reducing results often correlating strongly with fluxing agents such as iron. The analyses were also carried out under oxidizing conditions as the gasifier is running with steam and oxygen as agent.

From experience, the ideal gasifier operation condition is to operate at a temperature above the initial deformation temperature in order to obtain enough agglomeration to improve bed permeability, but to operate below the AFT (flow temperature) to prevent excessive clinking. Secunda and Sasolburg coal sources currently used for gasification have an AFT of 1340°C (Table 3.4).

TABLE 3.4 AFT (OXIDISING CONDITIONS)

TEMPERATURE STAGE	Temperature (°C) of coal used in this study	Coal characteristic as used during previous base case tests (1998-2003)	
		Average (°C)	Variation of base case coal sample (minimum and maximum) (°C)
IDT	1300	1290	1230-1390
ST	1320	1300	1240-1420
HT	1330	1320	1200-1440
FT	1340	1340	1270-1470

Taken into account that the AFT analyses has an experimental error of $\pm 30^{\circ}\text{C}$ (ISO 540, 1995E), it can be concluded that the coal used in this study has for all practical reasons a similar AFT compared to the coal used for gasification purposes.

3.2 Ash composition

The ash composition (Table 3.5), specifically the Ca and Fe content in the coal, is believed to give a fair indication of the expected ash fusion behavior. A Ca and/or Fe rich coal source normally has a low AFT due to the fluxing properties of the Ca and Fe minerals, forming low ash melting temperature minerals.

TABLE 3.5 ASH COMPOSITION ANALYSIS (MASS %) OF THE SOUTH AFRICAN COAL BLEND

ELEMENT	Result of coal sample used in this study (mass %)	Coal characteristic as used during previous base case tests (1998-2003)	
		Average (mass %)	Variation (minimum and maximum) (mass %)
SiO ₂	50.1	48.7	40.0-51.9
Al ₂ O ₃	23.3	24.1	20.9-30.2
Fe ₂ O ₃	6.4	4.8	2.5-9.3
P ₂ O ₅	0.7	0.7	0.5-2.2
TiO ₂	1.0	1.4	1.0-1.6
CaO	8.1	7.9	6.1-11.6
MgO	2.7	2.5	1.9-3.2
K ₂ O	0.8	1.0	0.6-4.1
Na ₂ O	0.4	0.7	0.2-0.9
SO ₃	6.1	7.3	5.3-9.5

The ash composition analysis indicated that the coal used in this study is within the variation of the coal used for gasification purposes. A Ca and/or Fe rich coal source normally has a low ash fusion temperature due to the fluxing properties of the Ca and Fe minerals. Although the standard AFT analysis is currently used as prediction tool for AFT of coal ash, literature studies [Alpern *et. al.*, 1984] have shown that this may not represent the actual flow temperature of certain minerals and mineral phases. For example high iron (Fe) concentrations can lead to slagging properties at temperatures as low as 700°C and then the phase can solidify again. Visual investigation of actual ash produced from a fixed bed gasifier showed that the coarse and fine ash is sometimes extracted from the gasifier with the important middle fraction being absent. This can possibly be explained by the fact that some minerals already slag and clinker

at low temperatures and for this reason it is important to also have a detail finger print of the ash composition of a coal source.

3.3 Computer-controlled scanning electron microscopy (CCSEM)

A detail summary of the mineral proportions as analyzed by CCSEM and reported by Van Alphen [2004], is given in Table 3.6. The mineral proportions as given in Table 3.6 will be used as composition for the ash content.

TABLE 3.6 MINERAL COMPOSITION MASS % [VAN ALPHEN, 2004]

Mineral	Formula	Mass %	Mass flow (kg/hr)
Pyrite	FeS ₂	4.0	526
Quartz	SiO ₂	20.0	2631
Microline	KAlSi ₃ O ₈	1.9	250
Muscovite / Illite	KAl ₃ Si ₃ O ₁₀ (OH) ₂	2.9	381
Kaolinite	Al ₂ O ₃ .2SiO ₂ .2H ₂ O	52.5	6913
Anatase (rutile)	TiO ₂	0.3	39
Ankerite	Ca(Mg, Fe, Mn)(CO ₃) ₂	0.0	-
Siderite	Fe(CO ₃)	0.0	-
Calcite	CaCO ₃	6.7	881
Dolomite	CaMg(CO ₃) ₂	10.1	1328
Apatite	Ca ₅ (PO ₄) ₃ (F, OH)	0.5	65
Gypsum	CaSO ₄ .2H ₂ O	1.1	144
TOTAL		100	13158

According to the CCSEM analysis, the main minerals consist of kaolinite clay, quartz, pyrite, calcite and dolomite.

3.4 Morphology analysis

The physical and chemical morphology analysis of the coal were performed on a prepared sample of the original coal to -250µm, with a similar set of analysis also performed on a sample of the original coal prepared (screened) to -1mm and -20mm respectively. The average chemical composition as given of the different prepared size fractions in Table 3.7 were calculated from the chemical composition of 12 individual point counts.

TABLE 3.7 AVERAGE ELEMENTAL COMPOSITION OF COAL (MASS %) OF SPECIFIC PREPARED PARTICLE SIZE FRACTIONS

Prepared coal fraction	Na	Mg	Al	Si	P	S	Cl	K	Ca	Ti	Fe	Ba	O
-250µm	0.5	4.8	9.3	15.1	0.7	0.0	0.0	0.3	29.5	0.0	0.8	1.7	37.3
-1mm	0.8	4.1	9.8	19.2	0	4.8	0	0.5	9.4	6.4	0.4	3.8	40.6
-20mm	1.3	1.8	19.2	21.7	0.0	0.0	0.1	0.1	30.6	0.0	0.6	1.7	23.0

From the elemental composition of the -250 μ m prepared coal fraction (Table 3.7) the following conclusions and remarks can be drawn:

- The types of mineral particles within the coal ranges from large irregular minerals to small irregular minerals or small minerals on the edge of coal particles (Figure 3.2).

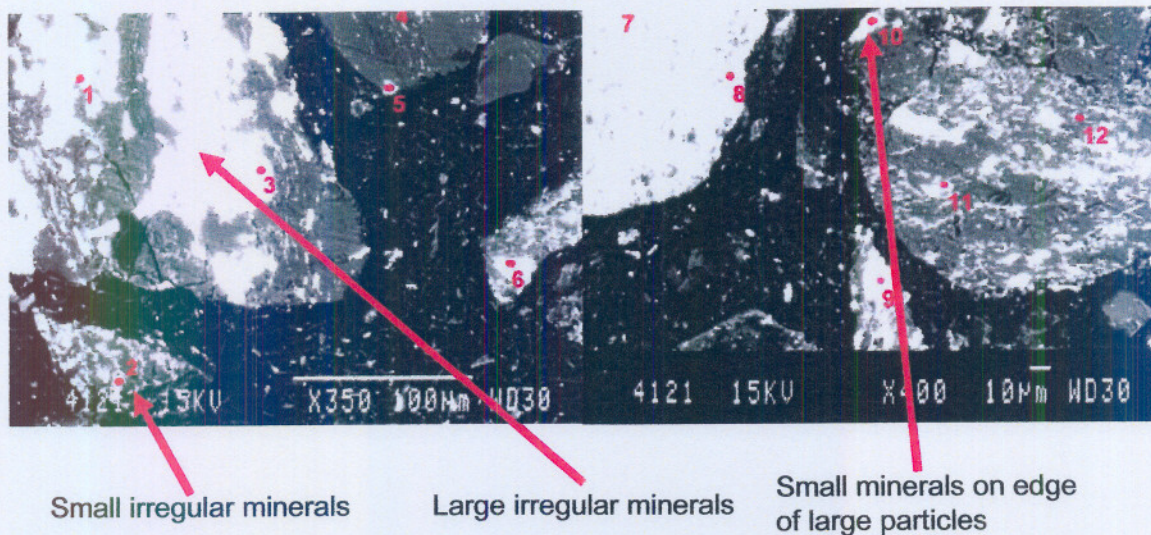


FIGURE 3.2 MINERAL VARIATIONS IN COAL STRUCTURE (IMAGE TAKEN BY M LAUMB, MTI)

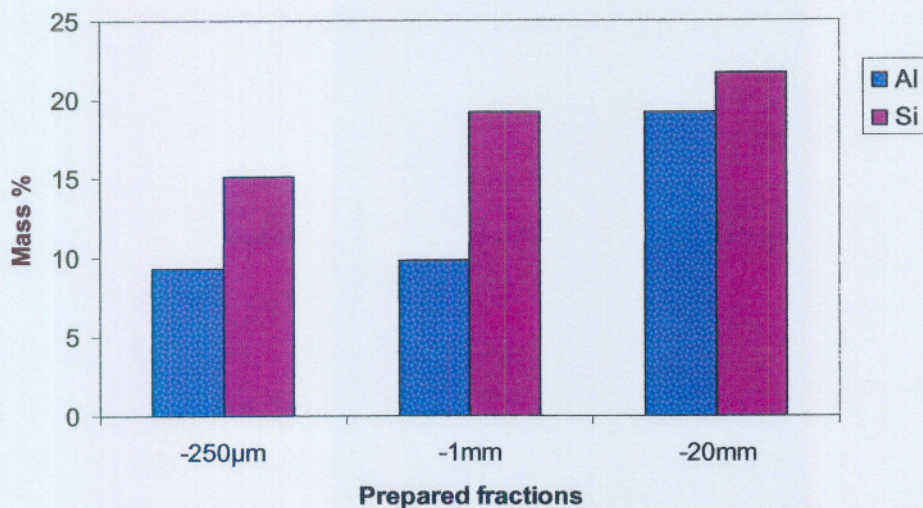


FIGURE 3.3 INCREASING MASS % IN SI AND AL ABUNDANCE IN DIFFERENT SIZE FRACTIONS

An abundance of calcium-rich particles were observed which are a combination of calcite and dolomite. These minerals are observed throughout the coal structure and not specifically to one type of mineral grain or structure (Table 3.7). This conclusion was also confirmed by HT-XRD results. It is also interesting to note the increase in Si and Al abundance in the 3 different prepared coal fractions with increasing particle size distribution (Figure 3.3). This supports findings that the high density fractions (high concentration of Si and Al) are mainly situated in the coarser particles.

4 EFFECT OF SILICA (SiO₂), ALUMINA (Al₂O₃) AND TITANIA (TiO₂) AS PURE COMPOUNDS ON THE AFT

With the specific aim of this study to increase the AFT, and from literature results presented in **Chapter 1**, experimental AFT determination on coal blends with the addition of some acidic components are necessary to quantify the effect of the additives, before the mechanistic path can be addressed and studied. The acidic components used as pure additives were silica (SiO₂), alumina (Al₂O₃) and titania (TiO₂). These compounds were selected, based on the results obtained by Vassilev *et. al.* (1995) where the effect of silica (SiO₂), alumina (Al₂O₃) and titania (TiO₂) on the AFT were studied. It should be noted that although these components are part of the overall mineral composition, and will not only change the chemistry per sae, but will also react with other phases present.

Blends with the SCS coal sample and SiO₂, Al₂O₃ and TiO₂ were prepared and the average AFT (average of duplicate prepared sample analyses) of the different blends are given in Table 3.8. The effect of the individual compounds on the AFT of the coal blend is graphically illustrated in Figure 3.4. The confidence intervals included are the standard experimental error ($\pm 33^{\circ}\text{C}$) of an AFT analyses.

TABLE 3.8 AFT OF BLENDS WITH Al₂O₃, TiO₂ and SiO₂ ADDITION ($^{\circ}\text{C}$)

Additive (mass %)	Al ₂ O ₃	TiO ₂	SiO ₂
0 (Base case)		1340	
2	1460	1380	1360
4	1530	1370	1390
6	1600	1440	1330
8	1600	1460	1360
10	1600	1470	1360

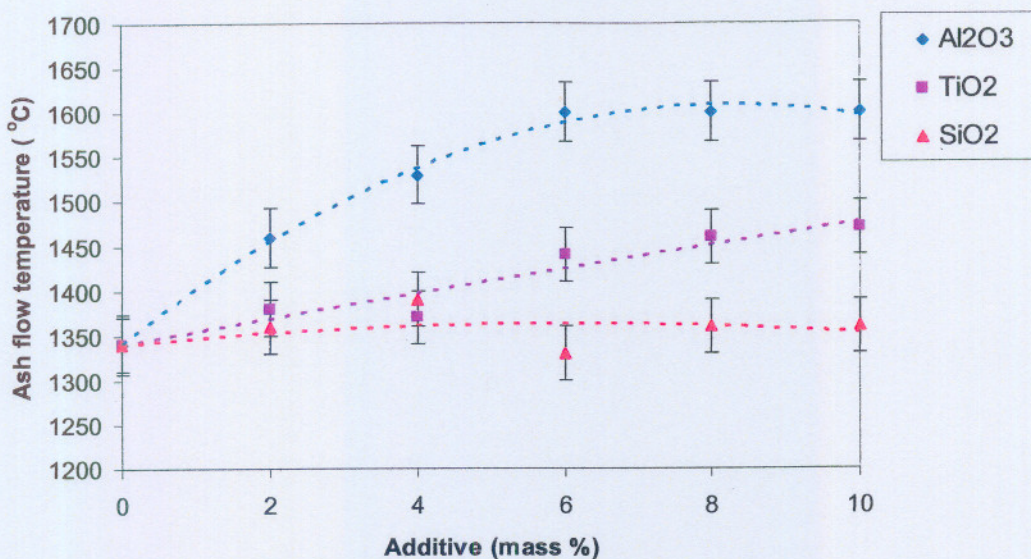


FIGURE 3.4 EFFECT OF INDIVIDUAL COMPOUNDS ON AFT

The experimental data points of the AFT at 6, 8 and 10 mass % Al₂O₃ additive were all taken at 1600°C, but the temperature was probably higher than that reported. AFT results are only reported to 1600°C due to safety reasons and equipment limitations. Normal AFT analytical equipment only ramped to 1600°C.

From Figure 3.4 it is clear that Al₂O₃ had the biggest and most significant effect on the AFT, even with the smallest addition to the coal blend. The effect of SiO₂ and TiO₂ are very similar with regards to the effect on the AFT, which stayed almost constant. Based on the error bars included in the graphs ($\pm 33^\circ\text{C}$), statistically it can be concluded from the 3 different trend lines that Al₂O₃ addition has a significant effect with increasing percentage additive, while the addition of SiO₂ or TiO₂ has a smaller effect on the AFT in comparison to Al₂O₃. The trend line of the Al₂O₃-addition is also a good fit as it has a good correlation coefficient (R^2) of 0.99.

According to literature [Vassilev, *et. al.*, 1995] on related work on the mineral and chemical compositions of coal, the higher AFT is a result of decreased concentrations of fluxing agents (Ca, Fe and Mg components) and that the coals with high AFT ashes have an advanced rank and increased Si, Al and Ti concentration. After comparing the increase in AFT for a specific coal source at a temperature of 1300°C as indicated in Figure 3.5 [Vassilev, *et. al.*, 1995], the amount of Al₂O₃ needed to achieve a similar increase was <7 mass% (from ± 15 to ± 22 mass%). For the other pure oxide SiO₂, almost 15% (from ± 40 to ± 55) was needed to increase the AFT also to 1300°C. The emphasis needs not to be on the actual temperatures mentioned in Figure 3.4, but on the amount of material that was needed and the difference in masses between SiO₂

and Al_2O_3 to reach the same temperature. The minerals have thus different behaviours during heating and therefore each one of them has a different influence on AFT. It was concluded from that study that the main refractory minerals are quartz, mullite and rutile [Vassilev *et. al.*, 1995]. This implies that clay or other similar substances can be used in the gasification operation to increase the AFT.

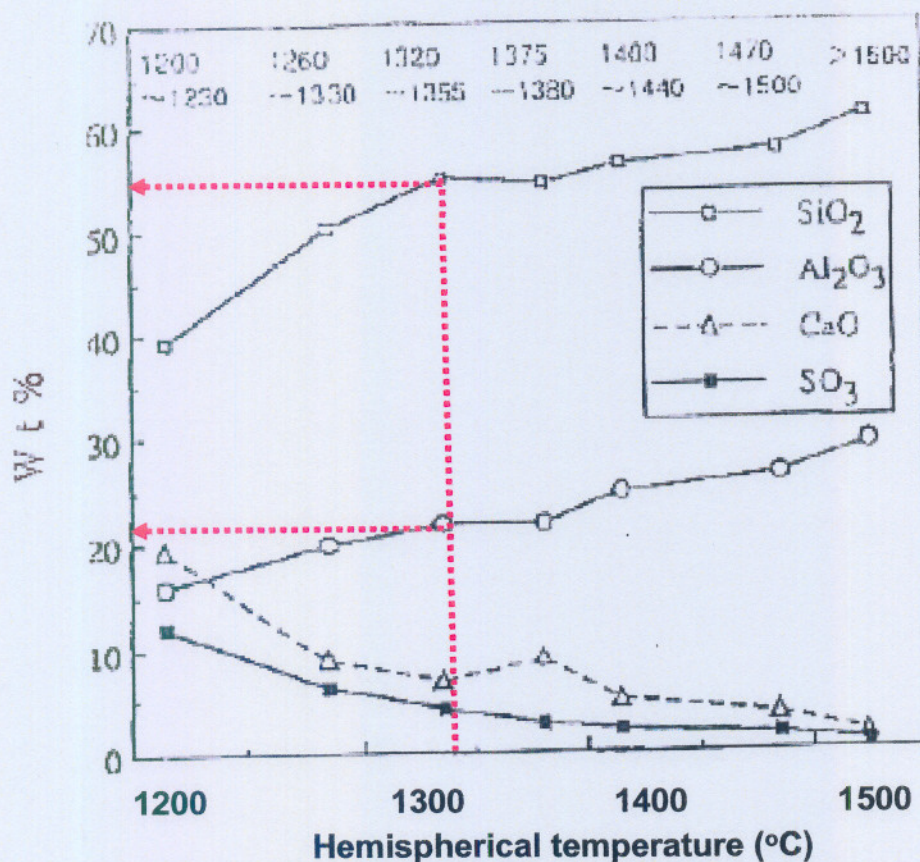


FIGURE 3.5 CORRELATION TRENDS AS PUBLISHED BY VASSILEV *ET. AL.* [1995]

The question remains why Al_2O_3 , as pure oxide component, does react differently and increases the AFT to a certain temperature with less addition in comparison to the addition of TiO_2 and SiO_2 as pure oxide components? Based on literature, Duffy and Ingram [in Allibert *et. al.* [1995]] reported that the shifts in frequency of the absorption band associated with the 6s-6p electron movements observed in the ultraviolet region of the spectrum relates to the basicity of a glass or slag. The shift can be considered as a measure of the electron donor power and is usually expressed in terms of the optical basicity (Λ) defined in equations 1 to 3 where the subscript "free" refers to the probe ion, e.g. Pb^{2+} .

$$\Lambda = (\text{electron donor power of slag}) / (\text{electron donor power of CaO}) \quad (1)$$

$$\Lambda = \Lambda_{\text{free}} - \Lambda_{\text{slag}} / \Lambda_{\text{free}} - \Lambda_{\text{CaO}} \quad (2)$$

$$\Lambda = (60700 - \Lambda_{slag}) / 31000 \quad (3)$$

Values reported in literature are given in Table 3.9 [Allibert *et. al.* 1995].

TABLE 3.9 OPTICAL BASICITY VALUES [Allibert *et. al.* 1995]

Component	Ion-oxygen attraction (Λ_{th})
SiO ₂	-6.31
Al ₂ O ₃	-0.2
TiO ₂	-4.97

The difference in optical basicity (Λ) can be considered as a measure of the electron donor power and is usually expressed in terms of the optical (Λ) basicity. The ion-oxygen attraction and the stronger (more positive) value for Al₂O₃ in comparison with TiO₂ and SiO₂ possibly explain why Al₂O₃ has a bigger influence and effect on increasing the AFT. When the AFT of the pure compounds were compared, it can also be concluded that the Al₂O₃ has the highest AFT of 2040°C, with SiO₂ and TiO₂ having AFT's of 1710°C and 1830°C respectively [Time domain website, 2004].

4.1 Discussion of results by means of three-component phase diagrams

In order to bring this finding into perspective and to obtain a comparison with phase diagrams, the information as published in the 2nd Slag Atlas [Allibert *et. al.* 1995] will be used, together with FactSage modelling. The phase diagrams were developed and modelled with the software package FactSage.

4.1.1 Al₂O₃-SiO₂-TiO₂

From the phase diagram for the three-component system Al₂O₃-SiO₂-TiO₂ developed with FactSage (Figure 3.6) it is clear that Al₂O₃ has a significant different effect on the flow properties (solid-liquid phases) than SiO₂ and TiO₂.

FactSage 7.1 (win) - database: thermo: HSC 9.1.0-2700 (2.10) 3_1010101
 1600-1900°C, P=29 bar

SiO₂ - TiO₂ - Al₂O₃ SLAG-LIQUIDUS TRANSFORMATIONS

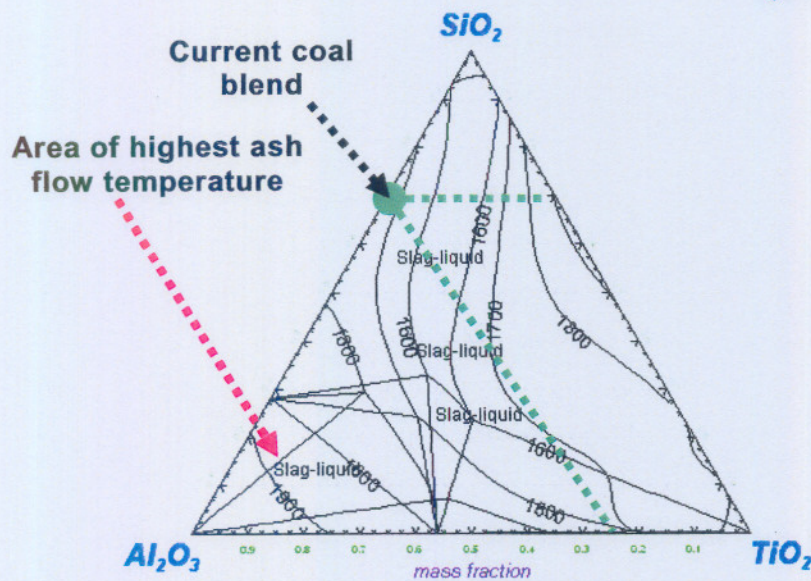


FIGURE 3.6 SLAG-LIQUIDUS SURFACE AND PHASE RELATIONS IN THE AL₂O₃-SiO₂-TiO₂ SYSTEM

The slag-liquid transformation temperature is the highest at the point where Al₂O₃ is a maximum, which is the point in the bottom left corner of Figure 3.6. The slag-liquid temperature at that point is >1900°C. In a two-dimensional area where Al₂O₃ is kept fixed at any point, the slag-liquid temperature in the levels between SiO₂ and TiO₂ are almost the same. The above result is in agreement with the results found on the effect of the individual components on the AFT presented in Figures 3.4 and 3.5, done on a South African coal source for this study, as well as a Northern hemisphere coal sources as presented by Vassilev *et al.* [1995]. The AFT might be lower because with liquidus temperatures, no crystal phases are present. The mineralogy of the coal is not an ideal three-component system, and from literature [Alpern *et al.* 1984, Seggiani, 1999] it is known that specifically Ca, Na and Fe play a dominant role in the ash component slag-liquidus systems. This might not be the only components affecting the mineralogy, but will be used as examples and to compare experimental findings as presented in **Section 3** of this chapter. The ash composition as given in **Section 3** of this chapter (Table 3.5) was reproduced as Table 3.10 and was used in the three-component systems, normalised to 100% (Table 3.11). Take note that although 5 elements are shown in Table 3.11, only 3 components were normalised to 100 mass % for each system. The influence of Na₂O is very limited and in this case does not have a major influence in determining the AFT. However, with a significant increase in Na₂O-content the AFT will decrease dramatically.

TABLE 3.10 ASH COMPOSITION (MASS %) OF COAL USED IN THIS STUDY

ELEMENT	Result of coal sample used in this study (mass %)
SiO ₂	50.1
Al ₂ O ₃	23.3
Fe ₂ O ₃	6.4
P ₂ O ₅	0.7
TiO ₂	1.0
CaO	8.1
MgO	2.7
K ₂ O	0.8
Na ₂ O	0.4
SO ₃	6.1

TABLE 3.11 ASH COMPOSITION NORMALISED TO THREE-COMPONENT SYSTEMS

Three-Component system	SiO ₂	Al ₂ O ₃	CaO	Fe ₂ O ₃	Na ₂ O	Total
SiO ₂ - Al ₂ O ₃ - Fe ₂ O ₃	62.8	29.2	-	8.0	-	100
SiO ₂ - Al ₂ O ₃ - Na ₂ O	67.9	31.6	-	-	0.5	100
SiO ₂ - Al ₂ O ₃ - CaO	61.5	28.6	9.9	-	-	100

4.1.2 Al₂O₃- SiO₂-Fe₂O₃

The Al₂O₃-SiO₂-Fe₂O₃ system (the liquidus phase relations) was developed and modelled with FactSage and is presented in Figure 3.7, with the coal blend mineralogy of the sample used in this study, highlighted by the green dot.

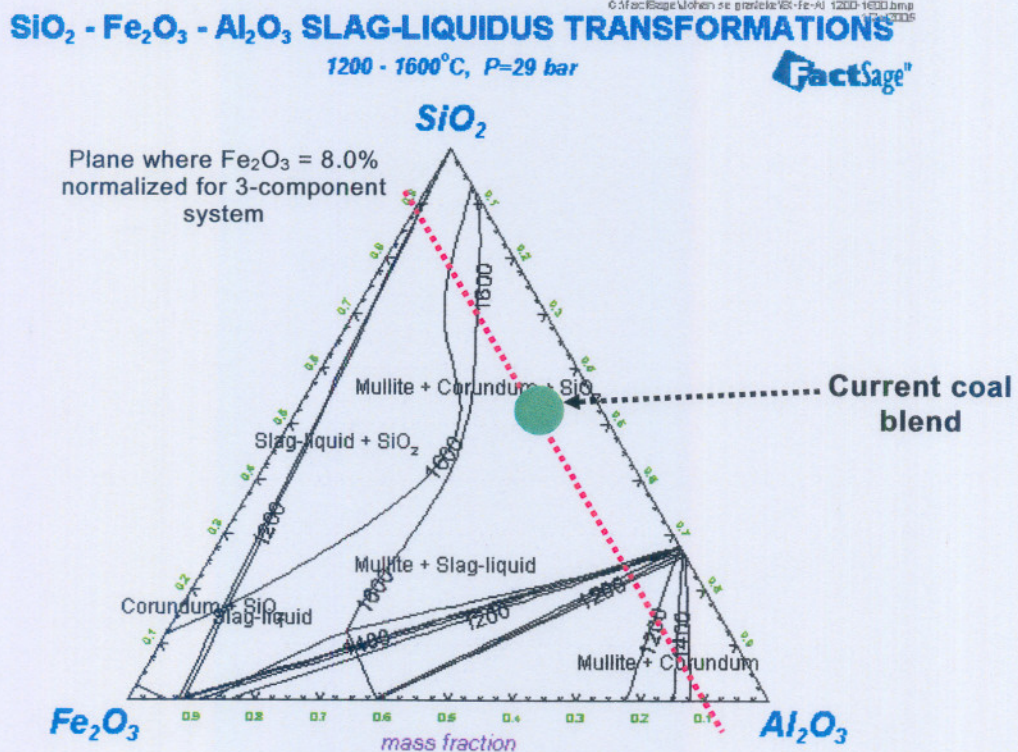


FIGURE 3.7 LIQUIDUS SURFACE AND PHASE RELATIONS IN THE AL₂O₃- Fe₂O₃-SiO₂ SYSTEM

The percentage Fe_2O_3 in the coal sample used in this study was 6.4 mass% (8.0 mass% normalised for the three-component $\text{Al}_2\text{O}_3\text{-Fe}_2\text{O}_3\text{-SiO}_2$ system). The area where the current coal composition is shown (green dot), is in the area where mullite forms. This is indeed the case with the coal within the gasification process. Although this is for an ideal three-component system, the slag-liquidus temperature is in the $>1600^\circ\text{C}$ area. This implies that the three-component system $\text{Al}_2\text{O}_3\text{-Fe}_2\text{O}_3\text{-SiO}_2$ is not one of the critical phase formations affecting the AFT in the blend, as the AFT really depends on the amount of slag or liquid – amount of oxides present.

However, when the Fe-content shifts towards the left bottom corner on Figure 3.7, the Fe-containing phases which starts to form with a similar Si/Al ratio have a significant lower melt temperature and moves in the slag-liquidus area. The Fe_2O_3 content only then may starts to play a dominant role for the AFT. When the Si/Al ratio is decreased (shift towards higher Al) liquidus temperatures are not relevant for the gasifier operating window and the blend composition moves then to outside the slag-liquidus region. In order to explain the above reasoning it can be visualised by means of Figure 3.8, where the three-component system was changed in composition.

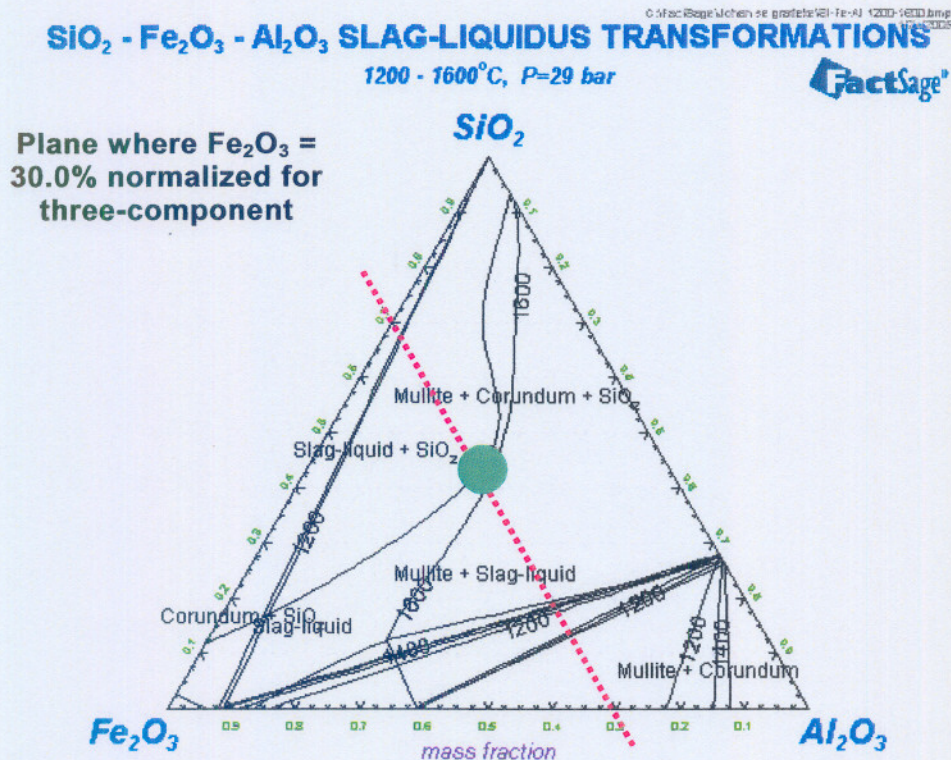


FIGURE 3.8 LIQUIDUS SURFACE AND PHASE RELATIONS IN THE $\text{Al}_2\text{O}_3\text{-Fe}_2\text{O}_3\text{-SiO}_2$ SYSTEM

When the Fe_2O_3 -content, normalised for the three-component system to a Fe_2O_3 content of 30 mass%, liquid temperatures decrease to the region close to the AFT.

This implies that Fe only plays a significant role in the AFT when it occurs in higher concentrations in the coal blend.

When the Fe_2O_3 -content increases from 8% the composition moves from mullite if the Fe_2O_3 content is increased to 30% Fe in the system and it changes to hercynite [Allibert *et. al.* 1995]. At this point the flow temperature drops to $<1500^\circ\text{C}$, with the presence of a slag-liquid in the blend. Thus the result that the current Fe-content has not a significant effect on the AFT within the current variation of Fe in the blend, also explains the finding that Fe_2O_3 has a very low correlation (0.39) with the AFT [Van Dyk *et. al.* 2004]. Even for 30 mass % Fe_2O_3 , very small amounts of melt would be present.

4.1.3 Al_2O_3 - SiO_2 - CaO

The Al_2O_3 - CaO - SiO_2 system as calculated with FactSage is presented in Figure 3.9. A similar trend is observed as with Fe_2O_3 for the current coal blend as both Fe_2O_3 and CaO occur in about the same abundance in the coal blend used for gasification.

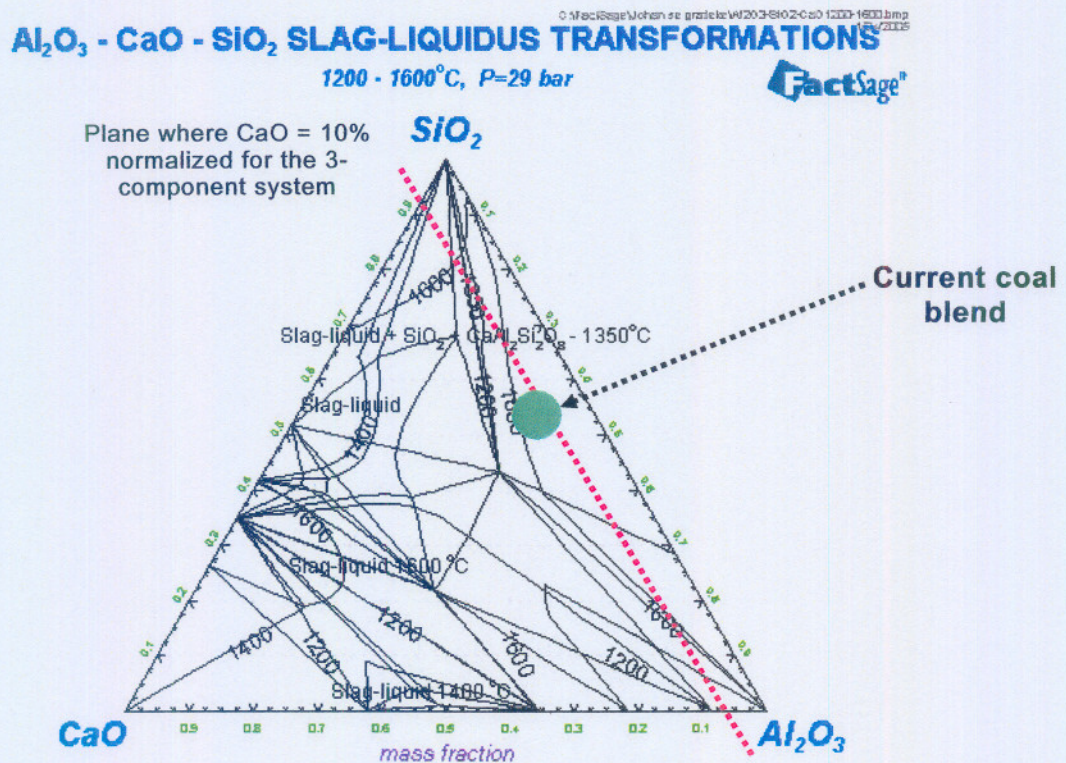


FIGURE 3.9 LIQUIDUS SURFACE AND PHASE RELATIONS IN THE Al_2O_3 - CaO - SiO_2 SYSTEM

According to the phase diagram presented in Figure 3.9, the area where the current coal blend is shown, is in the area with a liquidus temperature of 1300 to 1400°C . This

implies that, although the calculation is for an ideal three-component system, the AFT from this system is firstly in the range where the current coal source to AFT is. Secondly it is within the range of slag formation. This also indicates that the critical phase assemblages affecting the AFT in the coal blend is within the critical temperature range, implying that changes to the blend will significantly affect the AFT.

4.1.4 Al_2O_3 - SiO_2 - Na_2O

The three-component Al_2O_3 - Na_2O - SiO_2 system, for the current coal blend, is given in Figure 3.10, with a Na_2O -content of 0.5%.

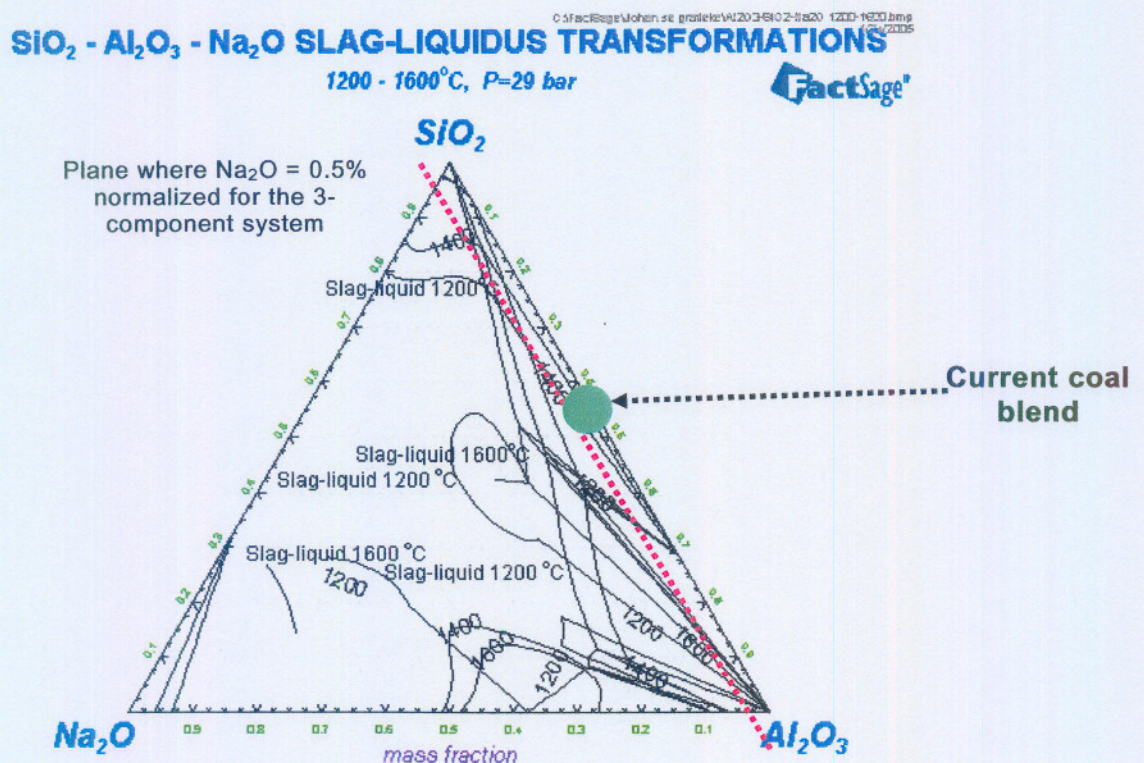


FIGURE 3.10 LIQUIDUS SURFACE AND PHASE RELATIONS IN THE Al_2O_3 - Na_2O - SiO_2 SYSTEM

Although the Na_2O -content is very low, it can be seen that a relatively small change in the Na_2O -content may have a significant effect on the AFT. By increasing the Na_2O -content from the current 0.5% content in the coal to 10%, the liquidus decrease from $>1500^\circ C$ in the current system to as low as $1200^\circ C$. Gruber and Kalmanovitch [1989] indicated in studies done for fixed bed gasification (DGC), that the economic impact of clinkering is substantial enough to warrant close monitoring of the sodium in the gasification feed and that with blending the sodium content must be maintained below 8 mass %.

4.2 Effect of silica (SiO₂), alumina (Al₂O₃) and titania (TiO₂)-containing substances (i.e. kaolinite and siltstone) on the AFT

Taken into account the results of **Section 4.1** indicating that SiO₂, Al₂O₃ and TiO₂ all have an increasing effect on the AFT it is worthwhile to investigate what the effect quartz (SiO₂), alumina (Al₂O₃) and titanium (TiO₂)-containing substances will have on the AFT. Examples of such substances are kaolinite and siltstone. Kaolinite contains mainly SiO₂ and Al₂O₃ as (Al₂O₃)(SiO₂)₂(H₂O)₂. Siltstone is a combination of mineral species, is usually found as part of the roof and floor partings of the mine stope. The roof and floor of the coal seam are normally not mined as part of the whole seam, as the roof and floor rocks consist mostly of Si and Al, with a total ash content of >80%, with only a small percentage of carbon present. For the purpose of this study the so-called roof and floor are treated separately. The mineral composition of the roof and floor are shown in Table 3.12.

TABLE 3.12 AVERAGE PROPERTIES OF THE ROOF AND FLOOR OF THE TOTAL COAL SEAM [VAN DYK AND KEYSER, 2002]

	ROOF	FLOOR
% Ash	91.4	86.6
% Fixed carbon	1.9	3.1
Difference (moisture + volatile matter)	6.7	10.3
Ash composition (%)		
SiO ₂	80.1	71.5
Al ₂ O ₃	11.3	22.1
Fe ₂ O ₃	3.6	1.9
P ₂ O ₅	0.1	0.1
TiO ₂	0.5	0.7
CaO	1.2	0.4
MgO	0.3	0.3
K ₂ O	1.4	1.4
Na ₂ O	0.2	0.3
SO ₃	0.7	0.1
AFT (°C)(Oxidizing)		
DT	1558	1588
HT	1585	1591
FT	1600	1593
XRD-analyses		
Pyrite	2.7	1.4
Quartz	55.2	25.3
Calcite	1.5	0.1
Siderite	1.3	0.0
Dolomite	0.0	0.0
Illite	7.0	19.4
Kaolinite	26.5	50.8
Microlite	4.4	1.4

The general properties of the roof and floor can be summarized as follows:

Roof - Low volatile matter content in the order of 6%. The C-content in the single coal source and coal blend is <3% and the S-content <1.8% (air dry basis). Both the single coal source and coal blend have a high SiO₂-content of >80%. XRD-analyses showed high quartz (>50%) and kaolinite (±20%) contents, as well as illite (7%) and pyrite (2.7%). The AFT were determined and found to be in the order of 1550-1600°C.

Floor - Low volatile matter content in the order of 7-8%. The C-content of the floor is <5% and the S-content in the order of 1% (air dry basis). Both the single coal source and coal blend have a high SiO₂-content ±(70%) and Al₂O₃-content (±20%). XRD-analyses showed concentration of quartz (25.3%), illite (19.4%) and microcline (1.4%) contents, with traces of other minerals. The AFT were determined to be in the order of 1550-1600°C.

Blends with the SCS coal sample and kaolinite, roof and floor were prepared and the AFT of the different blends were determined and given in Table 3.13. The effect of the individual elements on AFT of the coal blend is graphically shown in Figure 3.11.

TABLE 3.13 AFT OF BLENDS WITH ADDITIVE (ROOF AND FLOOR) ADDITION (°C)

Additive (mass %)	Kaolinite	Roof	Floor
0 (Base case)	1340		
2	1420	1430	1440
4	1440	1420	1440
6	1430	1430	1440
8	1460	1420	1460
10	1440	1450	1470

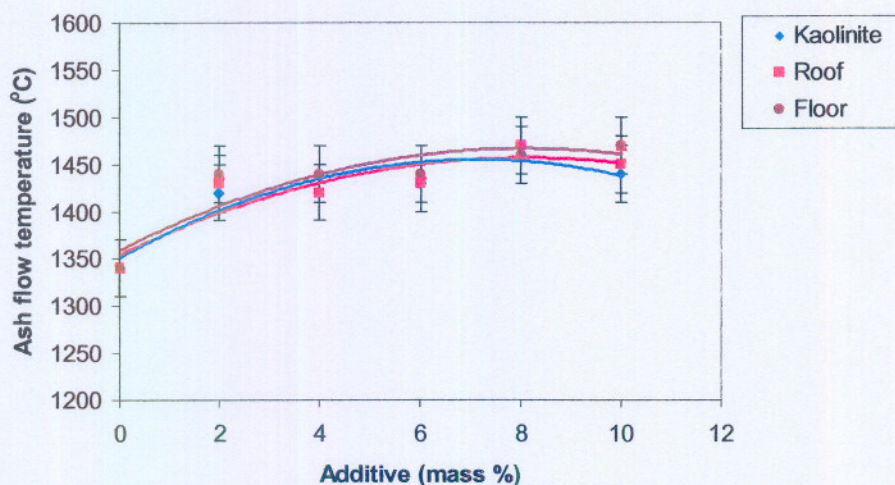


FIGURE 3.11 EFFECT OF ADDITIVES ON THE AFT

From these results it can be concluded that all three substances have an increasing effect on the AFT. The effect is not as significant as that obtained for pure Al_2O_3 as an individual compound, but definitely the AFT increased by more than 50°C initially, whereafter it gradually stabilised. Based on the error bars included in the graphs ($\pm 30^\circ\text{C}$), statistically it can be concluded from the 3 different trend lines that all three substances have a significant effect from 0 mass% to a 2 mass% addition. The trend lines indicate that the AFT increase with a bigger degree in the smaller addition ranges and have a lesser effect with the addition of higher percentages of additive.

4.3 *Other experimental findings on manipulating the mineral composition of a coal blend versus ash fusion temperature with statistical evaluations as support of the mechanism for increasing the AFT*

The purpose of this part of the investigation was to evaluate the statistical correlation of mineral composition on AFT by means of the impact of dense medium separation (destoning) and leaching on coal properties such as ash composition and ash fusion properties as discussed in **Section 4.1 Chapter 2**. The results were then statistically evaluated. These studies supplement the valuable insight gained in the previous sections and findings, with specific examples and explanation to previous conclusions.

4.3.1 *Effect of dense medium separation of coal on mineral composition and ash fusion properties*

The purpose of this part of the investigation was to evaluate the impact of dense medium separation (destoning), and specifically at different relative densities on coal properties such as ash composition and AFT in order to obtain insight to the effect of Si, Al and Ti on the AFT. A typical Secunda run-of-mine (ROM) coal blend was used where coal washing was performed according to the ISO 7936 standard. The samples were washed at different relative densities from RD 1.4 to RD 2.1 with increments of 0.1. The cumulative dense medium curve is given in Figure 3.12.

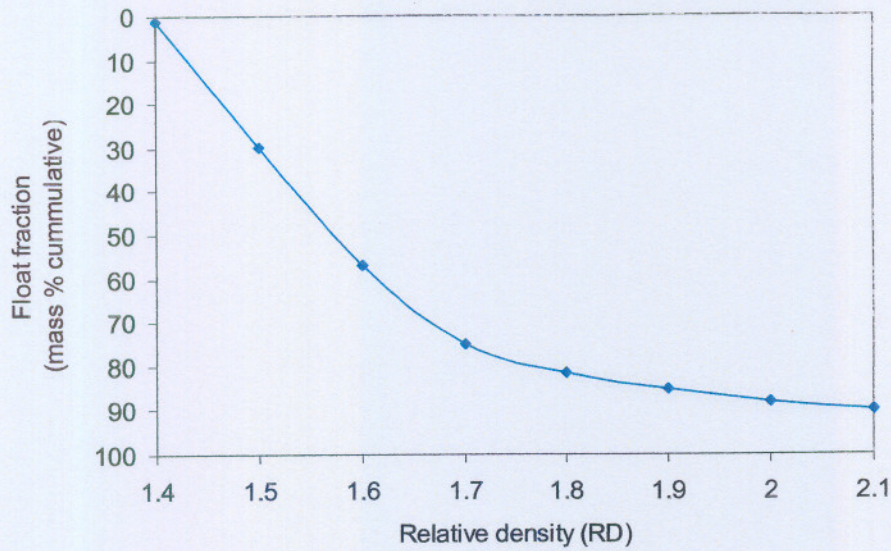


FIGURE 3.12 DENSE MEDIUM CURVE

The AFT was determined on the individual density fractions and is given in Figure 3.13.

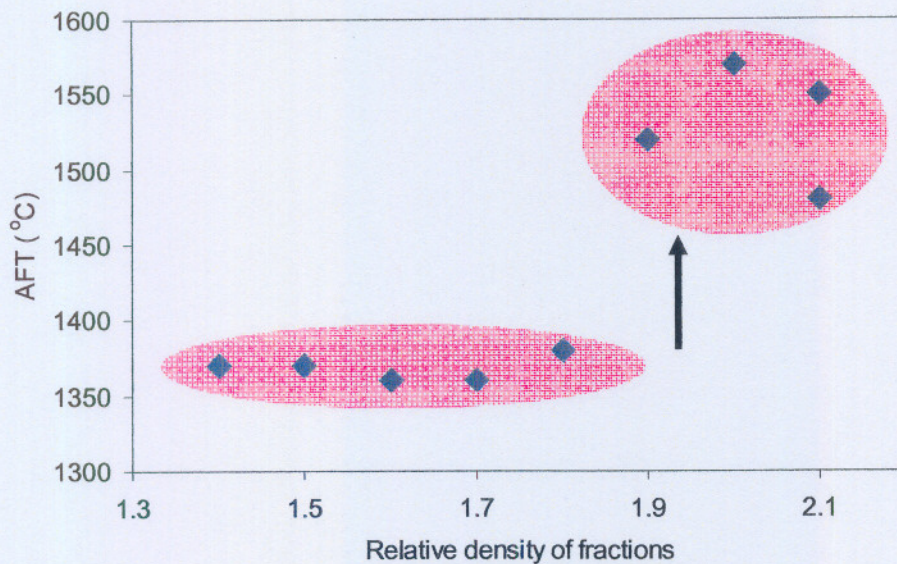


FIGURE 3.13 EFFECT OF DENSE MEDIUM SEPARATION (DESTONING) ON AFT FOR INDIVIDUAL DENSE MEDIUM FRACTIONS

These results indicated that dense medium separation at a RD = 1.4 to RD = 1.8 did not significantly affect the AFT, where (from a relative density greater than 1.9) the AFT increased significantly in specific fractions. The AFT has increased >200°C from 1340°C of the original coal to 1570°C. The original data are given in Appendix B Table G.

From Figure 3.14 the mass % SiO₂ and Al₂O₃ are shown against the AFT and the following conclusions can be drawn:

- The Al_2O_3 and TiO_2 concentration remained constant through all the dense medium fraction, but the SiO_2 concentration increased with increasing AFT.

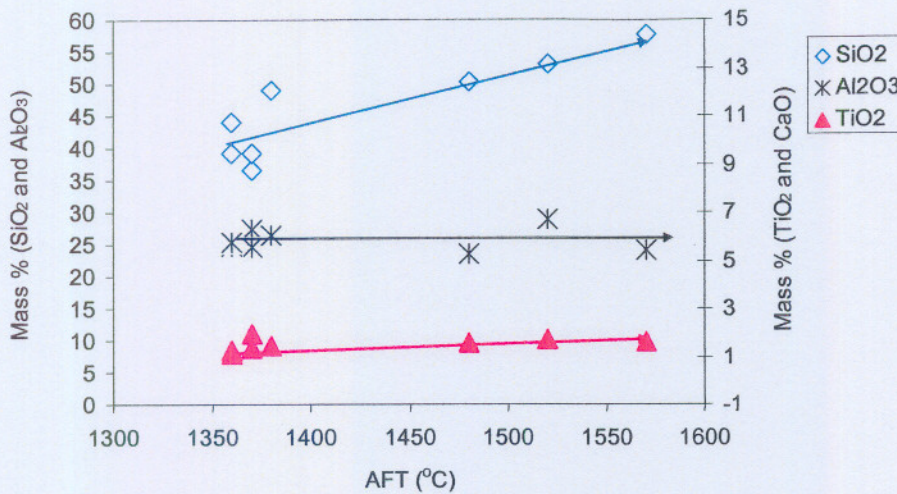


FIGURE 3.14 SiO_2 , Al_2O_3 and TiO_2 PERCENTAGE VERSUS THE AFT OF THE DENSE MEDIUM FRACTIONS

Subsequently the Si/Al ratio was drawn against the AFT to determine if any relation existed. The ratio versus AFT graph is shown in Figure 3.15. The variation in Si/Al ratios were obtained by dense medium separation.

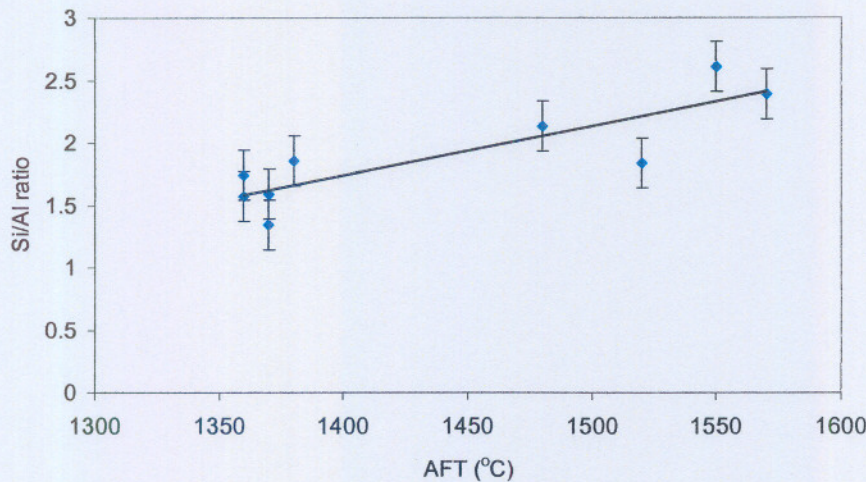


FIGURE 3.15 Si/Al RATIO VERSUS ASH FUSION TEMPERATURE

It is clear from Figure 3.15 that the AFT increased with increasing Si/Al ratio. Furthermore an increasing Si/Al ratio in the dense medium separation fractions were obtained. The Al amount decreased in relation to Si, as some mineral fractions were removed by density differences from the total coal fraction. The Al present in the mineral structure is not “free” Al_2O_3 or clays, and the actual effect of decreasing or increasing the AFT with varying Si/Al ratios, is actually the result of the SiO_2 (quartz)

in the structure. The SiO_2 acts as a dilutant and as the SiO_2 concentrated in the fractions with higher percentages, the AFT decreases and the effect of SiO_2 is more a physical effect. The inconsistent trend can possibly explained by the heterogeneous nature of the coal source, experimental error in the coal or even due to sample and preparation of the coal blend.

The mechanism changed from a physical effect in increasing the AFT by dilution, to a chemical process where the Al_2O_3 added, then reacted with the SiO_2 in the mineral structure to form mullite species, which have a high AFT. This chemical effect was discussed in **Section 5** of this chapter and will be elaborated on in **Section 6** as well. Seggiani [1999] stated similar results that the acid-base ratio is the most frequently used parameter for correlating ash fusibility, although the work was done on northern hemisphere coal sources.

4.3.2 *The statistical evaluation of the effect of leaching (chemical fractionation) of coal on the AFT*

The purpose of this section is to discuss the statistical results on the effect of leaching on coal sources to quantify the effect of different mineral species and mineral/mineral ratios on the AFT of the coal sources [Van Dyk et. al., 2004].

Another means of manipulating the mineral composition, is by leaching the coal source with specific leachates which will also result in different Si, Al and Ti concentrations in the coal. The purpose of the work was not to determine the effect of the leaching agents, but more specifically to change the mineral composition.

The statistical correlations between the AFT and the ash composition were calculated in Microsoft Excel™ with the Data Analysis Tool Pack. This relationship can be approximated by a polynomial function in ten mixture components. The relationship between a response, in this case AFT, and the ten mixture components can best be predicted by a Scheffe polynomial [Scheffe, 1958 and Cornell, 1981]. The relationship between the AFT and ash composition were statistically evaluated by means of a Scheffe polynomial (mixture model) and the AFT was therefore expressed as a mixture model of ten mineral components. The significance of the complete model is presented in Table 3.14. The coefficient estimates of the polynomial model are given in Appendix B Table J. The binary mixtures between SiO_2 and Al_2O_3 , as well as between SiO_2 and P_2O_5 , were also included to improve the fit of the mixture model.

The coefficient estimates in Appendix B Table J are shown in pseudo or coded component units. The conventional pseudo component transformation z_i :

$$z_i = \frac{(x_i - L_i)}{(1 - \sum_{i=1}^q L_i)} \quad (4)$$

where x_i denotes the actual component proportion and L_i the lower bound for component i . Notice that pseudo components are calculated from component proportions. The pseudo units are independent of the actual units of the components. The parameters in the model were estimated through least-squares estimation with the Design-Expert® software [Stat-Ease, 2000]. Table 3.14 depicts the statistics for the fit of the mixture model. The sum of squares (SS) for the model (SSM) is the SS for all the terms in the model and indicates the total variability explained by the complete model. The SSE is the variability not explained by the model and the total SS (SST) is the total variability in the data. In this case, the adjusted R^2 of the model is equal to 0.87. In other words, the mixture model explains 87% of the variability in the data. Therefore, it can be concluded that the mixture model fits the data well.

From Table 3.14 it can be concluded that the mixture model is significant at the 5% significance level since, according to statistical principles, the p-value is smaller than 0.05. Therefore, it is at least 95% certain that the components in the mixture model explain the variability in the AFT data. Finally, the residual standard error (RSE) of the model is the square root of the SSE divided by the DF for error. In this case, $RSE = \sqrt{7738.30/3} = 50.79$. The RSE is in the same units as the response and is therefore an indication of the experimental error [Cornell, 1981].

TABLE 3.14 SUMMARY OF MODEL STATISTICS FOR THE AFT

	Sum of Squares	DF	F Value	p-value
Model	278301.70	11	9.81	0.0428
Residual	7738.30	3		
Cor Total	286040.00	14		

The effects of the components on the AFT can best be interpreted through evaluating the coefficients estimates in the model together with their standard errors. Notice that the AFT can be predicted with the coefficient estimates in Appendix B Table J. The significance of each component or term in the mixture model is determined through evaluating the 95% confidence interval of the coefficient estimate depicted in the last two columns of Appendix B Table J.

If the confidence interval does not include 0 then the component or term in the model is significant at the 5% significance level. The following deductions can be made with regards to the Si, Al and Ti components:

- Based on the 95% confidence intervals (low and high predictions) depicted in Appendix B Table J the following components can be highlighted as having a statistical significant effect on the AFT:
 - $\text{SiO}_2\text{-Al}_2\text{O}_3$ combination
 - $\text{Al}_2\text{O}_3, \text{Fe}_2\text{O}_3, \text{CaO}, \text{MgO}, \text{P}_2\text{O}_5$

These findings are in agreement with previous results [Alpern, et. al., 1984 and Seggiani, et. al., 1999]. However, it must be stressed that these are components of the ash composition and cannot be interpreted individually. This is so since the significant as well as the non-significant components are always present in the mixture. The significant components are the ones that have the greatest effect on AFT.
- These evaluations again highlights the fact and confirms work from other researchers that ash composition on its own does not explain the AFT behavior of coal ash accurately [Slegeir, et. al., 1988] and that it entails complex interactions between different mineral elements.

The following ratios from literature [Slegeir et. al. 1988, Seggiani, 1999 and Carpenter, 2002] were decided on and calculated for use in this study and the ash composition expressed as mass percentages:

$$\% \text{ Base} = \text{Na}_2\text{O} + \text{K}_2\text{O} + \text{CaO} + \text{MgO} + \text{Fe}_2\text{O}_3 \quad (5)$$

$$\% \text{ Acid} = \text{SiO}_2 + \text{Al}_2\text{O}_3 + \text{TiO}_2 \quad (6)$$

$$\text{Silica value} = \text{SiO}_2 / (\text{SiO}_2 + \text{Fe}_2\text{O}_3 + \text{CaO} + \text{MgO}) \quad (7)$$

$$\text{Dolomite ratio} = (\text{CaO} + \text{MgO}) / (\text{Fe}_2\text{O}_3 + \text{CaO} + \text{MgO} + \text{K}_2\text{O} + \text{Na}_2\text{O}) \quad (8)$$

$$\text{Acidity} = (\text{SiO}_2 + \text{Al}_2\text{O}_3) / (\text{Fe}_2\text{O}_3 + \text{CaO} + \text{MgO} + \text{Na}_2\text{O} + \text{K}_2\text{O}) \quad (9)$$

Correlation coefficients (r) between the calculated oxide ratios and AFT are given in Table 3.15. It can be concluded from Table 3.15 that the best correlation coefficient (r) with AFT is obtained with the dolomite ratio. A fairly good correlation of 0.7 was obtained between % acidic components and silica value with AFT. P_2O_5 abundance was very low in the coal studied and thus not further investigated.

TABLE 3.15 CORRELATION COEFFICIENTS (r) BETWEEN OXIDE RATIOS AND AFT

	% Base	% Acid	Silica value	Dolomite ratio	Acidity	FT
% Base	1					
% Acid	-0.99	1				
Silica value	-1.00	1.00	1			
Dolomite ratio	0.83	-0.84	-0.85	1		
Acidity	-0.90	0.88	0.89	-0.63	1	
FT	-0.70	0.71	0.71	-0.81	0.54	1

As already mentioned and indicated, one property that specifically gives more information on the suitability of a coal source for gasification purposes is the AFT. Conventional AFT analyses (SABS/ISO methods) gives an average flow property and does not indicate exactly at what temperature the first melt/sinter is occurring due to specific mineral matter transformations. Operating experience indicated that even when the gasifiers are operated at temperatures above the AFT as given by an AFT analysis, a percentage of slag (clinker) is formed. HT-XRD results on the base case sample as supplied by Corus R&D and the results as supplied by Sasol Technology R&D will be discussed together, and compared, as this is a newly developed and set-up technique at Sasol Technology R&D.

5.1 Mineral decomposition of base case coal sample

The predominant phases of the base case coal sample were quartz, muscovite, calcite, dolomite, FeS₂, anhydrite, rutile and kaolinite (Appendix B Table H) [Melzer, 2003].

It is interesting to note that kaolinite was only detected by Corus and not Sasol Technology. This might be explained by the fact the one sample (that of Corus) was not ashed before analysing, while the sample of Sasol Technology was first ashed at 500°C and kaolinite already starts to decompose below 500°C. As it is known that small amounts of kaolinite are present in the SCS coal sources, it will be discussed and the transformations interpreted according to the results obtained by Corus. As all other results and compositions compared well, it is accepted that all discussions further on will be on that of results and analysis done at Sasol Technology. The sample was first scanned at ambient conditions (25°C), although it was already ashed at 500°C (Appendix B Table H).

The mineral transformations from 500°C to 1400°C are discussed here based on Appendix B Table H and Figure 3.16, as well as the 3D graphically visualisation of the results in Figures 3.19 and 3.20. Figure 3.16 illustrates the mineral phase transformations of the base case mineral coal sample at ambient temperature. Figure 3.17 and 3.18 illustrate the mineral phase transformations of the minerals with and without Al₂O₃ addition from 500°C to 1400°C. Figure 3.19 and 3.20 are detail into the mineral transformations as given in Figure 3.16 at ambient temperature.

It should be noted that the HT-XRD graphs show the pattern intensity of a specific sample and HT-XRD run on the y-axis which is only a count and does not reflect the mass of direct mass ratio. It only has to be seen as a degree of presence of that specific mineral and the transformation over temperature. Figure 3.16 is a summary of the individual XRD-graphs that will follow from Figure 3.17.

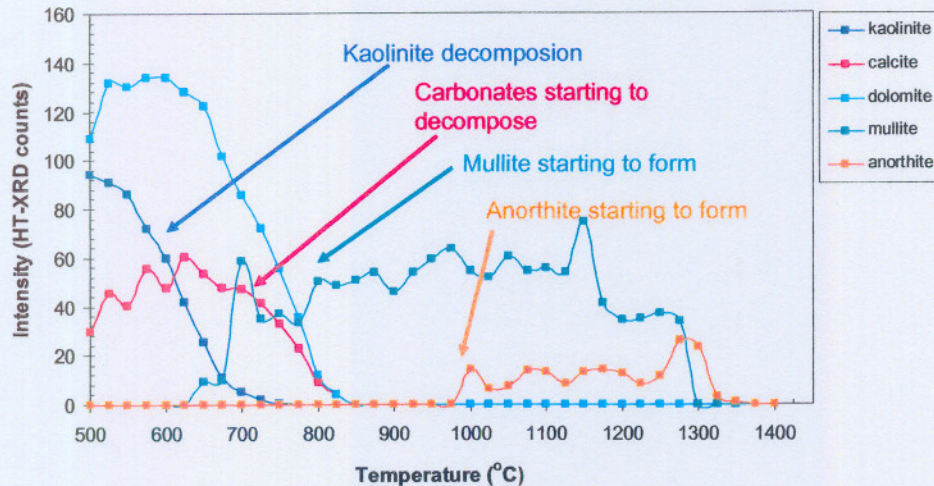
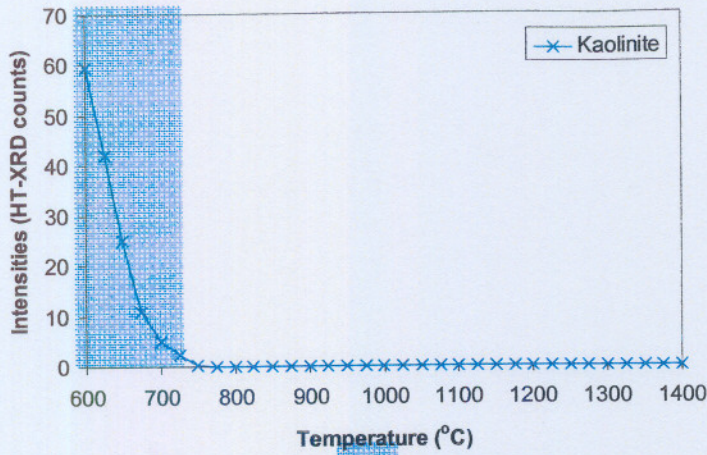


FIGURE 3.16 INTEGRAL INTENSITIES OF IDENTIFIED PHASES AS A FUNCTION OF TEMPERATURE

Between 600°C and 650°C kaolinite starts to disappear first (Figure 3.17). A graphical summary of the decomposition of kaolinite to mullite via metakaolinite is given in Figure 3.17. The onset of decomposition of kaolinite is from temperatures higher than 500°C, whilst the mullite has a melting temperature of 1850°C [Benson,1987].



**Decomposition of kaolinite
to formation of mullite via metakaolinite**

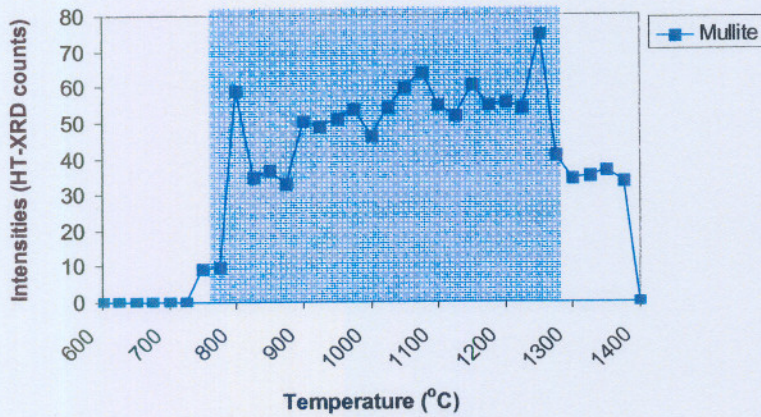


FIGURE 3.17 DECOMPOSITION OF KAOLINITE AND FORMATION OF MULLITE AS FUNCTION OF TEMPERATURE

In the temperature range $>500^{\circ}\text{C}$ to 900°C , the carbonates, calcite and dolomite, start to decompose (Figure 3.18) with the formation of lime and periclase.

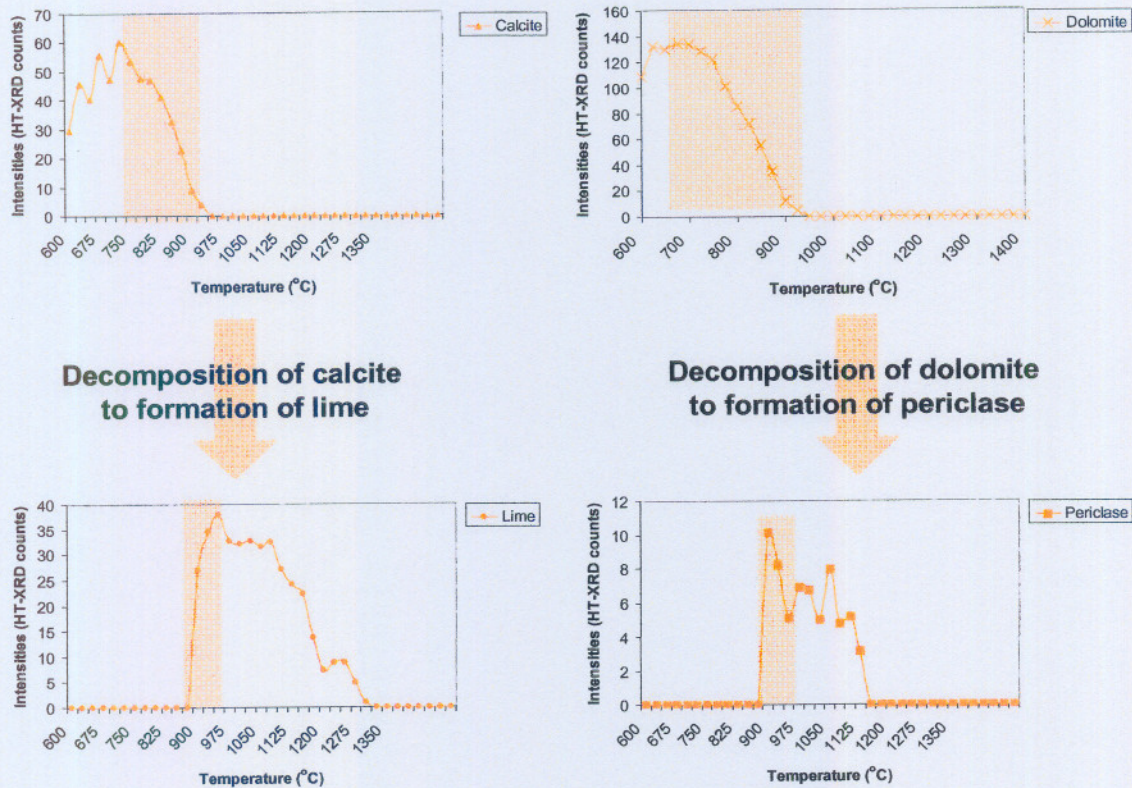


FIGURE 3.18 DECOMPOSITION OF CALCITE AND DOLOMITE AS FUNCTION OF TEMPERATURE

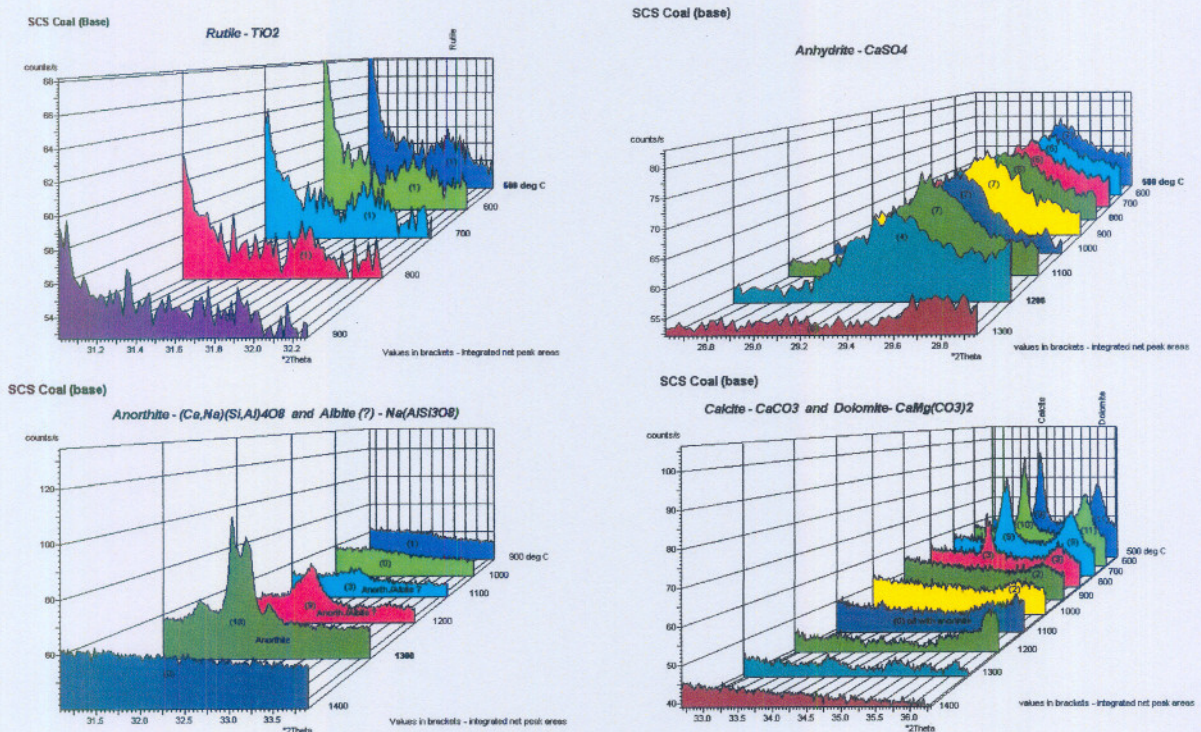


FIGURE 3.19 INTEGRAL INTENSITIES OF SPECIES (RUTILE, ANHYDRITE, ANORTHITE, DOLOMITE AND CALCITE) AS FUNCTION OF TEMPERATURE

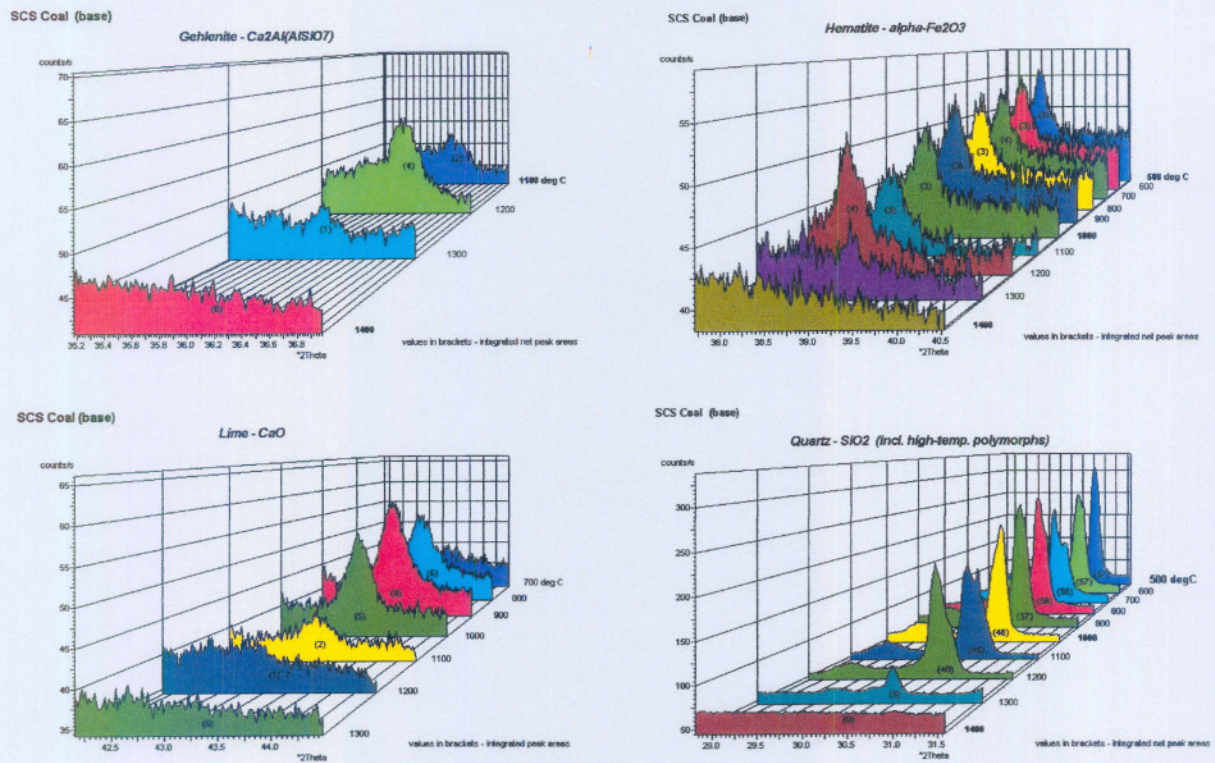


FIGURE 3.20 INTEGRAL INTENSITIES OF SPECIES GEHLENITE, HEMATITE, LIME AND QUARTZ AS FUNCTION OF TEMPERATURE

The formation of anhydrite (CaSO_4) takes place after the formation of calcite (Figure 3.21).

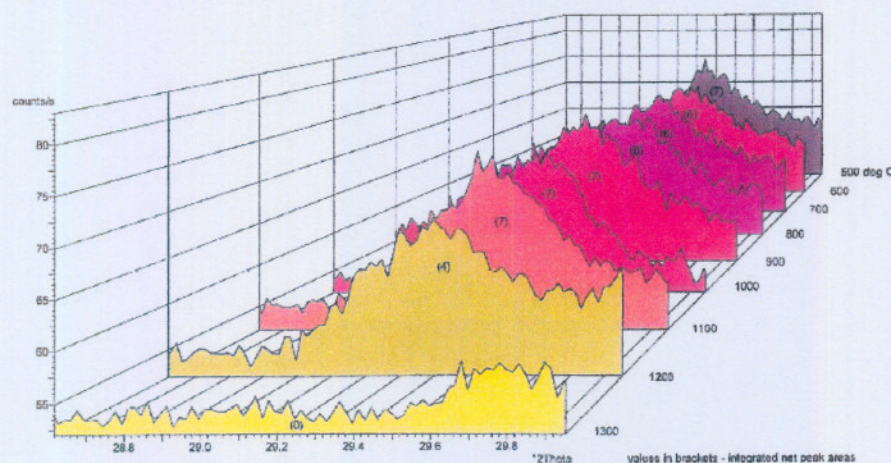


FIGURE 3.21 DECOMPOSITION OF CALCITE AND DOLOMITE AS FUNCTION OF TEMPERATURE

At 1000°C anorthite ($\text{CaAl}_2\text{Si}_2\text{O}_8$) and gehlenite ($\text{Ca}_2\text{Al}_2\text{SiO}_7$) start to crystallise, probably due to partial melting of the phase assemblage. Anorthite and gehlenite are formed as products from the crystallisation of a Ca-aluminosilicate melt at temperatures around 900°C to 1100°C [Alpern, et. al., 1984]. The formation from anorthite is graphically given in Figure 3.22.

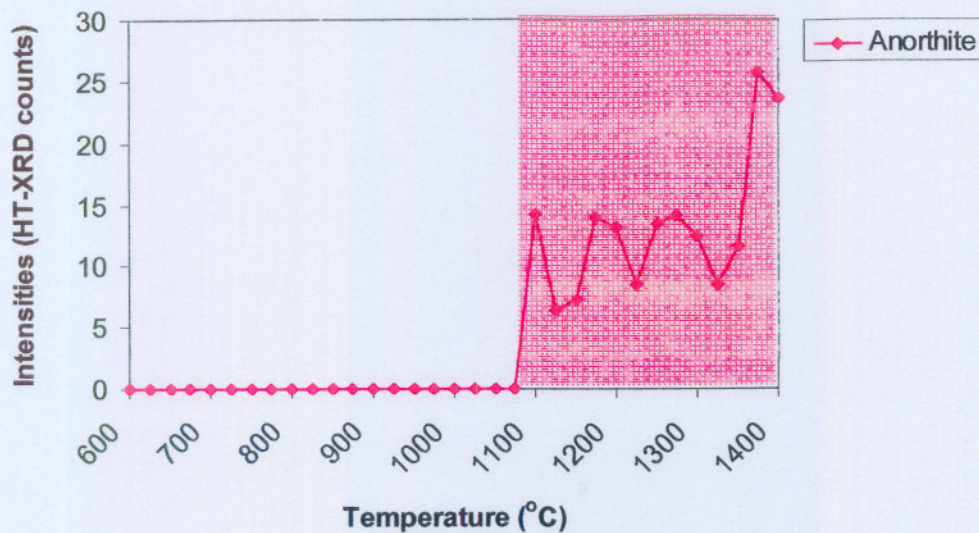


FIGURE 3.22 FORMATION OF ANORTHITE AS FUNCTION OF TEMPERATURE

Mullite melted at 1200°C (Figure 3.17), with dissociation starting during melting. Quartz and anorthite were observed up to 1350°C.

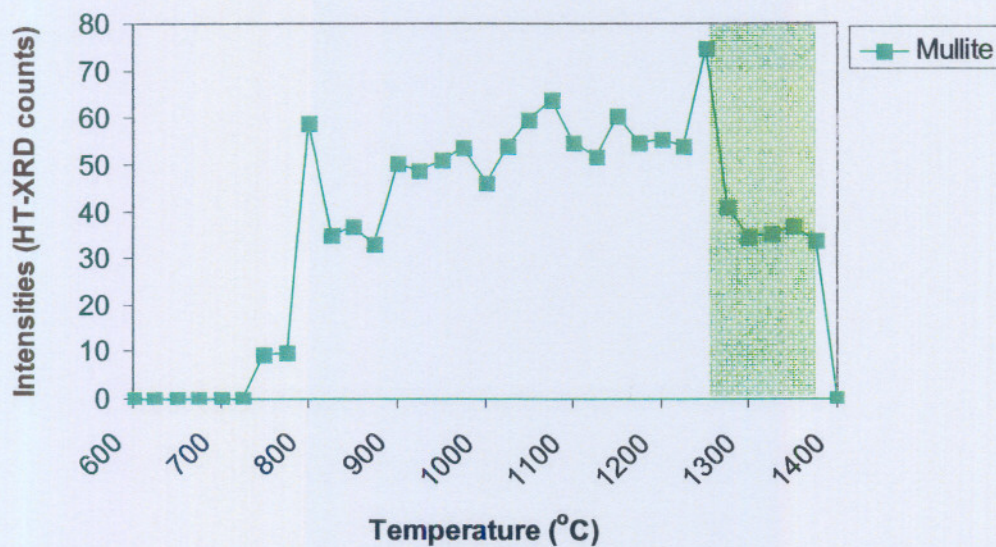


FIGURE 3.23 DECOMPOSITION OF MULLITE AS FUNCTION OF TEMPERATURE

Above 1350°C the whole phase assemblage found in coal was molten (Figure 3.24). The decrease in intensity of the mineral matter as function of temperature is not only a decomposition of some mineral phases, but also the formation of liquid (slag). At the temperature of 1400°C it was observed and that all the crystalline phases were molten.

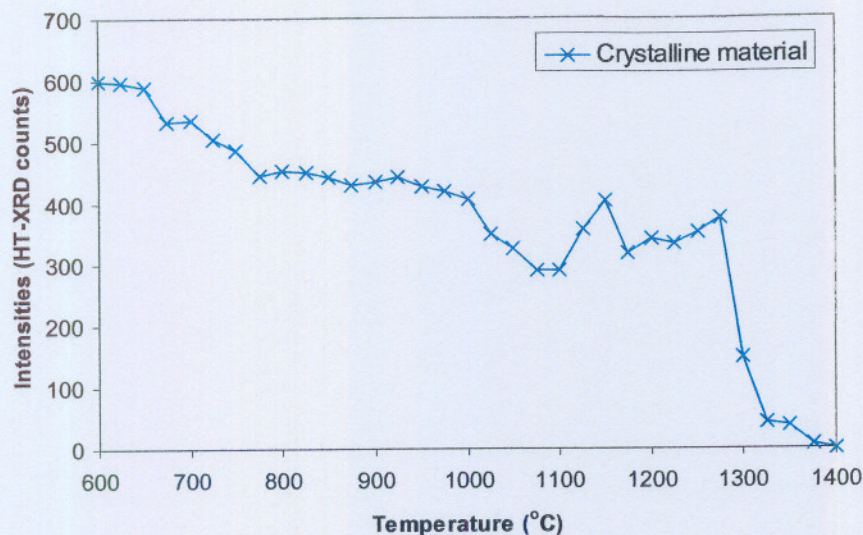


FIGURE 3.24 CRYSTALLINE MATERIAL (DECOMPOSITION OF MINERAL MATTER AND SLAG FORMATION AS FUNCTION OF TEMPERATURE)

Summary:

Based on HT-XRD analyses, the predominant phases of the base case coal sample were quartz, muscovite, calcite, dolomite, hematite, anhydrite, rutile and kaolinite. Between 600°C and 650°C kaolinite started to disappear first. The onset of decomposition of kaolinite occurred from temperatures higher than 500°C, whilst the mullite has a flow temperature of 1850°C. In the temperature range >500°C to 900°C, the carbonates, calcite and dolomite, started to decompose with the formation of lime and periclase. The formation of anhydrite (CaSO₄) took place after the formation of calcite. At 1000°C anorthite (CaAl₂Si₂O₈) and gehlenite (Ca₂Al₂SiO₇) become stable, probably due to partial melting of the phase assemblage. Anorthite and gehlenite were formed as products from anhydrite, alumina and silica at temperatures around 900°C to 1100°C, but gehlenite could also have formed directly from lime. Above 1350°C the whole phase assemblage of the coal was molten. The decrease in intensity of the mineral matter as function of temperature relates not only to a decomposition of some mineral phases, but also the formation of liquid (slag). At the temperature of 1400°C only liquid was observed and all the crystalline phases were molten.

5.2 Mineral decomposition of base case coal sample with various amounts of Al₂O₃ added

The base case sample was manipulated with the addition of 10 mass % Al₂O₃ and the HT-XRD analyses repeated as discussed in **Section 5.1**. A number of changes in

mineral decomposition and mechanistic differences were observed and compared with that of the base case sample. The crystalline phases in the manipulated coal sample at different temperatures are given in Appendix B Table I.

Similar trends and changes in the mineral behaviour were observed when Al_2O_3 was added as the base case coal sample (**Section 5.1** and Appendix B Table H). However, the intensities differ in specific minerals, as well as the temperature of formation and deformation of some minerals, as discussed below.

When comparing the base case sample with the Al_2O_3 -manipulated sample it is clear that the mullite is one mineral that showed a significant difference in formation and mechanistic behaviours. The differences and similarities are herewith discussed and graphically explained.

In the temperature range $>500^\circ\text{C}$ to 900°C , the carbonates, calcite and dolomite, started to decompose (Figure 3.25) with the formation of lime and periclase. The amount of Al_2O_3 added was 10 mass %.

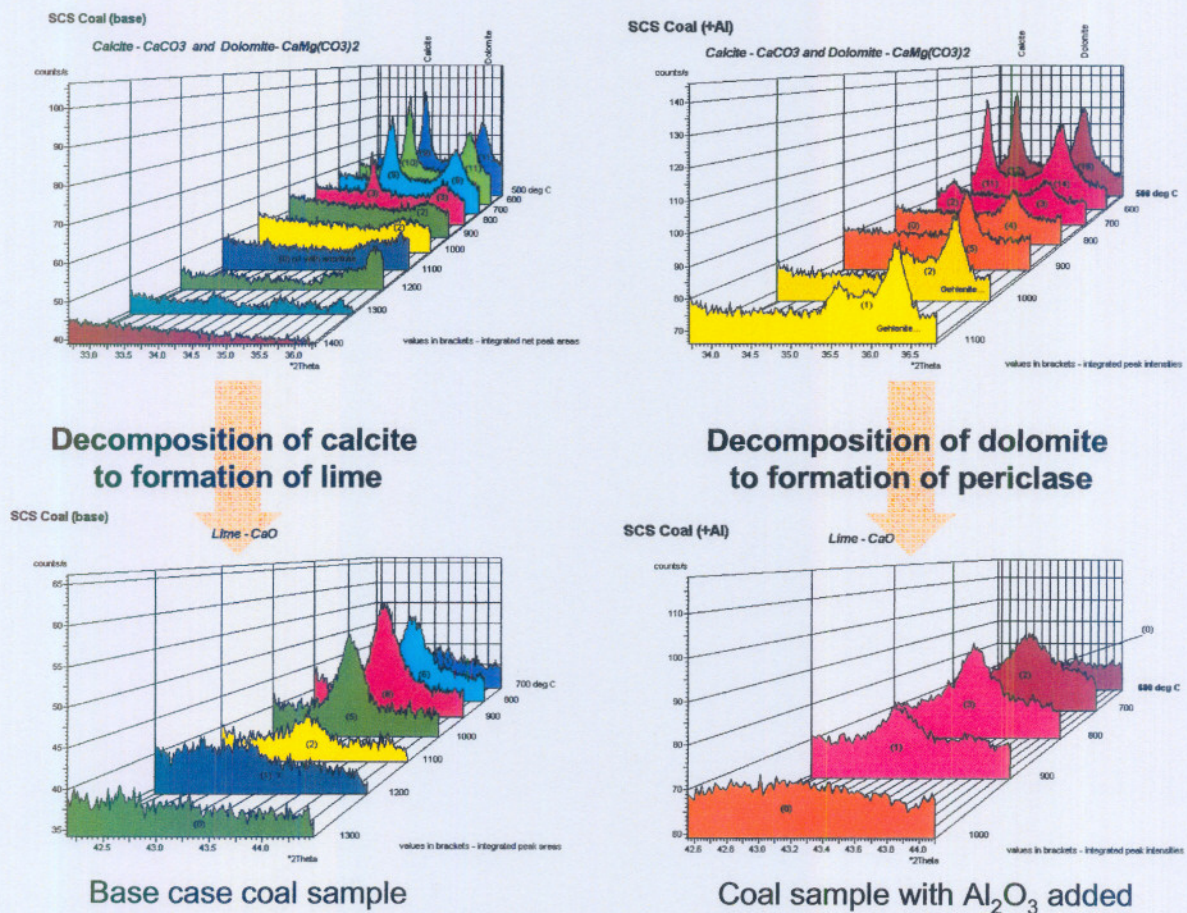
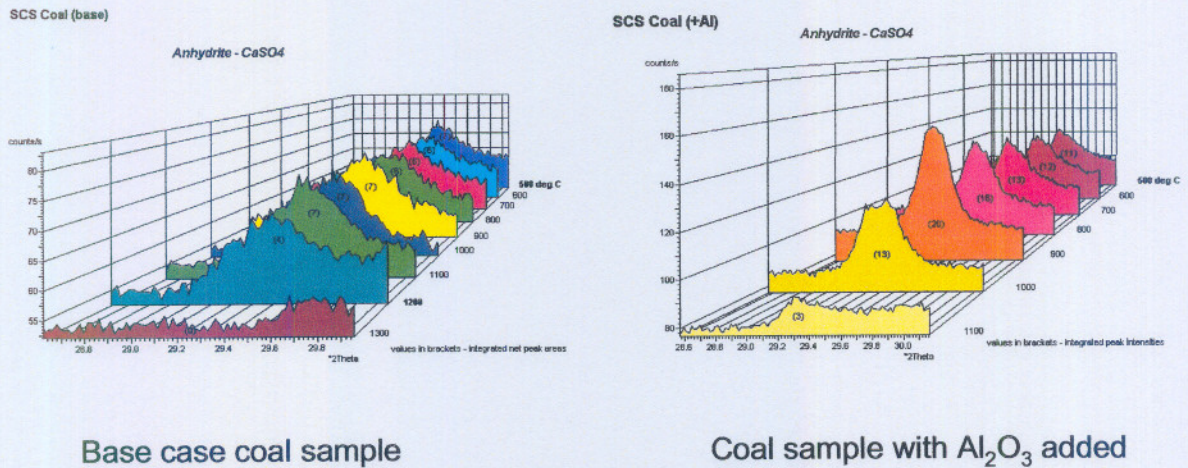


FIGURE 3.25 DECOMPOSITION OF CALCITE AND DOLOMITE AS FUNCTION OF TEMPERATURE

The formation of anhydrite (CaSO_4) in both the base case sample and manipulated coal sample took place after the formation of free lime and decomposed at the same temperature (Figure 3.26).

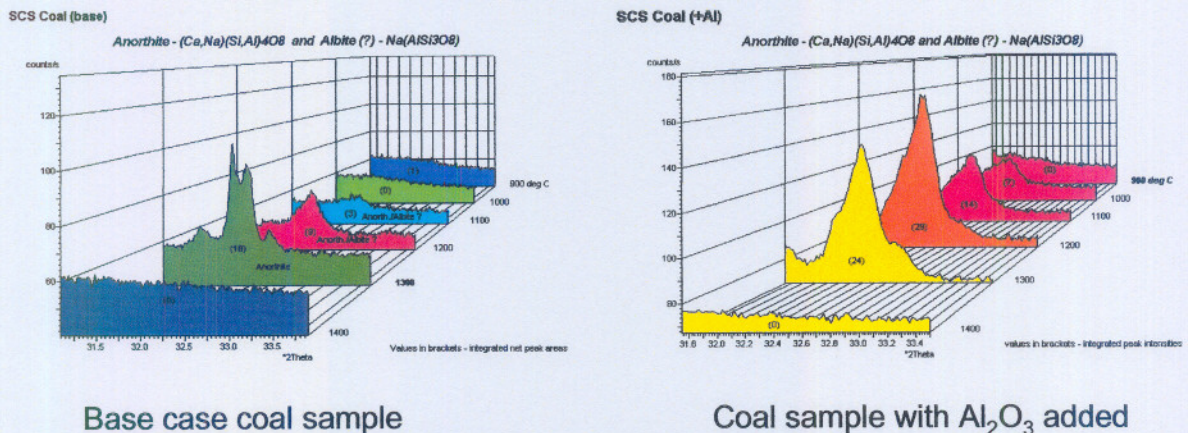


Base case coal sample

Coal sample with Al_2O_3 added

FIGURE 3.26 FORMATION AND DECOMPOSITION OF ANHYDRITE AS FUNCTION OF TEMPERATURE

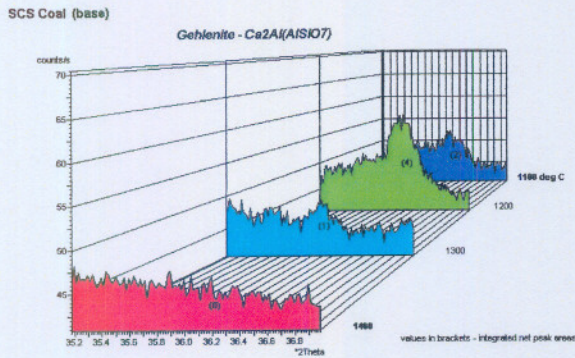
At 1000°C anorthite ($\text{CaAl}_2\text{Si}_2\text{O}_8$) and gehlenite ($\text{Ca}_2\text{Al}_2\text{SiO}_7$) started to crystallise. Anorthite and gehlenite were formed as product from anhydrite, alumina and silica at temperatures from 900°C to 1100°C (Figure 3.27 and 3.28).



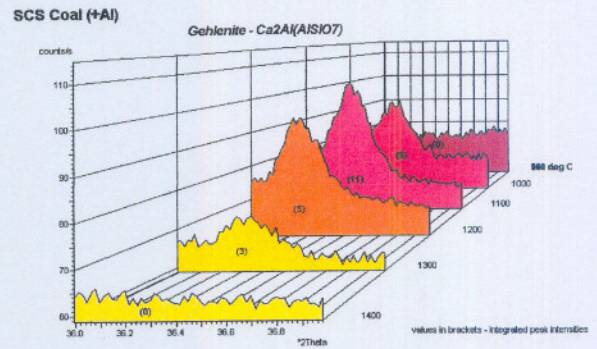
Base case coal sample

Coal sample with Al_2O_3 added

FIGURE 3.27 FORMATION OF ANORTHITE AS FUNCTION OF TEMPERATURE



Base case coal sample



Coal sample with Al₂O₃ added

FIGURE 3.28 FORMATION OF GEHLENITE AS FUNCTION OF TEMPERATURE

The biggest and most significant difference in mineral formation and mechanistic behaviour of the elements and minerals with the addition of Al₂O₃ is the formation of mullite. A summary of the HT-XRD results of mullite (as presented in Appendix B Table H and I) is given in Table 3.16.

TABLE 3.16 CRYSTALLINE PHASES OF MULLITE IN BASE CASE COAL SAMPLE AND MANIPULATED COAL SAMPLE WITH Al₂O₃ AND AT DIFFERENT TEMPERATURES

Identified mullite in SCS Coal (base) + Al ₂ O ₃ manipulated coal ashed to 500 °C	25	500	600	700	800	900	1000	1100	1200	1300	1400
Mullite Al ₆ Si ₂ O ₁₃ (Base case coal sample)	----	----	----	----	----	----	----	----	traces	traces	----
Mullite Al ₆ Si ₂ O ₁₃ (Manipulated coal sample)	---	----	----	----	----	----	----	Yes	Yes	Yes	Yes

From Table 3.16 it is evident that the appearance of mullite from 1100°C in the manipulated coal sample is very strong and can be identified up to a temperature of 1400°C. However, in comparison with last mentioned coal sample, the presence of mullite is only vaguely identified as a trace. The formation of mullite is also graphically given in Figure 3.29 as it formed in the coal sample with the Al₂O₃ added.

SCS Coal (+Al)

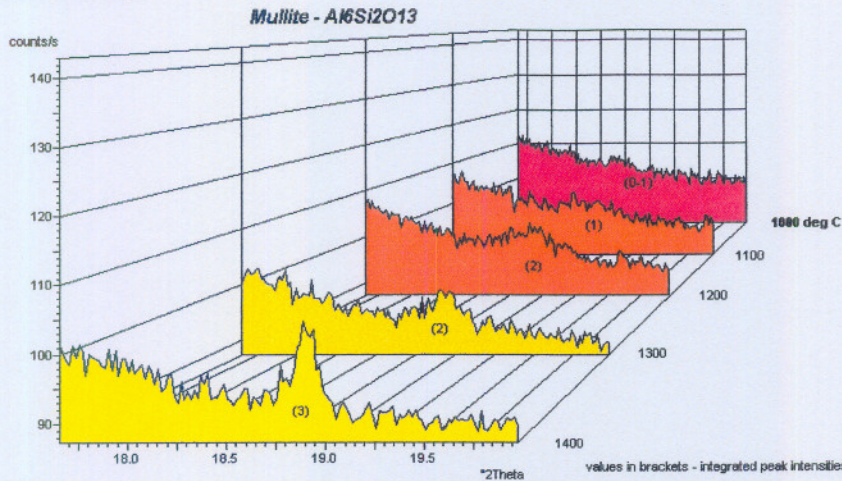
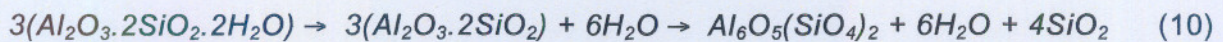


FIGURE 3.29 FORMATION OF MULLITE AS FUNCTION OF TEMPERATURE

The mechanistic formation of mullite under normal conditions in for example the base case coal can be described as the formation of mullite from kaolinite through a metastable phase called metakaolinite [Alpern, et. al., 1984].



Kaolinite decomposed to metakaolinite around 450°C to 800°C with the formation of mullite from a temperature of 850°C to 1000°C. The amount of mullite that can be formed is thus directly correlated with the amount of kaolinite in the coal sample. Mullite formation can also take place with the availability of free Al_2O_3 in the coal that can react with free SiO_2 . However, free Al_2O_3 is normally not present in coal.

With the addition of free Al_2O_3 to the coal, the free SiO_2 (quartz) in the coal can react with the Al_2O_3 to form mullite ($\text{Al}_6\text{O}_5(\text{SiO}_4)_2$) directly. The increase in mullite formation in the manipulated coal sample is thus explained by the chemistry where SiO_2 and Al_2O_3 react to form mullite. With the addition of Al_2O_3 more mullite crystallises. A network former, [Williamson, 2005 and Melzer, 2005], has the tendency to increase viscosity and durability of the silica melt. As mullite is a high temperature melting phase, this acts then as a dilutant in the mineral structure causing the AFT of the ash mixture to increase and less liquid to form. It has also been noted from Table 3.16 that the remaining Al_2O_3 not reacted with SiO_2 formed mullite and changed to a stable $\alpha\text{-Al}_2\text{O}_3$ at 1100°C.

CHAPTER 4

FACTSAGE MODEL DEVELOPMENT AND OTHER TOOLS USED FOR QUANTIFYING EXPERIMENTAL RESULTS

The tendency for coal ash to slag is related to the chemical composition and the AFT, which explains the reason why modelling tools such as viscosity modelling of the total ash blend to be an important tool in describing the ash properties and slagging tendency at specific temperatures [Gibb, 1996]. Even with the same chemical composition different flow temperatures may occur. Another software tool that was used in this study is FactSage and is described in **Section 4.1**. Viscosity and sintering modelling are also referred to in **Section 4.2**.

4.1 *FactSage modelling*

The theoretical FactSage 5.3 modelling program was used as modelling tool in this study, to confirm the results obtained with regards to slagging and flow properties of mineral matter during Sasol-Lurgi fixed bed gasification and to start initiating a modelling tool which can accommodate changes or influences of organic and inorganic components simultaneously.

The purpose of using the FactSage model in this study will only be to confirm the slagging behaviour and changes in mineral composition affecting slag formation in the gasification process with and without feed manipulation. The emphasis in this study was only on the **inorganic components and slag formation**, although the organic components were included in order to simulate the gasification process as close as possible to the actual operating conditions. The step-by-step guide on how the model was development is given in Appendix C.

4.1.1 *FactSage model development and inputs for base case model*

In order to simulate the Sasol-Lurgi fixed bed gasification process as close as possible to the actual gasification process, similar flows (kg/hr) and conditions (temperature, pressure and mass flows) were used in the modelling.

The average coal flow into a MKIV Sasol-Lurgi gasifier at a medium to high oxygen load of 11 500 kg/hr is 51 000 kg/hr as received (AR) coal. The coal consists of moisture, fixed carbon, volatiles and minerals and the 51 000 kg/hr AR coal feed is

the sum of these four components. This implies that the mass % as determined from the proximate analysis can be normalised to a mass flow (kg/hr) of 51 000 kg/hr as given in Table 4.1.

TABLE 4.1 MOISTURE, FIXED CARBON, VOLATILE MATTER AND ASH CONTENT OF SOUTH AFRICAN COAL BLEND USED IN THIS STUDY

Component	Mass %	Mass flow (kg/hr)
Moisture	5.0	2550
Fixed carbon	46.3	23613
Volatile matter	22.9	11679
Ash	25.8	13158
TOTAL	100	51000

The input into FactSage has to be in elemental form i.e. carbon (C), hydrogen (H), nitrogen (N), sulphur (S) and oxygen (O), and the sum of the fixed carbon and volatile matter is assumed to be the flow of the elemental components C, H, N, S and O. Taken into account that most models do not treat or incorporate tar, the tar and oil portion first have to be deducted from the mass flow portion of fixed carbon plus the volatile matter. Thermodynamic software i.e. SimuSage cannot treat tar as a component. The composition of the volatile matter as given in Table 4.1 can be split into the different elements shown in Table 4.2. The volatile matter composition was determined by means of a pyrolysis experiment, where the tar and char were measured, and the gas was captured and analysed. The sum of the volatile matter, as indicated in Table 4.2 was taken as the volatile matter component as shown in Table 4.1.

TABLE 4.2 COMPOSITION OF VOLATILE MATTER

Property	Mass %	Mass flow (kg/hr)
H ₂ O	2.9	1479
H ₂	0.15	76
CH ₄	4.01	2045
CO	0.98	499
CO ₂	7.2	3672
N ₂	2.1	1050
Tar and oils	5.6	2858
TOTAL	22.9	11679

The amount of tar and oils that have to be deducted from the mass flow for fixed carbon plus volatile matter was taken as 2858 kg/hr. The flow for fixed carbon and volatile matter then equals 23613 kg/hr of fixed carbon plus 11679 kg/hr volatile matter minus 2858 kg/hr for the tar and oil portion, which then results in a mass flow of 32434 kg/hr. Tar and oils cannot be treated in the current model and databasis linked to FactSage.

The mass flow for the fixed carbon and volatile matter are then further normalised to an elemental composition similar to that of an ultimate analysis and is given in Table 4.3.

TABLE 4.3 CARBON, HYDROGEN, NITROGEN, SULPHUR AND OXYGEN (DRY ASH FREE BASIS) FLOW OF SOUTH AFRICAN COAL BLEND USED IN THIS STUDY

Property	Mass %	Mass flow (kg/hr)
Carbon (C)	78.8	25557
Hydrogen (H)	4.1	1329
Nitrogen (N)	2.2	713
Sulphur (S)	2.1	681
Oxygen (O) by difference	13.0	4154
TOTAL	100	32434

The mass ash flow amount of 13158 kg/hr consists of different mineral species [Van Alphen, 2004] as analyzed by CCSEM technique and then the ash flow is normalised to a mass flow for the different mineral species and is given in Table 4.4.

TABLE 4.4 MINERAL COMPOSITION MASS FLOW OF SOUTH AFRICAN COAL BLEND USED IN THIS STUDY

Mineral	Formula	Mass %	Mass flow (kg/hr)
Pyrite	FeS ₂	4.0	526
Quartz	SiO ₂	20.0	2631
Microcline	KAlSi ₃ O ₈	1.9	250
Muscovite / Illite	KAl ₃ Si ₃ O ₁₀ (OH) ₂	2.9	381
Kaolinite	Al ₂ O ₃ .2SiO ₂ .2H ₂ O	52.5	6913
Anatase	TiO ₂	0.3	39
Ankerite	Ca(Mg, Fe, Mn)(CO ₃) ₂	0.0	-
Siderite	Fe(CO ₃)	0.0	-
Calcite	CaCO ₃	6.7	881
Dolomite	CaMg(CO ₃) ₂	10.1	1328
Apatite	Ca ₅ (PO ₄) ₃ (F, OH)	0.5	65
Gypsum	CaSO ₄ .2H ₂ O	1.1	144
TOTAL		100	13158

The gasification process was, for modelling purposes, divided into three distinct zones (Figure 4.1),

- (1) the drying and devolatilisation zone,
- (2) gasification zone and
- (3) the combustion and ash zone.

Each zone was treated as a separate zone for modelling purposes in FactSage.

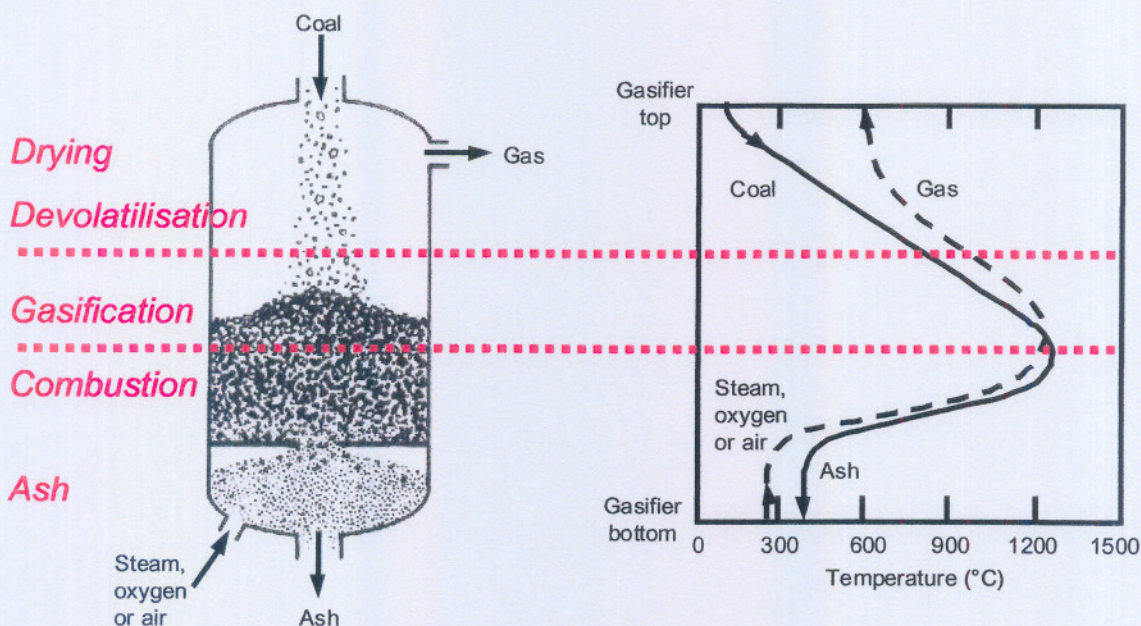


FIGURE 4.1 TYPICAL ZONES IN THE SASOL-LURGI GASIFICATION PROCESS [Slaghuys, 1993]

The inputs, as specified in Tables 4.3 and 4.2, together with the gas flow and temperature zones, as specified for each zone from the current ASPEN model (Table 4.5), were used as parameters for the FactSage model.

TABLE 4.5 TABULATED GAS FLOW FROM ZONES IN THE SASOL-LURGI GASIFIER (DATA FROM ASPEN THERMODYNAMIC MODEL)

Gas species	Gasification zone outlet gas into pyrolysis and drying zone (kg/hr)	Combustion zone outlet gas into gasification zone (kg/hr)	Agent flow into gasifier (kg/hr)
H ₂ O	27 159	59 099	50 900
O ₂	0	0	11 856
C	0	0	
H ₂	1 961	0	
CH ₄	6 417	0	
CO	15 761	0	
CO ₂	42 742	16 110	
N ₂	142	142	142
T(°C)	690	1200	344

The model operates on the principle that the coal (inorganic and organic components) flows from the top downwards in the gasifier and the gas from the zone below flows upwards into the zone that is being modelled, i.e. the coal that flows into the drying and devolatilization zone is brought into contact, to react with the gas that flows out of the gasification zone – thus a counter-current effect.

4.1.1.1 Drying and devolatilization zone

The 1st zone to be modelled was the drying and devolatilisation zone. The coal (organic and inorganic components) was introduced with the specific mass flow, as reactants, whereas each element, reactant or species was added separately. A summary of the elements added as the total coal stream is given in Table 4.6.

TABLE 4.6 SUMMARY OF INPUT REACTANTS INTO FACTSAGE DEVOLATILIZATION AND DRYING ZONE

Element	Mass flow (kg/hr)
H ₂ O	2550
C	25557
H	1329
N	713
S	681
O	4154
Pyrite	526
Quartz	2631
Microline	250
Muscovite / Illite	381
Kaolinite	6913
Anatase	39
Ankerite	-
Siderite	-
Calcite	881
Dolomite	1328
Apatite*	65
Gypsum	144
Tar and oils**	2858
TOTAL	51000

* Not included in model due to FactSage software limitations.

** Not included in model.

The gas flow from the gasification zone was added as reactants that reacted with the coal (Table 4.7). The temperature range according to the ASPEN model for this zone was from ambient conditions when the coal enters the gasifier to 690°C, the end of the pyrolysis zone.

TABLE 4.7 GAS FLOW FROM GASIFICATION ZONES

Gas(kg/hr)	Gasification zone outlet gas into pyrolysis and drying zone
H ₂ O	27 159
O ₂	0
C	0
H ₂	1 961
CH ₄	6 417
CO	15 761
CO ₂	42 742
N ₂	142
T(°C)	690

Schematically this implies that the up-flowing gas from the gasification zone reacts with the down flowing coal and mineral matter into the gasifier as shown in Figure 4.2.

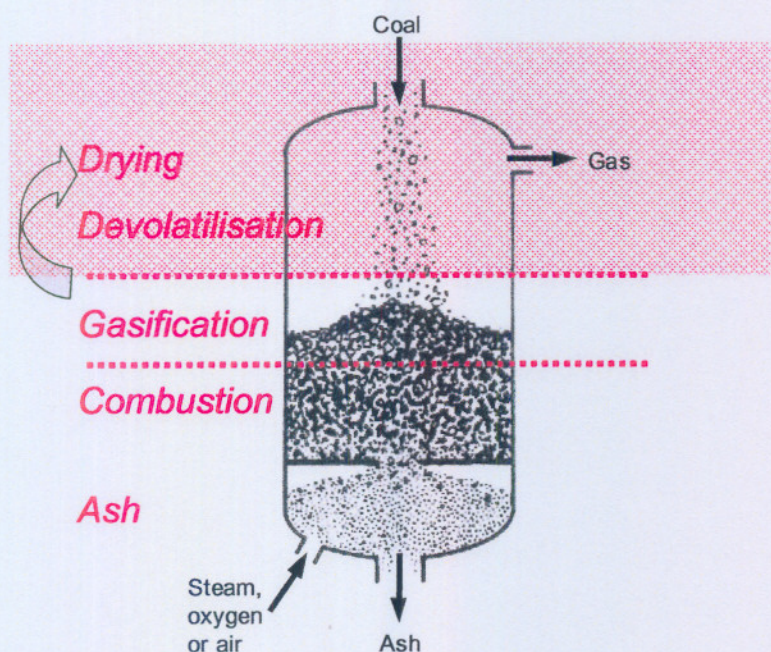


FIGURE 4.2 GAS AND SOLIDS FLOW IN DRYING AND PYROLYSIS ZONE

4.1.1.2 Gasification zone

A similar approach and procedure, as used for the drying and devolatilization zone, was followed in order to model the gasification zone. The differences in the models were mainly in the temperature ranges and reactants as input. The results with regards to the mineral matter from the drying and devolatilization zone, were then subsequently used as input for the FactSage gasification zone model.

The temperature range for the gasification zone was specified as 690°C when the coal enters the zone and reacted with the up-flowing gas from the combustion zone with a temperature of 1200°C. The reactants in the model for the gasification zone were those from the drying and devolatilization zone obtained for the coal flow from the FactSage model, together with the up-flowing gas from the combustion zone as obtained from the Aspen model.

4.1.1.3 Combustion zone

A similar approach and procedure as for the drying and devolatilization and gasification zone was followed in order to model the combustion zone. The differences in the models were mainly in the temperature ranges and reactants as

input. The results with regards to the mineral matter from the gasification zone as per the FactSage model were used as input for the FactSage combustion zone model.

The temperature range for the gasification zone was specified as 1200°C when the coal and minerals enter the zone and reacted with the up-flowing agent into the gasifier with a temperature of 344°C. The reactants in the model for the combustion zone were those of the results from the gasification zone as obtained from the FactSage model for the coal flow, together with the up-flowing agent into the gasifier as obtained from the Aspen model.

4.1.2 FactSage modelling results

The discussion of the results, although integrated as one unit, will be done in three sections (drying and devolatilization, gasification and combustion). The focus on the discussion of the results will be on the slag formation and the mineral species affecting the slag and liquid formation inside the gasifier. The results of both the base case coal sample and the manipulated coal sample will be discussed. Although the results are discussed and presented as actual mass flows through a MKIV gasifier in kg/hr, the emphasis of the discussion of the results should be on the formation and transformation of mineral species, trends and variations, rather than on the actual flows. It has to be noted that no kinetic effect has been taken into account.

The input data to the model for the base case, and the blends with 2 mass % to 10 mass % Al_2O_3 addition, is given in Table 4.8. The addition of Al_2O_3 was decided on to be modelled in detail with FactSage based on the fact that Al_2O_3 has the biggest and most significant effect on the AFT with the smallest amounts added to the coal blend.

SiO_2 (s_x) refers to solid quartz that undergoes structural and volume changes.

TABLE 4.8 SUMMARY OF INPUT REACTANTS INTO FACTSAGE DEVOLATILIZATION ZONE

Element	Base case (kg/hr)	Base case + 2% Al ₂ O ₃ (kg/hr)	Base case + 4% Al ₂ O ₃ (kg/hr)	Base case + 6% Al ₂ O ₃ (kg/hr)	Base case + 8% Al ₂ O ₃ (kg/hr)	Base case + 10% Al ₂ O ₃ (kg/hr)
H ₂ O	2550	2499	2448	2397	2346	2295
C	25557	25046	24535	24024	23512	23001
H	1329	1302	1276	1249	1223	1196
N	713	699	684	670	656	642
S	681	667	654	640	627	613
O	4154	4071	3988	3905	3822	3739
Pyrite	526	515	505	494	484	473
Quartz	2631	2578	2526	2473	2421	2368
Microline	250	245	240	235	230	225
Muscovite / Illite	381	373	366	358	351	343
Kaolinite	6913	6775	6636	6498	6360	6222
Anatase	39	38	37	37	36	35
Ankerite	-	0	0	0	0	0
Siderite	-	0	0	0	0	0
Calcite	881	863	846	828	811	793
Dolomite	1328	1301	1275	1248	1222	1195
Apatite*	65	64	62	61	60	59
Gypsum	144	141	138	135	132	130
Tar and oils**	2858	2801	2744	2687	2629	2572
Al ₂ O ₃ added	-	1020	2040	3060	4080	5100
TOTAL	51000	51 000	51 000	51 000	51 000	51 000

* Not included in model due to FactSage software limitations.

** Not included in model.

4.1.2.1 The Drying and devolatilization zone

The drying and devolatilization zone only took into account the temperature range from 25°C to 690°C and the results from the model are given in Table 4.9.

TABLE 4.9 MINERAL MATTER OUTPUT FROM DRYING AND DEVOLATILIZATION ZONE WITH Al₂O₃ ADDITION at 690°C

Mineral composition (mass kg/hr)	Base case	2% Al ₂ O ₃	4% Al ₂ O ₃	6% Al ₂ O ₃	8% Al ₂ O ₃	10% Al ₂ O ₃
CaAl ₂ Si ₂ O ₈ - Feldspar	4685	4589	4493	4402	4306	4214
SiO ₂ quartz(h)	2633	1979	1325	672	6	
Mg ₂ Al ₄ Si ₅ O ₁₈ cordierite	2106	2063	2020	1979	1936	1895
Al ₂ SiO ₅ andalusite	598	2208	3818	5426	7019	7238
KAlSi ₂ O ₆ leucite(rhf)-b	404	396	388	380	372	780
FeS	342	335	294	280	246	-
(FeO) ₂ (TiO ₂) ulvospinel	-	-	86	103	100	-
(FeO)(TiO ₂) ilmenite	74	72	11	-	-	66
FeAl ₂ O ₄ hercynite	-	-	-	-	-	619
Al ₂ O ₃	-	-	-	-	-	521
Fe ₃ Al ₂ Si ₃ O ₁₂ almandine	-	-	-	-	52	-

No slag formation in the base case coal was observed, as was to be expected. However, some interesting findings from the modelling of the drying and devolatilization zone on the base case coal blend are graphically illustrated in Figure 4.3.

The naming convention SiO_2 (sx) refers to a stable phase for a specific mineral. For example SiO_2 (s1) and SiO_2 (s2) refers to stable mineral phases at that specific temperature transformed to the other stable phase, i.e. α - SiO_2 to β - SiO_2 . This is specifically observed with SiO_2 and will be observed in all FactSage graphs that will follow. For example, SiO_2 (s3) indicates β - SiO_2 to tridymite and SiO_2 (s4) that of tridymite to cristobalite.

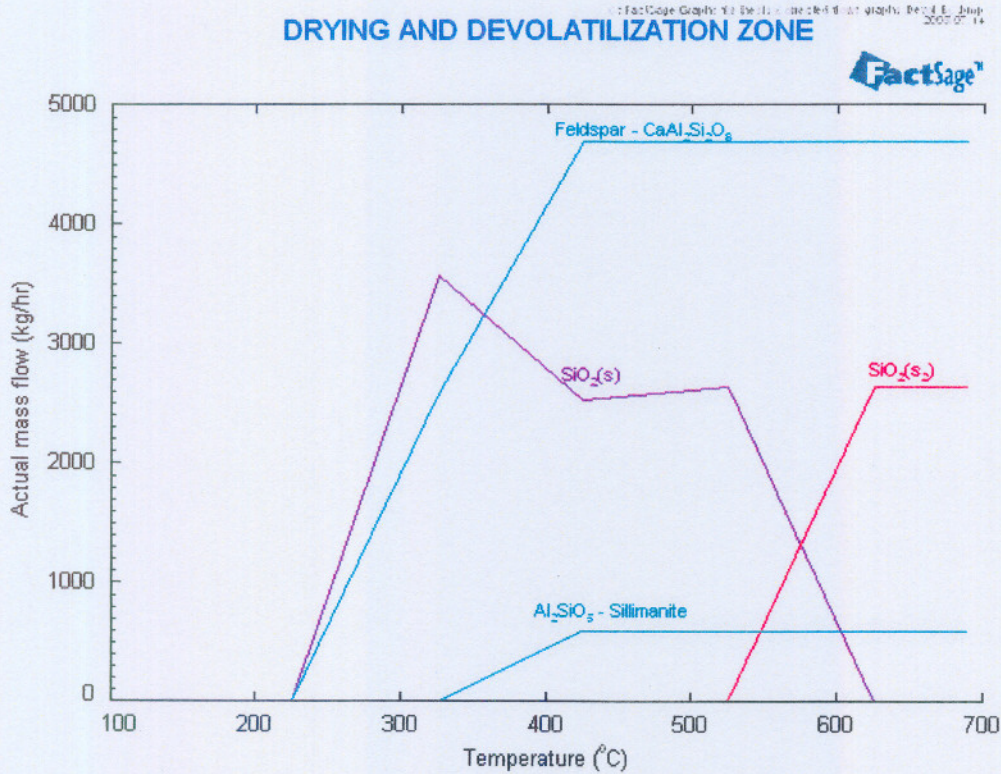
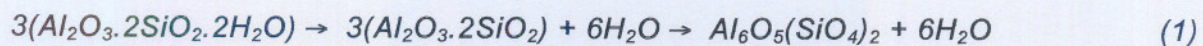


FIGURE 4.3 MODELLING RESULTS OF MINERAL MATTER IN DRYING AND DEVOLITILIZATION ZONE RESULTS OF BASE CASE COAL

The formation of sillimanite (Al_2SiO_5) was most probably formed due to the decomposition of the kaolinite present in the base case coal sample. Kaolinite starting to decompose to metakaolinite at about 450°C with the formation of amongst others mullite at a temperature of 850°C to 1000°C . The observed sillimanite is possibly the on-set towards (intermediate mineral) the meta-kaolinite formation [Alpern, *et. al.*, 1984]:



Kaolinite is only a group name and can stoichiometrically also be given as $(\text{OH})_8\text{Al}_4\text{Si}_4\text{O}_{10}$ [Slaghuys, 1989]. Kaolinite is a mineral with a certain specific composition, which of course can be written in different ways. The amount of

metakaolinite and mullite that can be formed is directly correlated with the amount of kaolinite in the original coal sample. Mullite formation can also take place with the availability of free Al_2O_3 in the coal that can react with SiO_2 . However, free Al_2O_3 is normally not present in coal and the presence of the Al_2SiO_5 , formed as an intermediate phase during the decomposition of kaolinite, and the onset of sillimanite as the intermediate phase towards the formation of mullite. The mechanistic formation of mullite under normal conditions, as already referred to in for example the base case coal, can be described as the formation of mullite from kaolinite through a metastable phase called metakaolinite or sillimanite [Alpern, *et. al.*, 1984]. The feldspar that formed, probably formed as a product between the SiO_2 , Al_2O_3 and Ca-containing species. Feldspar is one is the mineral species which has the lowest melting temperature and causes the highest amount of slag-liquid.

The naming sillimanite from the FactSage program probably refer to meta-kaolinite.

In explaining the formation of sillimanite, it has been observed that the sillimanite formation further increased with the addition of Al_2O_3 (Figure 4.4).

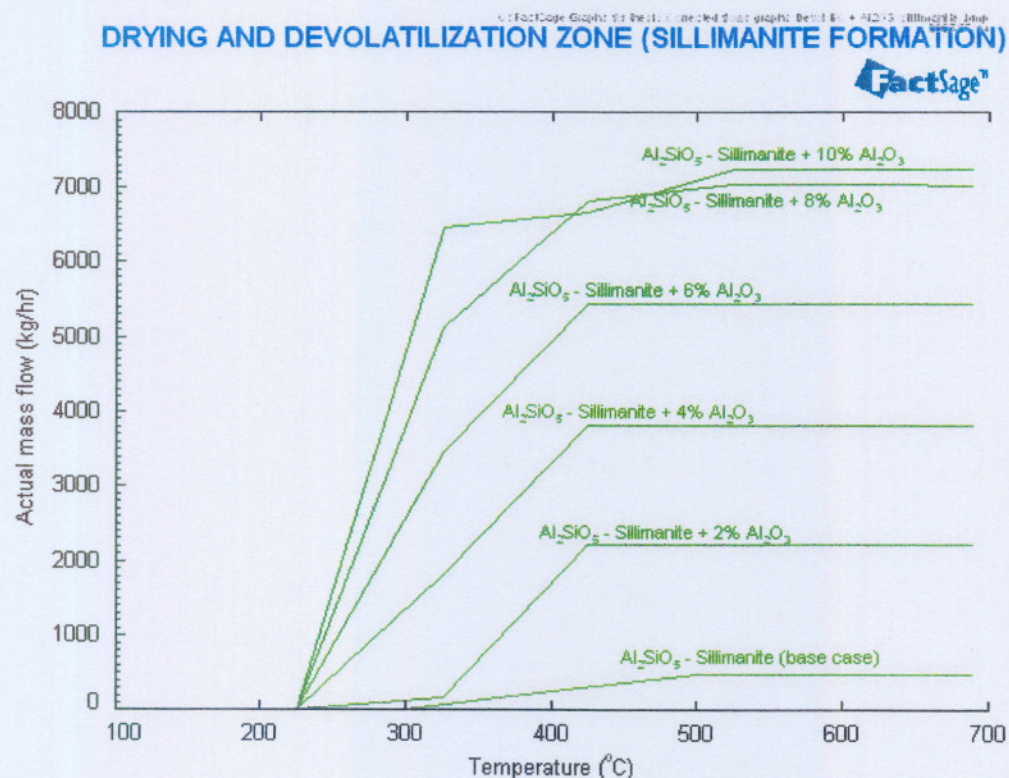


FIGURE 4.4 SILLIMANITE FORMATION IN DRYING AND DEVOLATILIZATION ZONE WITH Al_2O_3 ADDITION

The formation of sillimanite increased from the base case coal up to an addition of 8%

Al_2O_3 , after which it did not increase any more. The additional sillimanite that form can also be a product of the direct reaction between the Al_2O_3 added and the SiO_2 in the coal, as mullite formation from kaolinite is taking place with the decomposition of kaolinite to metakaolinite. If the sillimanite formation is a direct reaction between Al_2O_3 added and the SiO_2 in the coal, then the SiO_2 trends have to show similar trends as for the sillimanite formation, up to about 8% addition where all the SiO_2 will be taken up by the Al_2O_3 .

If it is true that the mullite or intermediate phases were formed as a product between the Al_2O_3 added and the SiO_2 in the coal, then a decrease in SiO_2 content has to be seen as is shown in Figure 4.5.

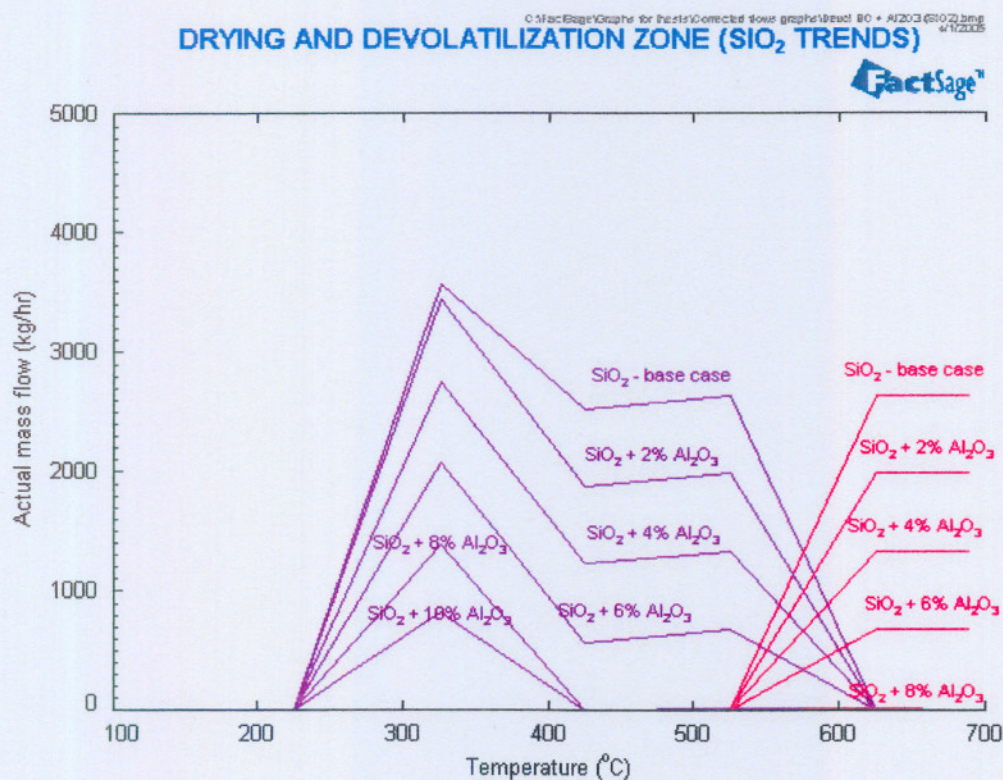


FIGURE 4.5 SiO_2 TRENDS IN THE DRYING AND DEVOLATILIZATION ZONES WITH Al_2O_3 ADDITION

From the graph it can be seen that the SiO_2 content decreased with the formation of sillimanite, implying that a reaction between the Al_2O_3 and SiO_2 definitely took place in order to form sillimanite or the intermediate, sillimanite/metakaolinite up to the formation of mullite. At 8% Al_2O_3 addition, at the temperature of 400°C, the SiO_2 has been taken up or already reacted.

4.1.2.2 The Gasification zone

The gasification zone is in the temperature range of 690°C to 1200°C and the output results from the gasification model are given in Table 4.10.

TABLE 4.10 MINERAL MATTER OUTPUT FROM GASIFICATION ZONE WITH Al_2O_3 ADDITION AT 1200°C

Mineral composition (mass kg/hr)	Base case	2% Al_2O_3	4% Al_2O_3	6% Al_2O_3	8% Al_2O_3	10% Al_2O_3
Mullite	724	2126	3528	4944	6351	7752
Slag-Liquid composition						
MgO	150	146	143	140	137	130
FeO	315	305	301	293	285	285
SiO ₂	1766	1727	1685	1656	1615	1358
TiO ₂	37	36	35	35	34	35
Ti ₂ O ₃	0.001	0.001	0.001	0.001	0.001	0.001
CaO	219	214	250	205	200	242
Al ₂ O ₃	635	621	726	595	571	726
K ₂ O	3	3	3	2	2	0.01
MgS	0.001	0.001	0.001	0.001	0.001	0.001
CaS	0.001	0.001	0.001	0.001	0.001	0.001
FeS	0.001	0.001	0.001	0.001	0.001	0.001
K ₂ S	0.001	0.001	0.001	0.001	0.001	0.001
CaAl ₂ Si ₂ O ₈ Feldspar	3600	3527	3457	3384	3314	3356
SiO ₂ tridymite(h)	1922	1489	1056	604	167	0
Mg ₂ Al ₄ Si ₅ O ₁₈ cordierite	1017	997	980	958	940	946
KAlSi ₂ O ₆ leucite(rhf)-b	388	380	372	365	357	778

The most important findings from the modelling results of the gasification zone on the base case coal blend are graphically illustrated in Figure 4.6.

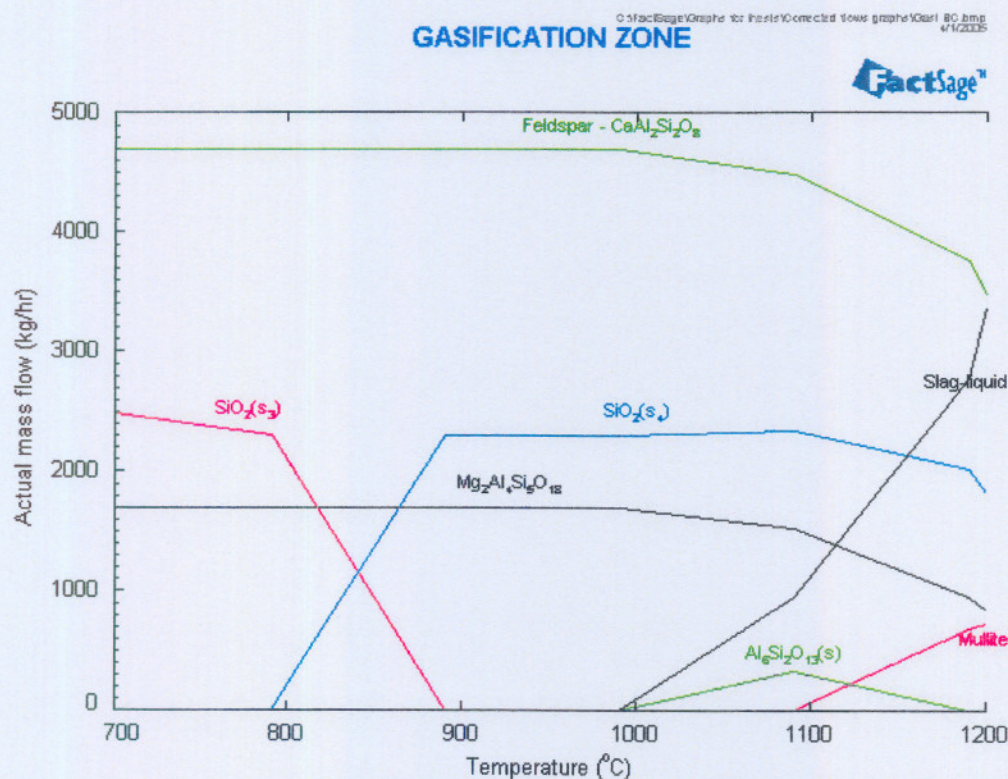


FIGURE 4.6 MODELLING RESULTS OF MINERAL MATTER IN THE GASIFICATION ZONE OF CHAPTER 4: FACTSAGE MODEL DEVELOPMENT AND OTHER TOOLS USED FOR QUANTIFYING EXPERIMENTAL RESULTS

THE BASE CASE COAL

From Figure 4.6 it is clear that slag-liquid formed at a temperature of 1000°C, with a decrease in the feldspar content. Mullite formation was also observed in the base case sample in the temperature range 1000°C and 1100°C. The decrease in the amount of SiO₂ at 1100°C is related to the formation of mullite, but also that the slag-liquid phase contained an amount of SiO₂. Take note that this mineral blend has already passed the gasification zone with temperatures >1250°C and is now in the combustion phase where cooling is taken place. The small amount of Al₆Si₂O₁₃ is probably a product of the decrease in mullite, which then also decomposes with cooling. However, this amount is negligibly small in comparison to the total amount of minerals. These findings on the slag-liquid and mullite formation were also observed from the HT-XRD analyses and discussed in **Section 5 of Chapter 3**. The findings from the experimental work and FactSage modelling are in agreement.

The changes in the slag-liquid formation in the gasification zone with Al₂O₃ addition to the base case coal sample are given in Figure 4.7.

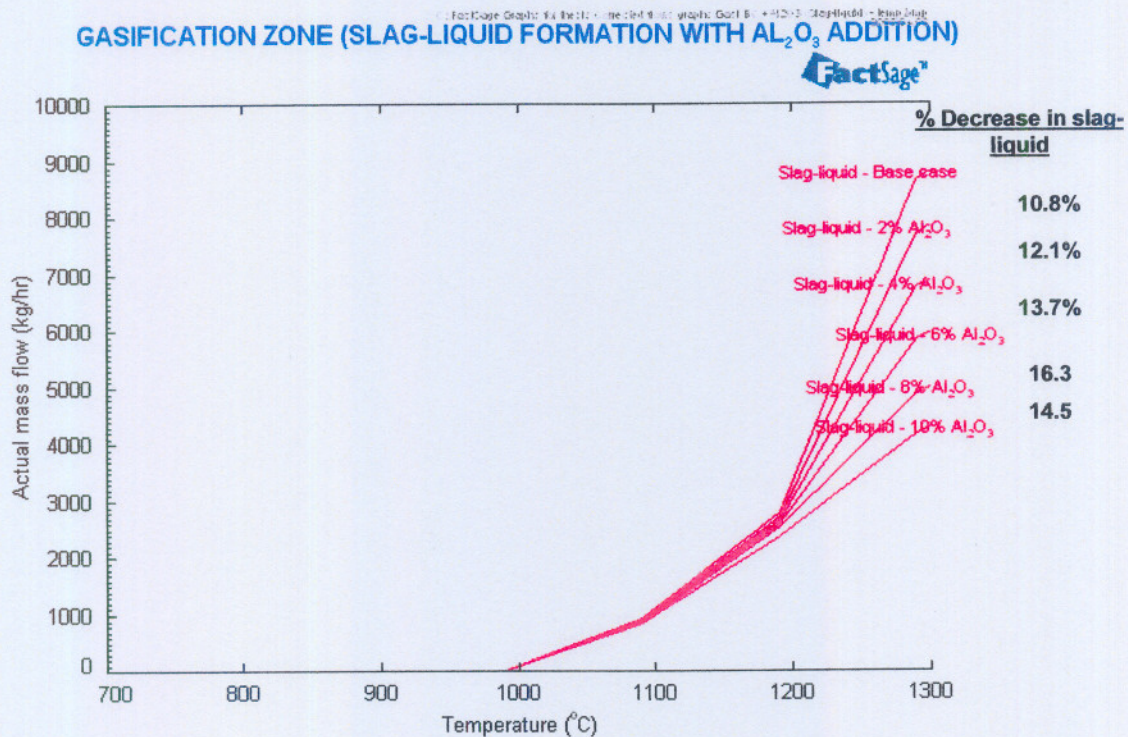


FIGURE 4.7 CHANGES IN SLAG-LIQUID FORMATION WITH AL₂O₃ ADDITION

The main conclusion clearly visible from Figure 4.7 is that the slag-liquid content decreased with the addition of Al₂O₃ only when the temperature was greater than

1100°C, with the most significant effect at temperatures greater than 1200°C, where the effect of the Al₂O₃ addition was significantly more visible, which is of importance in the operating region where the proposed higher gasifier temperature of more than 1250°C, is aimed for. The percentage of slag-liquid decreased with between 10 mass% and 16 mass % with every 2 mass % Al₂O₃ that was added, which is directly related to the amount of feldspar that is still present in a crystalline structure (not liquid or glass). It seems, according to these modelling results, that a saturation point has not been reached with up to 10% Al₂O₃ addition.

With the higher amount of Al₂O₃ added to the base case coal sample, the increased formation of sillimanite or meta-kaolinite and finally the formation of mullite was thus not only visible in the drying and devolatilization zone, but also in the gasification zone (Figure 4.8).

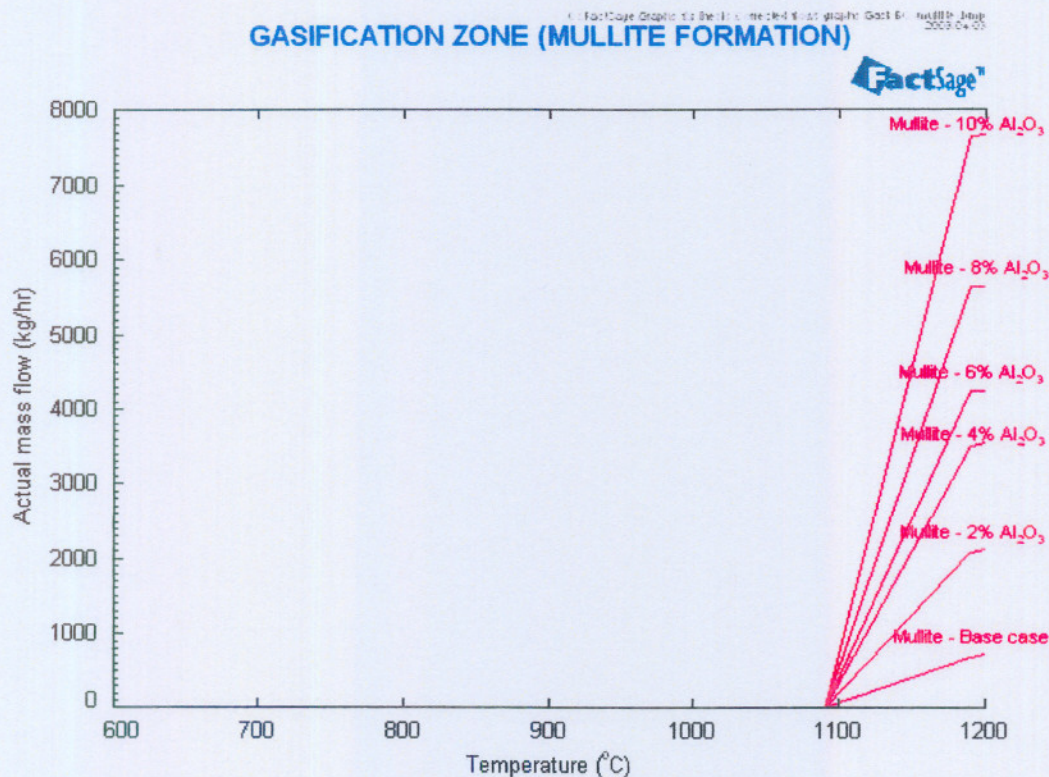


FIGURE 4.8 FORMATION OF MULLITE IN THE GASIFICATION ZONE

4.1.2.3 The Combustion zone

The combustion zone only took into account the temperature range from 1200°C to 344°C, which is a cooling step from gasification to the temperature where the agent (oxygen and steam) enters the gasifier at 344°C. The FactSage modelling output results of the combustion zone are given in Table 4.11.

TABLE 4.11 MINERAL MATTER OUTPUT FROM COMBUSTION ZONE WITH AL₂O₃ ADDITION AT 344°C

Mineral composition (mass kg/hr)	Base case	2% Al ₂ O ₃	4% Al ₂ O ₃	6% Al ₂ O ₃	8% Al ₂ O ₃	10% Al ₂ O ₃
SiO ₂ quartz(l)	3331	3271	2542	1926	1392	697
CaAl ₂ Si ₂ O ₈ anorthite	2967	89	-	-	-	-
CaAl ₄ Si ₂ O ₁₀ (OH) ₂ margarite	2460	6440	6723	6299	6163	5205
Mg ₅ Al ₂ Si ₃ O ₁₀ (OH) ₈ clinocl	800	781	766	750	735	718
KAl ₃ Si ₃ O ₁₀ (OH) ₂ muscovite	733	718	704	683	668	1420
Fe ₃ Al ₂ Si ₃ O ₁₂ almandine	650	629	622	603	-	-
(FeO)(TiO ₂) ilmenite	70	68	66	66	65	-
Al ₂ SiO ₅ andalusite	-	-	1546	3265	5099	7453
Fe ₃ O ₄ Magnetite	-	-	-	-	273	-
CaSO ₄ Anhydrite	-	-	-	-	-	450
Fe ₂ O ₃	-	-	-	-	-	316
TiO ₂ Rutile	-	-	-	-	--	35

The general mineral and slag-liquid trends are given in Figure 4.9, where it should be noted that the graphs in this section have to be read from right to left in order to obtain the actual picture of the coal and mineral flow from the top to the bottom in the gasifier. The temperature range is a cooling process from a temperature of 1200°C to 344°C in the bottom of the ash bed.

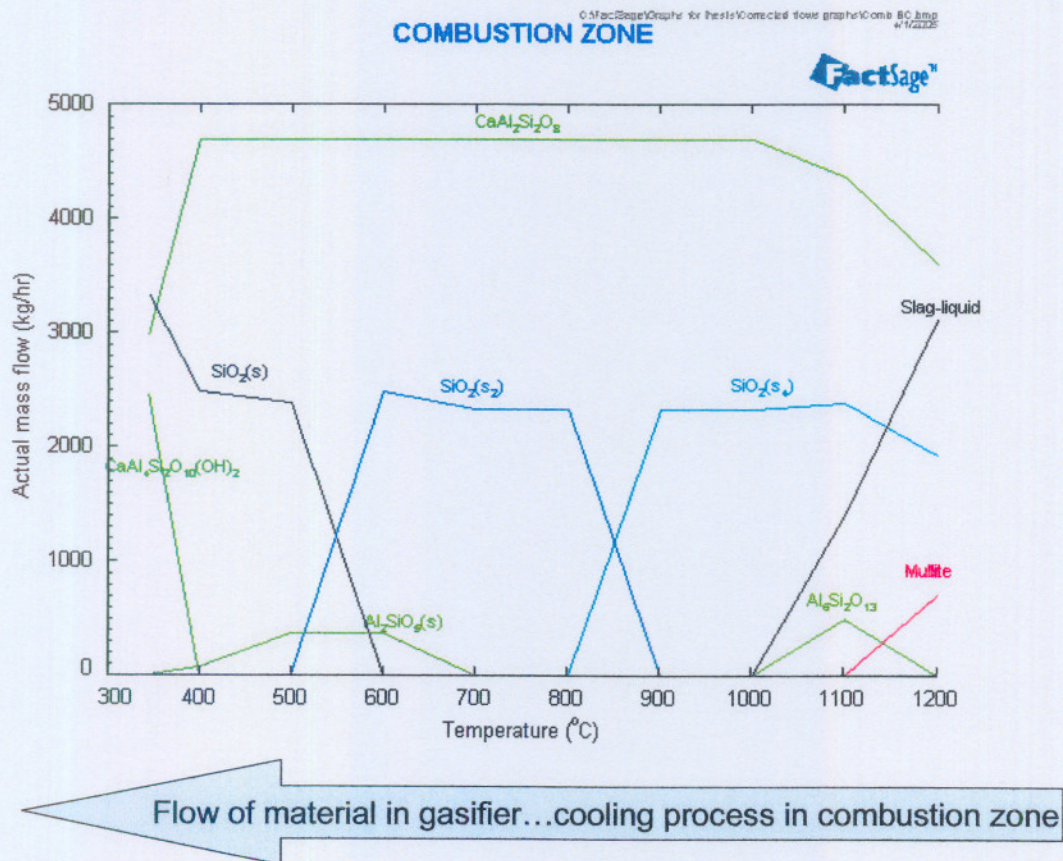


FIGURE 4.9 COMBUSTION ZONE OF BASE CASE COAL

From Figure 4.9, the decrease in slag-liquid content confirmed the cooling and actual mineral behaviour within the gasifier (combustion zone).

In conclusion, the HT-XRD findings were supported with FactSage thermochemical modelling of the gasifier, and indicated that feldspar formation (including anorthite) correlated with slag formation at temperatures around 1000°C. No slag formation in the base case coal was observed in the drying and devolatilization zone, as was to be expected. The formation of sillimanite (Al_2SiO_5) was most probably formed due to the decomposition of the kaolinite present in the base case coal sample. Kaolinite started to decompose to metakaolinite at about 450°C with the formation of amongst others mullite at a temperature of 850°C to 1000°C. The observed sillimanite species is possibly the on-set towards the meta-kaolinite formation. The amount of metakaolinite and mullite that can be formed is directly correlated with the amount of kaolinite in the original coal sample. The feldspar formed probably as a product between the SiO_2 , Al_2O_3 and Ca-containing species. In the gasification zone it was clear that slag-liquid formed at a temperature of 1000°C, with a decrease in the feldspar content. Mullite formation was also observed in the base case sample in the temperature range 1000°C and 1100°C. The decrease in the amount of SiO_2 at 1100°C is related to the formation of mullite, but also that the slag-liquid phase also contains an amount of SiO_2 in the molten form. The small amount of $\text{Al}_6\text{Si}_2\text{O}_{13}$ observed is probably a product of the decrease in mullite, which then also decomposes upon cooling.

4.2 Viscosity and sintering modelling

Viscosity modelling can be another tool for predicting slag mineral behaviour and used as a predicting tool. A conclusion made by Gibb (1996), to address all aspects of slagging, was that the key to the behaviour of ash deposits lies in understanding their consolidation by a viscous flow mechanism and the effect of the main fluxing agents on the viscosity of the minerals. The reason why viscosity and other mechanisms are also used together with the conventional AFT analysis is that the study of the AFT and cone deformation alone can be meaningless. Experimental evidence shows that the slag performance of blended coals can be either worse or better than the performance of the individual coals [Goni, *et. al.*, 2003]. If the liquid phase is highly fluid (low viscosity), it will enhance flow, but the un-melted solids can make the cone behave as a pseudo-plastic solid. It has also been mentioned and observed that the conditions at which conventional AFT analyses are conducted differ

significantly from real operating environments [EPRI, 1980].

The model used in this study for viscosity predictions was that of Kalmanovitch or the so-called modified Urbain model [Kalmanovitch, 1988]. This model was also used by Benson [1987] on similar studies. According to Benson [1987] sintering due to a viscous liquid phase occurred when the liquid on each particle exerted a surface tension force pulling the particles together. The model has been described in **Chapter 2**.

4.2.1 Viscosity modelling of mineral matter compositions obtained by dense medium separation of coal

The data obtained by means of dense medium separation, are presented by means of viscosity trends. The same data (Appendix B Table G) were used as input to the model to predict the viscosity of the individual dense medium fractions at different temperatures, and is given in Figure 4.10.

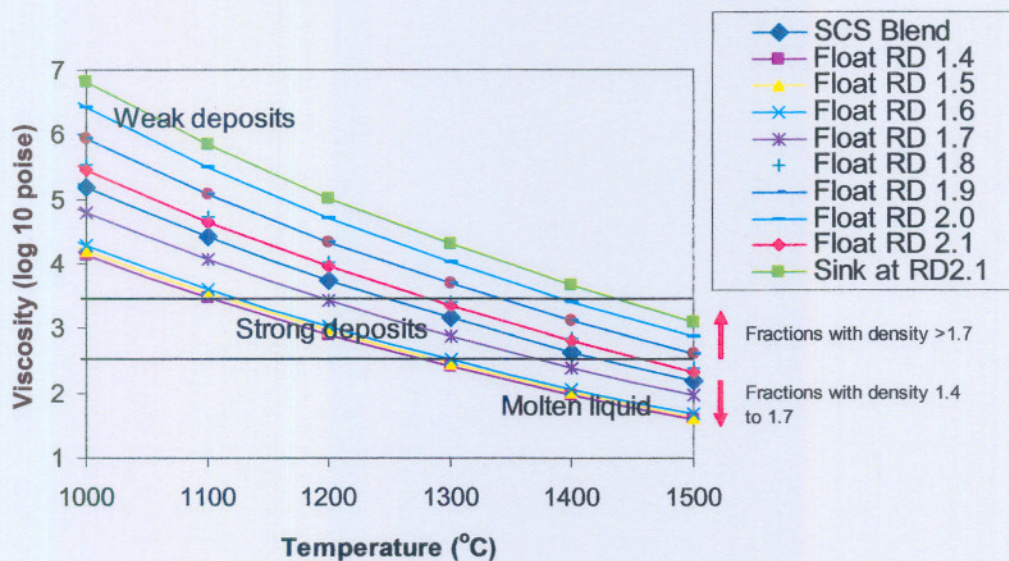


FIGURE 4.10 PREDICTED VISCOSITIES AT DIFFERENT TEMPERATURES FOR EACH INDIVIDUAL DENSE MEDIUM FRACTION

A weak deposit implies a viscosity where the minerals are not highly liquid and that the flowing properties increase (become more liquid) with increasing temperature. The Urbain predictions assume the composition to be completely molten and that the equation cannot accommodate the effect of undissolved or solid phases. With increasing temperature the viscosity becomes more liquid and moves from a weak deposit (less liquid) towards a strong deposit (more liquid) and eventually a molten liquid (highly viscous).

From Figure 4.10 the following conclusions can be drawn:

- Higher viscosity with an increasing relative density fraction can be seen for all temperatures. As an example, the relationship between the viscosity and the relative densities at 1300°C is given in Figure 4.11. The data at relative density = 2.1 is not only observed in the viscosity predictions, which are based on the ash composition data, but also from the AFT analysis. The sink at a relative density of 2.1 is defined as material with a relative density greater than 2.1, which is the high ash content material.

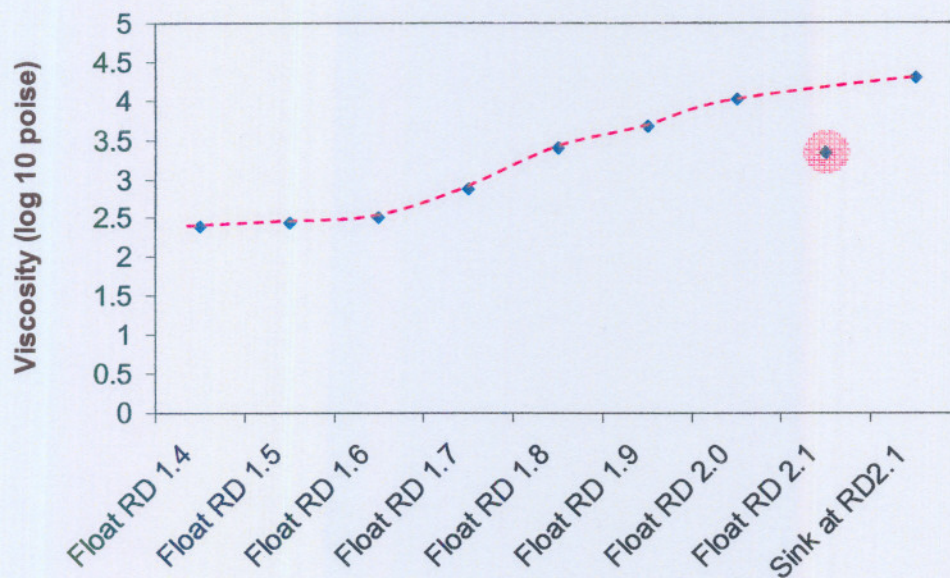


FIGURE 4.11 PREDICTED VISCOSITIES AT 1300°C FOR EACH INDIVIDUAL DENSE MEDIUM FRACTION

- The float fractions with a relative density <1.7 have lower predicted viscosities than the coal blend, and the fractions with a relative density >1.7 have a viscosity higher than the coal blend. This is in agreement with the AFT results indicated that the AFT of the lower density fractions have a lower AFT (Figure 4.12). The higher density fractions are also the fractions which contain more extraneous minerals (or stone particles) with higher concentrations of SiO_2 and Al_2O_3 , which are also the fractions with the higher AFT.

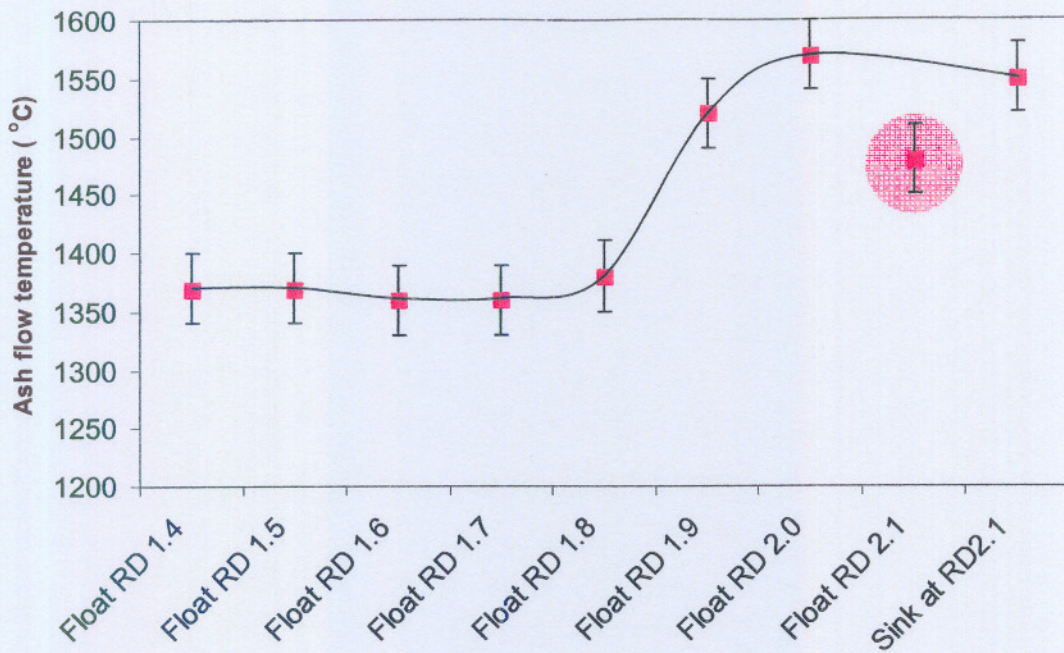


FIGURE 4.12 ASH FUSION TEMPERATURES FOR EACH INDIVIDUAL DENSE MEDIUM FRACTION

- The viscosity prediction of the mineral fraction and the AFT of the relative density = 2.1 fraction can be explained by the higher Fe_2O_3 -content of that specific fraction (see Appendix B Table G). The Fe_2O_3 -content in the relative density = 2.1 fraction was 14%, whereas in the other fractions, it was not more than 7%. Fe-containing compounds are known to lower the AFT and can be used as a fluxing agent.

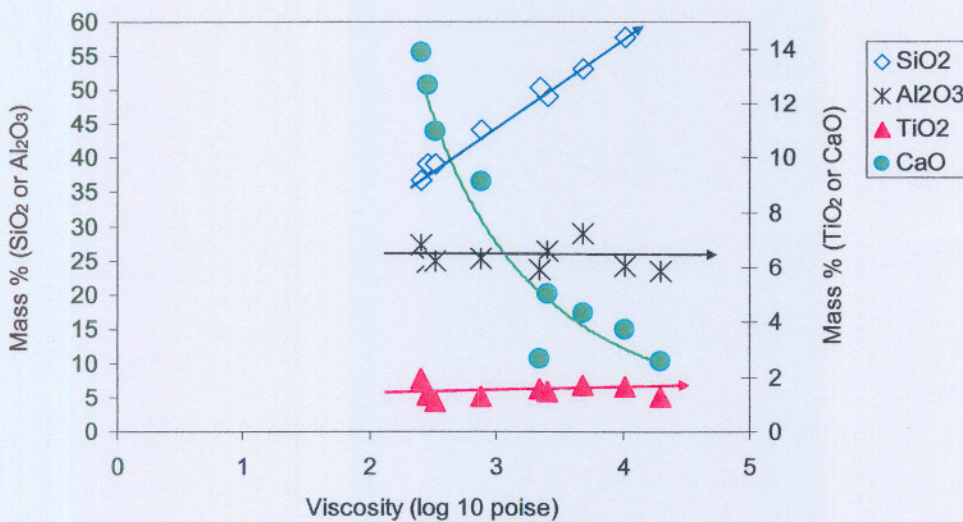


FIGURE 4.13 SiO_2 , Al_2O_3 , TiO_2 and CaO TRENDS VERSUS VISCOSITY AT 1300°C OF ALL DENSE MEDIUM FRACTIONS

- The trends for CaO, SiO₂, Al₂O₃ and TiO₂ versus the viscosity at 1300°C of the ash are graphically illustrated in Figure 4.13. The Al₂O₃ and TiO₂ trends remained constant for all the dense medium fractions, despite the change in viscosity prediction. The SiO₂ trend increased with increasing viscosity, whilst the mass % CaO decreased with increasing viscosity. The reason the viscosity of the mineral fractions changed, although the Al₂O₃ content remained constant, is due to the fact that the mineral content in the coal did not contain “free” Al₂O₃. All Al³⁺-ions are bonded mainly in kaolinite form, where as in the case with the SiO₂, a percentage is bonded as SiO₂ for example in kaolinite. The Al present in the mineral structure is not “free” Al₂O₃ or Al³⁺ species, and that the actual effect of decreasing or increasing AFT with varying Si/Al ratios, is actually the result of the SiO₂ (quartz) in the structure. The SiO₂ acts as a diluting agent and as the SiO₂ concentrated in the fractions to higher percentages, the AFT is decreased. The effect of SiO₂ is more a physical effect. When Al₂O₃ is added as “free” Al₂O₃, then the mechanism is totally different, where the mechanism changed from a physical effect in increasing the AFT by dilution, to a chemical process where the Al₂O₃ added then reacted with the SiO₂ in the mineral structure to form mullite species, which have a high melt temperature.

4.2.2 Viscosity modelling of base case mineral matter compositions with added mineral matter from the roof and the floor of the coal seam

It is known that in some areas of the mine and in the roof and floor of some mining areas, discards or high-ash coal is not mined. However, these roof and floor sections, which contain mainly siltstone layers, have high AFT properties which might be suitable for use as diluting agent to the current coal in order to increase the AFT of the feed. Taking into account the fact that SiO₂, Al₂O₃ and TiO₂ all have an increasing effect on the AFT, it is worthwhile to investigate the effect silica (SiO₂), alumina (Al₂O₃) and titania (TiO₂), as well as substances such as kaolinite and siltstone found in the roof and floor of the coal seam on the AFT. Kaolinite contains mainly SiO₂ and Al₂O₃ as (Al₂O₃)(SiO₂)₂(H₂O)₂, whilst siltstone is a combination of mineral species which are usually found as part of the roof and floor partings of the coal seam in the mine. For the purpose of this study the roof and floor were treated separately, and effect investigated on the AFT. The mineral composition of the roof and floor was given in Table 3.12 and was used to obtain Figures 4.14 and 4.15.

TABLE 4.12 AVERAGE PROPERTIES OF THE ROOF AND FLOOR OF A COAL SEAM

	ROOF	FLOOR
% Ash	91.4	86.6
% Fixed carbon	1.9	3.1
Difference (moisture + volatile matter)	6.7	10.3
Ash composition (%)		
SiO ₂	80.1	71.5
Al ₂ O ₃	11.3	22.1
Fe ₂ O ₃	3.6	1.9
P ₂ O ₅	0.1	0.1
TiO ₂	0.5	0.7
CaO	1.2	0.4
MgO	0.3	0.3
K ₂ O	1.4	1.4
Na ₂ O	0.2	0.3
SO ₃	0.7	0.1
AFT (°C)(Oxidizing)		
DT	1558	1588
HT	1585	1591
FT	1600	1593
XRD-analyses		
Pyrite	2.7	1.4
Quartz	55.2	25.3
Calcite	1.5	0.1
Siderite	1.3	0.0
Dolomite	0.0	0.0
Illite	7.0	19.4
Kaolinite	26.5	50.8
Microlite	4.4	1.4

The roof and floor materials are neither ash nor coal defined, but as the high ash content layer around a coal seam, which normally contains >80% ash. The effect of the addition of roof and floor material on the viscosity of the minerals are graphically illustrated in Figures 4.14 and 4.15.

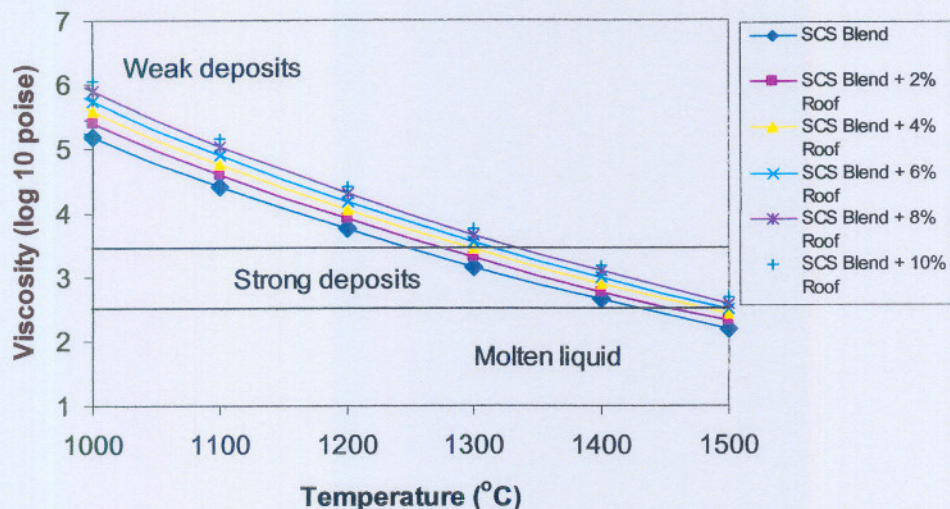


FIGURE 4.14 VISCOSITY PREDICTIONS AT DIFFERENT TEMPERATURES WITH THE ADDITION OF ROOF MATERIAL TO THE COAL BLEND

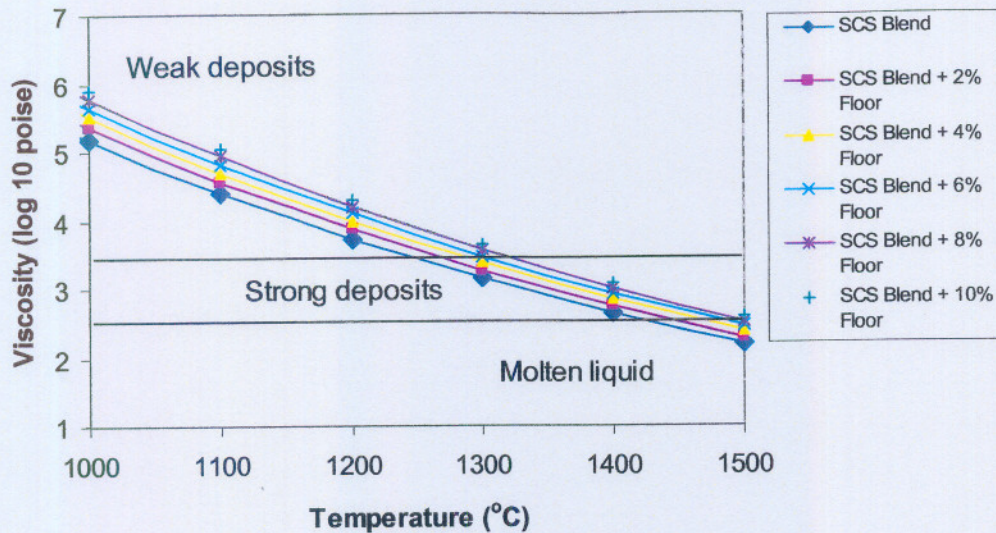


FIGURE 4.15 VISCOSITY PREDICTIONS AT DIFFERENT TEMPERATURES WITH THE ADDITION OF FLOOR MATERIAL TO THE COAL BLEND

From these results it can be concluded that both substances have a similar effect on the viscosity trends as in both cases the viscosity increased. It was decided to test the concept of so-called “sintering growth” in order to experimentally test the concept on the coal blend used in this study, but also to better understand the concept of sintering growth. Coal samples of -1mm particle size were heated at a rate of 10°C/min under ambient conditions to 1200°C, 1300°C and 1400°C respectively. The 1st sample was removed from the furnace when the initial temperature was reached. The 2nd, 3rd and 4th samples were left at the temperature for 1 hour, 2 hours and 3 hours respectively before removed from the furnace. Sintering was visible and shown in Figure 4.16. Sintering growth was both visible with increasing time as well as increasing temperature.

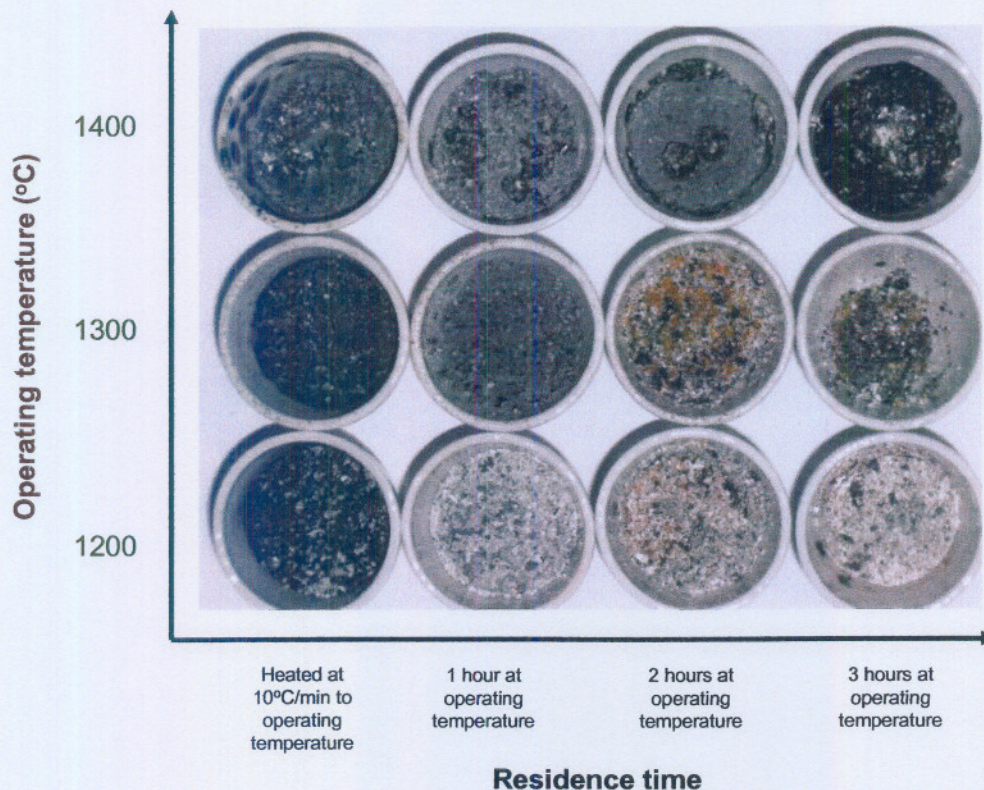


FIGURE 4.16 SINTERING GROWTH BY VISUAL OBSERVATION

From the visual observation a clear trend of increased sintering can be seen in both the vertical (temperature dependence) and the horizontal (time dependence) axes. Sintering growth increases both with increasing temperature and time [Raask, 1986 and Benson, 1987]. Figure 4.16 is just a visual explanation of the increase in liquid (slag) formation with increasing temperature and residence time, and the flow of mineral species.

In general it can be concluded that FactSage, viscosity and sintering modelling as tools for predicting mineral behaviour and slag formation, all have a role to play in different scenarios and applications. The purpose of this study was not to compare the different tools, but it can be highlighted that it will be difficult to conclude on the best model as each model has each own application and output results. From a thermodynamic point of view in the gasification environment, it might be worth to mention that FactSage is able to handle organic and inorganic components and might be a first decision for further work and development in this area.

CONCLUSIONS

Sasol has been operating the **Sasol-Lurgi Fixed Bed Dry Bottom (FBDB)** coal gasification process for more than 50 years. Coal is a crucial feedstock for South Africa's unique synfuels and petrochemicals industry and it is used by Sasol as a feedstock to produce synthesis gas (CO and H₂). One property, that specifically gives detailed information on the suitability of a coal source for gasification purposes, is the AFT. Although the standard AFT analysis is currently used as the only predictive tool for the AFT of coal, it is known that this may not represent the actual flow temperature of certain minerals and mineral phases.

A unique opportunity exists, as shown in this study to increase the average AFT of the coal fed to the Sasol-Lurgi FBDB gasifiers to >1350°C by adding AFT increasing minerals or species, for example kaolinite, to the coal blend before it is fed into the gasification process.

According to the standard coal properties, i.e. ash content, volatile content, carbon content and maceral composition, the coal sample used in this study was representative and comparable with the coal currently used for gasification. Furthermore, Secunda and Sasolburg coal sources used for gasification have an AFT of (1300°C±30°C) (ISO 540, 1995E), the same as the coal used in this study with an AFT of (1340°C±30°C). Lastly the ash composition analysis indicated that the coal used in this study was within the variation of the coal typically used for gasification purposes.

The gasification process and the interpretation of results were modelled and explained, by dividing the gasifier into three distinct zones, namely (1) the drying and devolatilisation zone, (2) gasification zone and (3) the combustion and ash zone.

With the specific aim of this study, to increase the AFT, the determination of the AFT of the coal blends where some acidic components such as silica (SiO₂), alumina (Al₂O₃) and titania (TiO₂) were added was conducted. The oxide Al₂O₃ had the biggest and most significant effect on the AFT with the least addition to the coal blend. The effect of SiO₂ and TiO₂ were very similar with regards to the effect on the AFT. Less Al₂O₃ was needed to increase the AFT to a similar AFT level in comparison to the SiO₂ used and the question still remains why Al₂O₃ (as pure oxide component) did react different and increased the AFT to a certain temperature with less addition, in comparison to that of TiO₂ and SiO₂. The Al₂O₃ keeps the oxygen molecules stronger bound to the molecule than to the other components, and when

the element becomes "free", with free electrons, a different mineral phase can form with a different flow property.

In the **drying and devolatilization zone** no slag formation in the coal was observed, as was to be expected. Based on HT-XRD analysis the predominant minerals in the untreated coal sample were found to be quartz, muscovite, calcite, dolomite, rutile and kaolinite. The amount of meta-kaolinite and mullite that can be formed are directly correlated with the amount of kaolinite in the original coal sample. It should be noted that mullite formation can also take place if free Al_2O_3 is present in the coal that can react with free SiO_2 . However, free Al_2O_3 is normally not present in coal and the presence of the sillimanite (Al_2SiO_5), formed as an intermediate phase due to the decomposition of kaolinite which in turn formed to mullite.

From the modelling results it became clear that the SiO_2 changed from the α - SiO_2 to the β - SiO_2 phase in the temperature range 500°C and 600°C consistent with known literature. The feldspar ($\text{CaAl}_2\text{Si}_2\text{O}_8$) observed formed as a product between the SiO_2 , Al_2O_3 and Ca-containing species present in the coal.

The amount of sillimanite that formed increased from the untreated coal up to an addition of 8 mass% Al_2O_3 to the base case coal, after which its formation did not increase any more. The additional sillimanite formation can also be a product of the direct reaction between the Al_2O_3 added and the "free" SiO_2 in the coal, as mullite formation from kaolinite took place with the decomposition of kaolinite to meta-kaolinite. If the sillimanite formation is a direct reaction between the Al_2O_3 added and the "free" SiO_2 in the coal, then the SiO_2 trends have to show similar trends as for the sillimanite formation, up to the 8% addition where all the free SiO_2 will be taken up by the added Al_2O_3 . It was confirmed that the mullite or intermediate phases formed as product between the Al_2O_3 added and the "free" SiO_2 in the coal, caused the decrease in SiO_2 content.

In the **gasification zone** it was clear that slag (liquid) formed at a temperature of 1000°C, with a decrease in the feldspar content. Above 1350°C the whole mineral phase assemblage in the coal sample was molten. The decrease in abundance of the mineral matter, as function of temperature was not only a decomposition of some mineral phases, but also the formation of liquid or slag. At a temperature of 1400°C no crystalline phases were observed and phase assemblage was totally molten. Furthermore, mullite formation was also observed in the base case sample in the temperature range 1000°C and 1100°C, and the decrease in the amount of SiO_2 at a

temperature of 1100°C was related to the formation of mullite, but also that the slag-liquid phase contained an amount of SiO₂ in the molten form. When comparing base case sample with the Al₂O₃-manipulated sample it was clear that the mullite is one mineral that showed a significant difference in formation and mechanistic behaviours. It is evident that the appearance of mullite in the manipulated coal sample at a temperature of 1100°C was very strong and was identified up to a temperature of 1400°C.

In the **combustion zone** the decrease in the slag-liquid content confirmed the cooling and actual mineral behaviour within the gasifier combustion zone. The representative coal ash, as it was produced after gasification, showed evidence of crystallization from the melt phase and formed due to the interaction of specific mineral species to produce a molten phase that had the correct chemistry to crystallize again. The SEMPC analysis also indicating that although the amount of melt was fairly low at 1000°C, a percentage of melt was definitely present, which at this temperature is not reflected by conventional AFT analyses.

As mullite is a high temperature melting mineral, it causes the AFT of the ash mixture to increase, resulting in less liquid formation. The main conclusion of the addition of Al₂O₃ to the blend is that the slag-liquid content decreased with addition, only when the temperature was greater than 1100°C, with the most significant effect at temperatures greater than 1200°C, which is of importance in the operating region where the proposed higher gasifier temperature of more than 1250°C, is aimed for. The percentage of slag-liquid decreased with between 10 mass% and 16 mass% with every 2 mass% Al₂O₃ added. It seems, according to these modelling results, that a saturation point was not yet reached with up to 10 mass% Al₂O₃ addition to the coal sample. With the higher amount of Al₂O₃ added to the untreated coal sample, the increased formation of sillimanite or meta-kaolinite and finally the formation of mullite was thus not only visible in the drying and devolatilization zone, but also in the gasification zone. With the increased formation of mullite in the gasification zone, the deformation or decrease in SiO₂ content was also clearly observed.

Another observation from the AFT results was that the AFT was definitely non-additive (not a linear weighted calculated average) and not the weighted average AFT as was expected for the other coal properties such as the ash content, for example. The ash slagging characteristics is a non-additive property of individual coal sources in the blend and therefore difficult to predict. Interaction between the individual coal sources as well as the different mineral species, has to be suspected as the main

reason behind the observed deviations, where agglomeration of solids or ash slagging is considered one of them. A higher viscosity for increasing relative density fraction samples were observed for all temperature ranges in comparison with the results obtained from the AFT analysis. The reason why the viscosity of the mineral fraction samples changed, although the Al_2O_3 content remained constant, is due to the fact that the mineral content in the coal did not contain free Al_2O_3 . All Al_2O_3 in the coal sample was bound mainly in kaolinite, where as in the case with the SiO_2 , a percentage was bound as SiO_2 for example in kaolinite, but also a percentage of free SiO_2 was present. The Al present in the mineral structure is not “free” Al_2O_3 or Al species, and that the actual effect of decreasing or increasing the AFT with varying Si/Al ratios, is actually the result of the “free” SiO_2 in the structure. The free SiO_2 acts as a diluting agent (helps to form less slag) and as the SiO_2 concentrated in the fractions to higher percentages, the AFT decreased, thus a physical effect was observed. When Al_2O_3 was added as free Al_2O_3 , then the mechanism was different, and changed from a physical effect in increasing the AFT by dilution, to a chemical process where the Al_2O_3 added, reacted with the free SiO_2 to form mullite, which has a high AFT.

In general it can be concluded that the unique opportunity exists to increase the AFT, was tested, proven and mechanistically outlined in this study on the coal source fed to the Sasol-Lurgi FBDB gasifiers. The AFT can be increased to $>1350^\circ\text{C}$ by adding AFT increasing minerals or species, for example Al_2O_3 or kaolinite, to the coal blend before it is fed into the gasification process. By increasing the AFT, the direct effect will be that steam consumption can be decreased, which in turn will improve carbon utilization. It can be recommended that roof and floor sections, containing mainly siltstone layers, have high AFT properties which might be suitable for use as dilution agent to the current coal in order to increase the AFT of the feed. From a thermodynamic point of view in the gasification environment, it might be worth to mention that FactSage modelling is able to handle organic and inorganic components and might be a first step for further work and development in this area.

APPENDIX A

**PROVISIONAL PATENT (F548)(Van Dyk, J.C., Coertzen, M. and Keyser, M.J.)
[Attorneys Van der Walt, 2004]**

5

10 THIS INVENTION relates to a method of operating a fixed bed dry bottom
gasifier.

 It is well known to add additives, e.g. calcium compounds, to carbonaceous
material being gasified in a slagging gasifier thereby to decrease the ash fusion
15 temperature. However, in the case of fixed bed dry bottom gasifiers such as the Sasol-
Lurgi fixed bed dry bottom gasifier, the slagging of ash is undesired as it leads to
unstable operation or inoperability of the gasifier. A fixed bed dry bottom gasifier must
thus be operated in a temperature region such that the maximum gasifier temperature is
below the ash fusion temperature of the carbonaceous material which is being gasified.
20 Conventionally, this is achieved by decreasing the oxygen load into the gasifier or by
operating the gasifier with an excess of steam as gasification or moderating agent.
Decreasing the oxygen load into the gasifier is undesirable as it results in a direct
reduction in synthesis gas production. Operating the gasifier with an excess of steam is
also not ideal as it results in decreased thermal efficiency of the gasification process as
25 more energy is required to generate the excess steam.

 Fixed bed dry bottom gasifiers such as the Sasol-Lurgi fixed bed dry bottom
gasifier is also known as a moving bed dry ash gasifier.

30 According to the invention, there is provided a method of operating a fixed
bed dry bottom gasifier, the method including

 feeding coarse particulate carbonaceous material with an average particle size of
at least 1 mm and an ash fusion temperature increasing agent into a gasification
chamber to form a carbonaceous material bed;

feeding a gasification agent into the gasification chamber;

gasifying the coarse particulate carbonaceous material in the gasification chamber to produce synthesis gas as well as ash, the ash being collected in an ash bed below the carbonaceous material; and

5 removing the synthesis gas and the ash from the gasification chamber.

Typically, the coarse particulate material and the ash fusion temperature increasing agent are fed into the gasification chamber through a lock located above the carbonaceous material bed, e.g. a coal lock.

10

Typically, the ash is withdrawn through an ash lock which is in communication with the gasification chamber via an ash discharge outlet in a bottom of the gasification chamber.

15

The gasifier typically includes a coarse particulate carbonaceous material distribution device which also defines a gas collection zone, with the synthesis gas thus being withdrawn from the gas collection zone.

20

Preferably, the carbonaceous material bed is a homogenously mixed bed comprising the coarse carbonaceous material and the ash fusion temperature increasing agent.

25

Preferably, the coarse particulate carbonaceous material has an average particle size of at least 3 mm, preferably at least 4 mm.

30

The particulate carbonaceous material is preferably coal.

The ash fusion temperature increasing agent may be a solid material or a solution, although the applicant expects that a solid material will be preferable. In this case, the carbonaceous material and the solid ash fusion temperature increasing agent will typically be in the form of a simple admixture, i.e. not pelletized or the like but a mixture of individual non-homogenised solid particles.

The ash fusion temperature increasing agent may be fed in an amount of less than 5 % by mass, preferably less than 4 % by mass, more preferably less than 3 % by mass, typically between about 1 % by mass and about 2 % by mass of the ash formed in the gasification chamber.

5

The ash fusion temperature increasing agent may be a substance capable of reacting with one or more of calcium, magnesium, iron, potassium or sodium at elevated temperatures to form products melting at higher temperatures than the salts or oxides of these elements present in the carbonaceous material. The ash fusion temperature increasing agent may thus be an acidic agent and may in particular be kaolinite (Al₂Si₂O₅(OH)₄), alumina (Al₂O₃), silica (SiO₂) or TiO₂.

10

When the carbonaceous particulate material is particulate coal, the coal may be gasified at a temperature above the ash fusion temperature of the coal. The gasification temperature may be at least 1330 °C, more preferably at least 1345 °C, even more preferably at least 1360 °C, most preferably at least 1375 °C, but below the ash fusion temperature of an admixture of the coarse particulate coal and the ash fusion temperature increasing agent.

15

When the carbonaceous material is particulate coal, the synthesis gas may have an H₂/CO mole ratio of less than 1.65, preferably less than 1.60, more preferably less than 1.50.

20

The invention will now be described, by way of example, with reference to the accompanying diagrammatic drawings.

25

In the drawings,

Figure 1 shows a schematic diagram of a fixed bed dry bottom gasifier;

Figure 2 shows a graph of a typical ash melting prediction curve; and

30

Figure 3 shows a graph of experimental ash fusion temperature measurements with various acidic ash fusion temperature increasing agents.

Referring to Figure 1 of the drawings, reference numeral 10 generally indicates a fixed bed dry bottom gasifier such as a Sasol-Lurgi gasifier. The gasifier 10

includes a coal lock 12, a gasification reactor 14, a rotating grate 16 and an ash lock 18. The gasifier 10 is a pressurised gasifier.

5 In use, a sized coal feed 20 with particles greater than 4 mm enters the gasification reactor 14 through the coal lock 12 and moves down through a bed formed inside the gasification reactor 14. An oxygen feed 22 and a steam feed 24 enter at a bottom of the bed, through the grate 16. Oxygen is required to combust some of the coal to supply energy for the endothermic gasification reactions. Typically, part of the steam that is used is generated in a gasifier jacket (not shown) from boiler feed water that is fed to the jacket. The steam has a pressure of 40 bar (gauge) and a temperature
10 of about 390 °C, with the boiler feed water being at a pressure of about 40 bar (gauge) and a temperature of about 105 °C and the oxygen being at a pressure of about 29 bar (gauge) and a temperature of 140 °C.

15 Within the gasifier bed, different reaction zones are distinguishable from top to bottom, namely a drying zone where moisture is released, a devolatilization zone where pyrolysis takes place, a reduction zone where mainly endothermic reactions occur, an exothermic oxidation or combustion zone, and an ash bed at the bottom of the gasifier bed. As a result of the counter-current mode of operation, hot ash exchanges heat with cold incoming reagents, such as steam and oxygen or air, while at the same
20 time hot raw gas exchanges heat with cold incoming coal. This results in an ash stream 28 and a raw gas stream 30, respectively leaving the gasifier 10 from the ash lock 18 and the gasification reactor 14, at relatively low temperatures compared to other types of gasifiers, which improves the thermal efficiency and lowers the steam and oxygen consumption of the gasifier. The ash passes through the rotating grate 16 and the ash
25 lock 18 before being removed.

In the pyrolysis zone of the gasifier, tars, oils and pitches and the like are released. These pyrolysis products are not destroyed, in view of the relatively low operating temperature of the pressurised dry ash moving bed gasifier 10. The pyrolysis
30 products can be used to create valuable co-products such as ammonia, sulphur, cresols and phenols.

The following reactions take place in the gasifier:

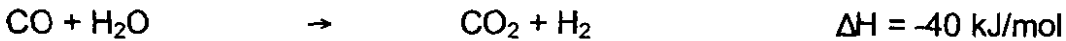
Combustion:



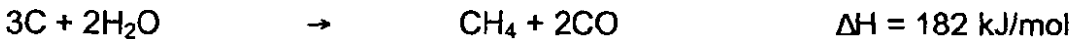
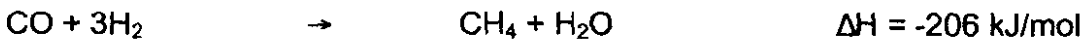
Reduction:



Water-gas shift:



10 *Methane formation:*



15 The temperature profile in the gasifier 10 varies between about 800 °C and 1200 °C as the coal moves through the different zones in the gasification reactor 14. The raw gas stream 30 leaves the gasification reactor 14 typically at a temperature of between about 460 °C and 500 °C, but may be lower.

20 The maximum temperature in the gasifier 10 is limited by the ash fusion temperature of the coal feed 20 as ash fusion creates removal problems of the ash at the bottom of the gasifier 10. Owing to this limitation, the temperatures can conventionally not be raised, causing more methane to form part of the raw synthesis gas than would be the case with higher temperatures. Conventionally, sufficient steam
25 is ejected to the bottom of the gasification reactor 14 to keep the temperature below the melting temperature of the ash.

In accordance with the invention, an ash fusion temperature increasing agent
30 is fed into the gasifier 10 thereby to raise the ash fusion temperature. A possible inlet location for the ash fusion temperature increasing agent is indicated by reference numeral 32. Thus, it is expected that the coarse particulate coal and the ash fusion temperature increasing agent will be fed into the gasification reactor 14 through the coal lock 12. A coal distributor (not shown) which is typically located below the coal lock 12

ensures that the coal and ash fusion temperature increasing agent are distributed in well mixed manner in the gasification reactor 14.

Figure 2 shows a typical ash melting prediction curve 34. Curves such as the curve 34 can be used to obtain a qualitative indication of the decrease in the percentage basic (calcium, magnesium, iron, potassium and sodium) components in the ash needed to effect a required increase in the ash fusion temperature. The calculated decrease in the percentage basic components is achieved by the addition of an acidic ash fusion temperature increasing agent.

The ash melting prediction curve 34 in Figure 2 is fairly accurately modelled by the following formula:

$$\text{Ash fusion temperature (}^{\circ}\text{F)} = 1.1914x^2 - 87.066x + 3867$$

where x is the mass % basic components (calcium, magnesium, iron, potassium and sodium) in the ash. The ash fusion temperature as a function of x is shown by the graph 36.

For the particular coal feed used to prepare the ash melting prediction curve shown in Figure 2, it is thus possible to calculate that for an increase in the ash fusion temperature of 37 °C to above 1350 °C, the amount of acidic component (e.g. kaolinite) in the ash needs to be increased by 1.9 mass %. It is then a simple calculation to determine how much of the ash fusion temperature increasing agent to add to the coal feed 20.

With reference to Figure 3, some experimental ash fusion temperature measurements with various acidic ash fusion temperature increasing agents are shown. As can be seen in Figure 3, when using alumina as ash fusion temperature increasing agent, fairly small amounts are required to obtain significant increases in the ash fusion temperature.

A computer simulation of a gasifier similar to the gasifier 10 was used to obtain a prediction of the improvement in gasifier thermal efficiency with increasing maximum gasifier operating temperature. The results were calculated at constant

gasifier load and coal feed. Excess steam is fed to the gasifier to control the maximum gasifier operating temperature and the increased thermal efficiency is thus reflected in a decreased high pressure (HP) steam consumption. The following table shows the calculated results:

5

Gasifier operating temperature (°C)	Percentage increase in HP steam consumption (%)	H ₂ /CO ratio (mole fractions)	Raw gas composition (mole fractions)			
			H ₂	CH ₄	CO	CO ₂
1325	0	1.71	0.382	0.089	0.223	0.288
1343	4	1.65	0.379	0.089	0.23	0.284
1355	6.3	1.61	0.378	0.089	0.235	0.281
1366	9.5	1.57	0.376	0.089	0.24	0.278
1416	18	1.41	0.367	0.089	0.261	0.265

As will be noted, the H₂/CO molar ratio decreases with increasing maximum gasifier operating temperature. Advantageously, as a result of being able to increase the maximum gasifier operating temperature, it is possible to match the H₂/CO ratio in the gasifier outlet to the needs of a downstream process which possibly also provides one with the opportunity of de-bottlenecking the downstream process.

10

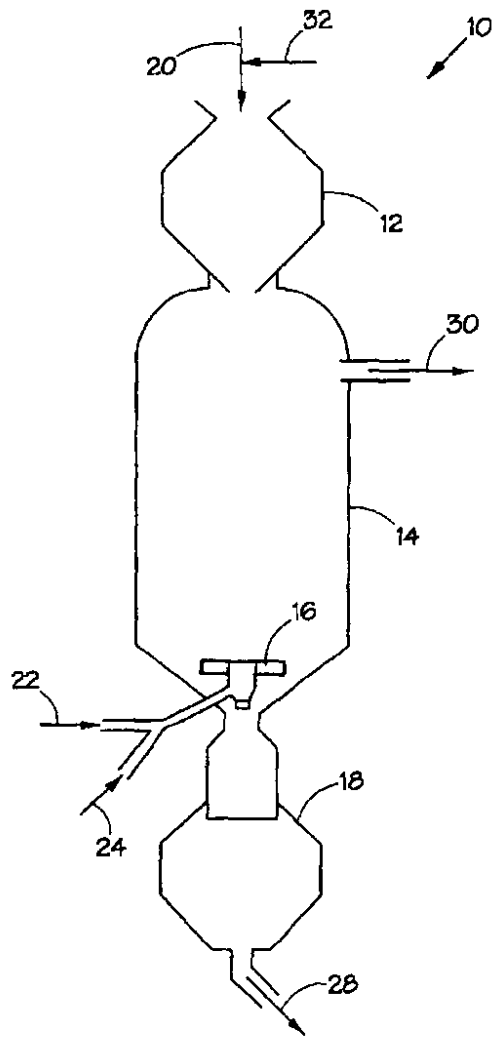


FIG 1

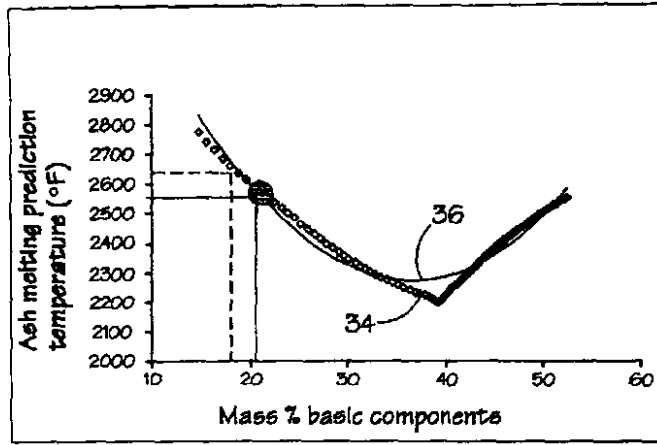


FIG 2

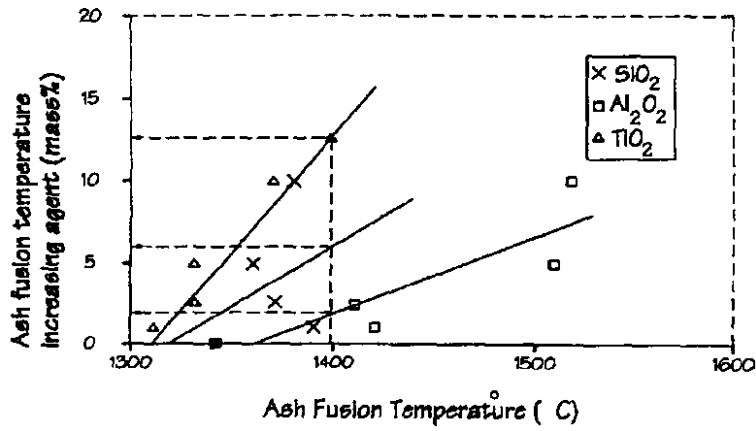


FIG 3

APPENDIX B

TABLE A

MORPHOLOGICAL RESULTS OF COAL (MASS %) (-250 μ M)

Point count	Na	Mg	Al	Si	P	S	Cl	K	Ca	Ti	Fe	Ba	O
1	0.0	11.6	0.0	0.7	0.0	0.0	0.0	0.0	44.8	0.0	1.4	0.0	41.5
2	1.2	0.0	31.4	49.3	0.0	0.0	0.0	0.0	0.0	0.0	0.0	0.0	18.1
3	0.0	19.2	0.0	0.9	0.5	0.0	0.0	0.0	27.9	0.0	1.3	3.1	47.1
4	1.4	0.0	28.2	26.9	7.3	0.0	0.0	3.3	3.2	0.0	0.0	4.5	25.0
5	0.0	18.6	0.0	0.7	0.0	0.0	0.0	0.0	30.4	0.0	0.0	0.0	50.4
6	0.0	0.0	0.0	0.0	0.0	0.0	0.0	0.0	100.0	0.0	0.0	0.0	0.0
7	0.0	1.1	0.0	0.6	0.6	0.0	0.0	0.0	40.7	0.0	1.8	5.9	49.3
8	0.0	2.0	0.0	0.7	0.0	0.0	0.0	0.0	45.6	0.0	2.8	0.0	48.9
9	1.2	0.0	26.8	25.5	0.0	0.0	0.0	0.0	0.0	0.0	0.0	0.0	46.5
10	0.0	5.0	0.0	0.9	0.0	0.0	0.0	0.0	61.0	0.0	0.0	7.3	25.7
11	2.3	0.0	24.9	26.4	0.0	0.0	0.0	0.0	0.0	0.0	0.9	0.0	45.4
12	0.0	0.0	0.0	49.1	0.0	0.0	0.0	0.0	0.0	0.0	1.5	0.0	49.4
Average bulk	0.5	4.8	9.3	15.1	0.7	0.0	0.0	0.3	29.5	0.0	0.8	1.7	37.3

TABLE B

MORPHOLOGICAL RESULTS OF COAL (MASS %)(-1MM)

Point count	Na	Mg	Al	Si	P	S	Cl	K	Ca	Ti	Mn	Fe	O
1	0.9	0	0	49.5	0	0	0	0	0	0	0	0	49.5
2	2.7	0	28.7	30.7	0	0	0	0.7	0	0	0	0	37.2
3	0	2.8	12.7	16.2	0	0	0	3.1	14.9	0	0	1.2	49.1
4	0	13.7	0	0.8	0	0	0	1.1	30.1	0	1.3	0	52.9
5	0	0	0	0.5	0	58.1	0	0	0	0	0	30.4	11
6	0.7	0	26.6	25	0	0	0	0	0	0	0	0	47.6
7	0	13.9	0	1	0	0	0	0	28.3	0	1.3	3.9	51.6
8	0	18.6	0	3.7	0	0	0	0	41.5	0	1.2	6.9	28.2
9	1.5	0	23.8	25.4	0	0	0	0.7	0.3	0	1	0.8	46.6
10	0	0	0	1.7	0	0	0	0	0.6	76.6	0	1.7	19.4
11	2.3	0	25.5	26.8	0	0	0	0	0	0	0	1.3	44.1
12	1	0	0	49.5	0	0	0	0	0	0	0	0	49.5
Average bulk	0.8	4.1	9.8	19.2	0	4.8	0	0.5	9.4	6.4	0.4	3.8	40.6

TABLE C

MORPHOLOGICAL RESULTS OF COAL (MASS %)(-20MM)

Photo (point)	Na	Mg	Al	Si	P	S	Cl	K	Ca	Ti	Mn	Fe	O
1	1.0	0.0	34.2	45.9	0.0	0.0	0.0	0.6	0.0	0.0	0.0	1.0	17.3
2	1.7	0.0	31.9	31.9	0.0	0.0	0.0	0.0	0.6	0.0	0.8	1.1	31.9
3	0.0	0.0	33.1	33.2	0.0	0.0	0.5	0.0	0.0	0.0	0.0	0.0	33.2
4	0.7	0.0	32.7	32.7	0.0	0.0	0.0	0.0	0.3	0.0	0.0	0.9	32.7
5	2.8	0.0	31.6	31.6	0.0	0.0	0.0	0.7	0.0	0.0	0.0	1.5	31.7
6	0.8	0.0	0.6	1.2	0.0	0.0	0.0	0.0	77.6	0.0	0.0	0.0	19.8
7	0.0	0.5	2.2	1.9	0.0	0.0	0.0	0.0	71.2	0.0	1.6	1.9	20.7
8	2.5	0.0	31.9	31.9	0.0	0.0	0.0	0.0	0.9	0.0	0.0	0.8	32.0
9	0.0	0.0	0.5	0.9	0.3	0.0	0.0	0.0	84.2	0.0	1.0	1.1	12.1
10	0.0	20.9	0.0	0.9	0.0	0.0	0.0	0.0	42.2	0.0	3.1	8.1	24.9
11	0.0	0.0	0.0	6.2	0.0	0.0	0.3	0.0	72.2	0.0	1.2	0.0	20.2
12	6.1	0.0	30.8	41.6	0.0	0.0	0.0	0.0	17.9	0.0	0.0	3.5	0.0
Average bulk	1.3	1.8	19.2	21.7	0.0	0.0	0.1	0.1	30.6	0.0	0.6	1.7	23.0

TABLE D

MORPHOLOGICAL RESULTS OF CALCIUM-RICH PARTICLES IN COAL ONLY (MASS %)(-250µM)

Photo (point)	Na	Mg	Al	Si	P	S	Cl	K	Ca	Ti	Fe	Ba	O
1	0.0	2.1	0.0	0.6	0.0	0.0	0.0	0.0	48.5	0.0	0.0	0.0	48.7
2	0.0	23.1	0.0	0.8	1.2	0.0	0.0	0.0	27.7	0.0	0.0	0.0	47.1
3	0.0	1.0	0.0	0.0	0.0	0.0	0.0	0.0	43.0	0.0	0.0	0.0	55.6
4	2.3	0.0	8.0	23.3	7.4	0.0	0.0	0.7	15.8	0.0	0.0	0.0	42.5
5	0.0	0.0	0.9	0.0	26.9	0.0	0.0	0.0	67.3	0.0	0.0	4.9	0.0
6	0.0	10.0	1.3	4.2	0.0	0.0	0.0	0.0	28.4	0.0	3.1	0.0	53.1
7	0.0	14.1	0.0	0.0	0.0	0.0	0.0	1.6	28.6	0.0	3.2	0.0	52.7
8	0.0	7.1	0.0	2.8	0.0	0.0	0.0	0.0	37.8	0.0	0.0	0.0	52.3
9	0.0	10.7	0.0	0.9	0.0	0.0	0.5	0.0	33.8	0.0	3.5	0.0	50.5
10	0.0	6.5	0.0	0.6	0.0	0.0	0.0	0.0	38.7	0.0	1.0	0.0	53.1
11	0.0	17.9	0.0	0.7	0.0	0.0	0.0	1.6	31.1	0.0	0.0	0.0	48.7
12	0.0	11.6	6.8	8.0	0.0	0.0	0.0	1.3	25.3	0.0	1.7	0.0	45.3
Average bulk	0.2	8.7	1.4	3.5	2.9	0.0	0.1	0.4	35.5	0.0	1.0	0.4	45.8

TABLE E

MORPHOLOGICAL RESULTS OF CALCIUM-RICH PARTICLES IN COAL (MASS %)(-1MM)

Photo (point)	Na	Mg	Al	Si	P	S	Cl	K	Ca	Ti	Mn	Fe	O
1	0.0	0.0	0.0	0.6	0.0	0.0	0.5	0.0	56.7	0.0	0.0	0.0	42.2
2	0.0	3.9	5.5	7.3	0.0	0.0	0.0	1.6	32.4	0.0	0.0	0.0	49.3
3	0.0	11.6	0.0	0.5	0.0	0.0	0.0	0.0	33.0	0.0	0.0	5.6	49.3
4	0.0	3.9	0.0	1.7	0.0	0.0	0.0	0.0	31.7	0.0	0.0	2.4	60.3
5	0.0	8.5	3.8	5.8	0.0	0.0	0.0	0.0	24.1	0.0	0.0	3.3	54.5
6	0.0	17.5	0.0	0.0	0.0	0.0	0.0	0.0	27.1	0.7	0.8	2.9	50.9
7	0.0	16.7	0.0	7.6	0.0	0.0	0.0	0.0	72.2	0.0	3.4	0.0	0.0
8	0.0	13.9	0.0	0.4	0.0	0.0	0.0	0.0	29.7	0.0	0.0	0.0	56.0
9	0.0	6.2	0.0	0.6	0.0	0.0	0.5	0.0	37.9	0.0	1.5	0.0	53.3
10	0.0	16.7	0.0	0.5	0.0	0.0	0.0	0.0	29.9	0.0	1.1	0.0	51.7
11	0.0	15.2	0.0	0.9	0.9	0.0	0.0	0.0	28.6	0.0	0.0	1.7	52.8
12	0.0	10.9	0.0	1.2	1.2	0.0	0.6	1.3	39.0	0.0	1.1	0.0	44.7
Average bulk	0.0	10.4	0.8	2.3	0.2	0.0	0.1	0.2	36.8	0.1	0.7	1.3	47.1

TABLE F

MORPHOLOGICAL RESULTS OF CALCIUM-RICH PARTICLES IN COAL (MASS %)(-20MM)

Photo (point)	Na	Mg	Al	Si	P	S	Cl	K	Ca	Ti	Mn	Fe	O
11(1)													
11(2)	0.0	14.2	0.8	3.2	0.0	0.0	0.0	0.0	52.7	0.0	0.0	1.9	27.2
11(3)	0.0	7.9	0.0	0.3	0.0	0.0	0.0	0.0	61.7	0.0	1.5	0.0	28.6
11(4)	0.0	19.0	0.0	0.0	0.0	0.0	0.0	0.0	54.6	0.0	0.0	1.1	25.3
11(5)	0.0	20.2	0.0	0.7	0.0	0.0	0.6	0.0	53.0	0.0	0.0	0.7	24.9
11(6)	0.0	6.6	0.0	0.9	0.0	0.0	0.0	0.0	60.0	0.0	1.3	1.6	29.8
12(7)	1.1	0.0	3.8	0.0	23.1	0.0	0.0	0.0	47.6	0.5	0.0	0.0	24.0
12(8)	0.0	3.1	2.6	2.6	0.0	0.0	0.3	0.0	62.9	0.0	0.0	0.0	28.5
12(9)	0.0	9.6	7.7	8.4	0.0	0.0	0.0	0.0	40.4	0.0	3.9	2.4	27.6
12(10)	0.0	0.5	2.6	2.7	0.0	0.0	0.0	0.0	72.4	0.0	0.0	0.0	21.8
12(11)	0.0	0.3	0.0	0.3	0.5	0.0	0.0	0.0	63.0	0.0	4.7	18.0	13.2
12(12)	0.0	4.6	0.0	0.7	0.0	0.0	0.0	0.0	70.8	0.0	0.5	0.5	22.8
Average bulk	0.1	7.8	1.6	1.8	2.1	0.0	0.1	0.0	58.1	0.0	1.1	2.4	24.9

TABLE G

ORIGINAL DATA SUPPORT TO SECTION 4.1 ON DENSE MEDIUM SEPARATION

	Original Coal Blend	Float RD 1.4	Float RD 1.5	Float RD 1.6	Float RD 1.7	Float RD 1.8	Float RD 1.9	Float RD 2.0	Float RD 2.1	Sink at RD2.1
Proximate analysis (air dry)										
Inh. H ₂ O	5	4.8	4.9	4.9	4.3	4	3.7	3.5	3.1	1.7
Ash	25.8	7.8	13.1	18.8	27.3	35.9	41.8	49.6	51.9	77.9
Vol.Mat	22.9	33.9	25.1	22.5	21.8	19.3	18.2	16.3	17	12
Fix.Carbon	46.3	53.5	56.9	53.8	46.6	40.8	36.3	30.6	28	8.4
Ash composition (mass %)										
SiO ₂	50.1	36.7	39.2	39.2	44.1	49.1	53.1	57.7	50.4	61.1
Al ₂ O ₃	23.3	27.4	24.7	24.9	25.3	26.4	28.9	24.1	23.6	23.4
Fe ₂ O ₃	6.4	3.65	2.93	5.11	4	5.62	4.17	5.59	14.0	6.17
P ₂ O ₅	0.7	1.46	2.13	1.83	0.87	0.72	0.68	0.4	0.42	0.16
TiO ₂	1	1.96	1.36	1.1	1.28	1.47	1.73	1.64	1.58	1.28
CaO	8.1	13.9	12.7	11	9.15	5.03	4.32	3.74	2.67	2.58
MgO	2.7	2.32	4.19	3.87	3.49	1.97	1.25	0.95	0.89	0.55
K ₂ O	0.8	0.55	0.49	0.54	0.67	0.88	0.82	0.72	0.77	1.27
Na ₂ O	0.4	0.92	0.89	0.68	0.54	0.53	0.49	0.45	0.4	0.34
SO ₃	6.1	13.1	13	13.7	11	8.5	6.33	5.4	5.4	2.72
AFT (oxidising to 1600°C)										
DT	1300	1330	1320	1320	1320	1260	1460	1460	1400	1500
ST	1320	1350	1330	1330	1340	1310	1490	1500	1430	1520
HT	1330	1360	1360	1340	1350	1340	1500	1540	1460	1530
FT	1340	1370	1370	1360	1360	1380	1520	1570	1480	1550
										230
Si/Al ratio	2.15	1.33	1.59	1.57	1.74	1.86	1.84	2.39	2.14	2.61
Yield (mass % cumulative)		1.25	29.81	57.04	75.06	81.56	85.24	88.07	89.79	100.01

TABLE H CRYSTALLINE PHASES IN BASE CASE COAL SAMPLE AND AT DIFFERENT TEMPERATURES (°C)

Minerals Identified SCS Coal (base) ashed to 500 °C	25	500	600	700	800	900	1000	1100	1200	1300	1400
α -Quartz SiO ₂	Yes	Yes	Yes	Yes	Yes	Yes	Yes	Yes	Yes	Yes	----
Kaolinite Al ₂ Si ₂ O ₅ (OH) ₄	----	----	----	----	----	----	----	----	----	----	----
Muscovite (Mica) Kal ₂ (Si ₃ Al)O ₁₀ (OH) ₂ F ₂	Yes	Yes	Yes	Yes	Yes	*	*	----	----	----	----
Calcite CaCO ₃	Yes	Yes	Yes	Yes	Yes	----	----	----	----	----	----
Dolomite CaMg(CO ₃) ₂	Yes	Yes	Yes	Yes	Yes	*	*	----	----	----	----
Hematite α -Fe ₂ O ₃	Yes	Yes	Yes	Yes	Yes	Yes	Yes	Yes	Yes	----	----
Rutile TiO ₂	Yes	Yes	Yes	Yes	Yes	(0)	----	----	----	----	----
Mullite Al ₆ Si ₂ O ₁₃	----	----	----	----	----	----	----	----	*	*	----
Anorthite (Ca,Na)(Si,Al) ₄ O ₈	----	----	----	----	----	----	----	Yes	Yes	Yes	----
Albite Na(AlSi ₃ O ₈)	----	----	----	----	----	----	----	----	*	*	----
Gehlenite Ca ₂ Al(AlSiO ₇)	----	----	----	----	----	----	----	Yes	Yes	Yes	----
Lime CaO	----	----	----	*	Yes	Yes	Yes	Yes	*	----	----
Periclase MgO	----	----	----	----	----	*	----	----	----	----	----
Anhydrite CaSO ₄	Yes	Yes	Yes	Yes	Yes	Yes	Yes	Yes	*	----	----
Cristobalite SiO ₂	----	----	----	----	----	----	----	----	----	*	----
Other high-temp. SiO ₂ polymorphs	----	----	----	Yes	Yes	Yes	Yes	Yes	Yes	Yes	----

* Trace

ND Not detected

TABLE I CRYSTALLINE PHASES IN MANIPULATED COAL SAMPLE WITH Al_2O_3 AND AT DIFFERENT TEMPERATURES

Minerals Identified SCS Coal (base) + Al_2O_3 ashed to 500 °C	25	500	600	700	800	900	1000	1100	1200	1300	1400
α -Quartz SiO_2 and/or polymorphs	Yes	Yes	Yes	Yes	Yes	Yes	Yes	Yes	Yes	Yes	----
Muscovite (Mica)	Yes	Yes	Yes	Yes	Yes	----	----	----	----	----	----
Calcite $CaCO_3$	Yes	Yes	Yes	Yes	----	----	----	----	----	----	----
Dolomite $CaMg(CO_3)_2$	Yes	Yes	Yes	Yes	Yes	Yes	Yes	*	----	----	----
Hematite α - Fe_2O_3	Yes	Yes	Yes	Yes	Yes	Yes	Yes	Yes	Yes	----	----
Rutile TiO_2	Yes	Yes	Yes	Yes	Yes	Yes	*	----	----	----	----
Anatase TiO_2	*	----	----	----	----	----	----	----	----	----	----
Mullite $Al_6Si_2O_{13}$	----	----	----	----	----	----	----	Yes	Yes	Yes	Yes
Anorthite $(Ca,Na)(Si,Al)_4O_8$	----	----	----	----	----	----	Yes	Yes	Yes	Yes	----
Albite $Na(AlSi_3O_8)$	----	----	----	----	----	----	----	----	*	*	----
Gehlenite $Ca_2Al(AlSiO_7)$	----	----	----	----	----	----	Yes	Yes	Yes	Yes	----
Lime CaO	----	----	----	Yes	Yes	Yes	----	----	----	----	----
Anhydrite $CaSO_4$	Yes	Yes	Yes	Yes	Yes	Yes	Yes	Yes	*	----	----
Additive: γ - Al_2O_3	Yes	Yes	Yes	Yes	Yes	Yes	Yes	----	----	----	----
α - Al_2O_3			----	----	----	----	----	*	Yes	Yes	Yes

TABLE J STATISTICAL RESULTS OF COEFFICIENT ESTIMATES

Component	Coefficient Estimate	Standard Error	95% CI	
			Low prediction	High prediction
A- SiO_2	-3338.794	1332.731	-7580.142	902.555
B- Al_2O_3	-3833.763	1070.254	-7239.790	-427.735
C- Fe_2O_3	11979.977	2689.257	3421.554	20538.401
D- P_2O_5	-43083.346	11166.607	-78620.505	-7546.187
E- TiO_2	194.599	3327.141	-10393.859	10783.056
F- CaO	2569.607	767.945	125.660	5013.555
G- MgO	5237.052	1420.052	717.809	9756.294
H- K_2O	-23855.420	9650.748	-54568.434	6857.593
J- Na_2O	1399.585	1341.741	-2870.438	5669.609
K- SO_3	1950.079	1326.121	-2270.233	6170.391
AB	25349.269	5372.732	8250.824	42447.715
AD	147475.480	51043.010	-14966.303	309917.263

APPENDIX C

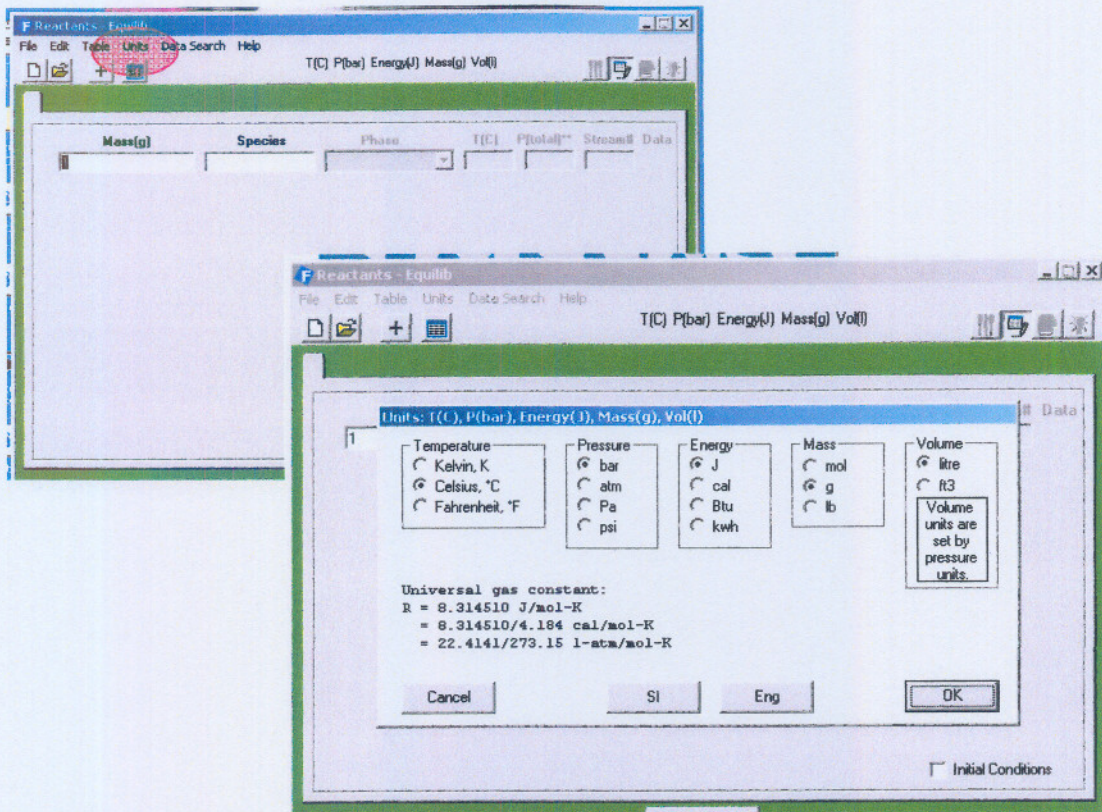
Introduction to Factsage modelling and programming

The purpose of the FactSage model for this study will only be to confirm the slagging behaviour and changes in mineral composition affecting slag formation in the gasification process with and without feed manipulation. The emphasis will only be on the inorganic elements and slag formation, although the organic components were included in order to simulate the gasification process as close as possible to the actual operating conditions. The model was only developed in this study for this purpose to obtain the results needed. The step-by-step guide on how the model was development is given herewith. FactSage 5.3 was used and the model developed with the Equilib model.

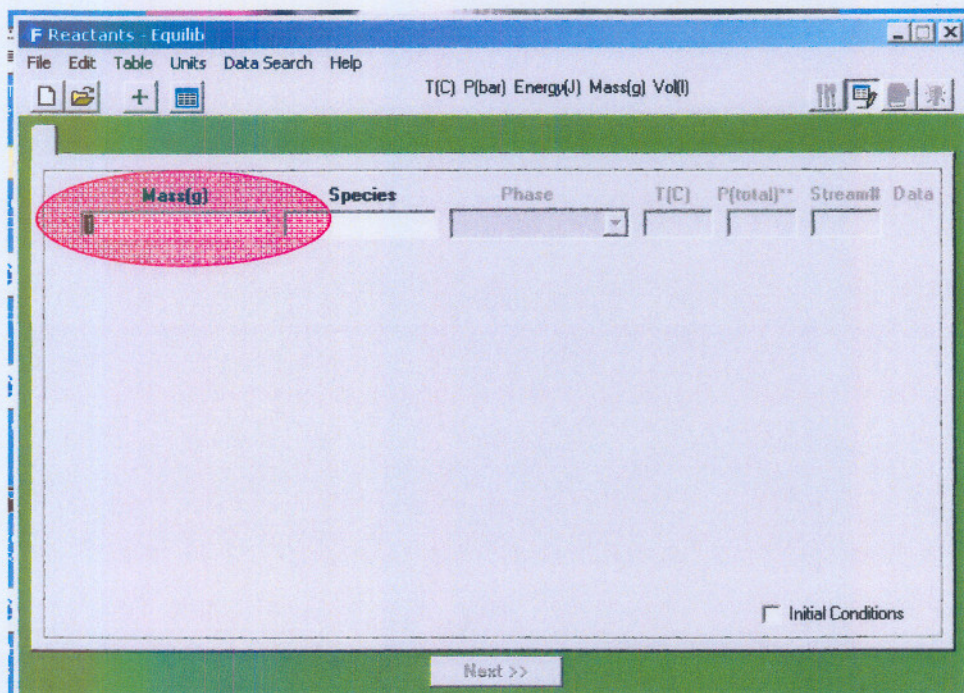
Take note that the actual flows in the screen pictures are just used as an illustration of the process and set-up procedure, and not the actual flows of a specific run or addition, unless otherwise stated. Screen images are only for illustration purposes.



Before the input elements and species were added, it was confirmed that all units are specified as needed for the model. Units were selected as °C, bar, J, g and litre.



Take note that although the mass is only given in g (grams), the flow was put in kg/hr. For example when the model results in a flow of 1000 g, it actually implies 1000 kg or 1000×10^3 g.



Drying and devolatilization zone

The 1st zone to be modelled was the drying and devolatilisation zone. The coal

(organic and inorganic components) as specified in **Chapter 4** was added with the specific mass flow as reactants. Each element, reactant or specie was added separately. A summary of the elements added as the total coal stream is given in Table A.1.

TABLE A.1 SUMMARY OF INPUT REACTANTS INTO FACTSAGE DEVOLATILIZATION ZONE

Element	Mass flow (kg/hr)
H ₂ O	2550
C	25557
H	1329
N	713
S	681
O	4154
Pyrite	526
Quartz	2631
Microline	250
Muscovite / Illite	381
Kaolonite	6913
Anatase	39
Ankerite	-
Siderite	-
Calcite	881
Dolomite	1328
Apatite*	65
Gypsum	144
Tar and oils**	2858
TOTAL	51000

* Not included in model due to FactSage software limitations.

** Not included in model.

The gas flow from the gasification zone was added as reactants that reacted with coal (Table A.2). The temperature range according to the ASPEN model for this zone was from ambient conditions when the coal enters the gasifier to 690°C the end of the pyrolysis zone.

TABLE A.2 GAS FLOW FROM GASIFICATION ZONES

Gas(kg/hr)	Gasification zone outlet gas into pyrolysis and drying zone
H ₂ O	27 159
O ₂	0
C	0
H ₂	1 961
CH ₄	6 417
CO	15 761
CO ₂	42 742
N ₂	142
T(°C)	690

Schematicly it implies that the up-flowing gas from the gasification zone reacted with the down flowing coal and mineral matter into the gasifier (Figure A.1).

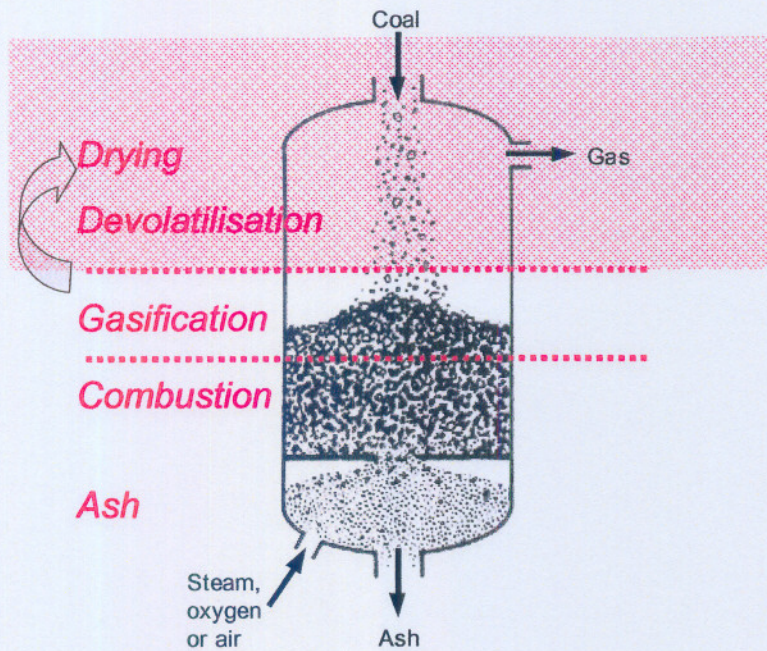


FIGURE A.1 DRYING AND PYROLYSIS ZONE

In total 27 reactants was added.

The image shows three overlapping screenshots of the FactSage 5.3.1 software interface, displaying reactant lists for different stages of the gasification process. Each window shows a table with columns for Mass(g), Species, Phase, T(C), P[total]**, Stream#, and Data.

Top Window (Reactants - Equilib):

Mass(g)	Species	Phase	T(C)	P[total]**	Stream#	Data
25557	C	solid-1-FACT graphit	25	29	1	FACT
1329	H	gas-FACT	25	29	1	FACT
713	N					
681	S					
4154	O					
1961	H2					
6417	CH4					
15761	CO					
42742	CO2					
142	N2					

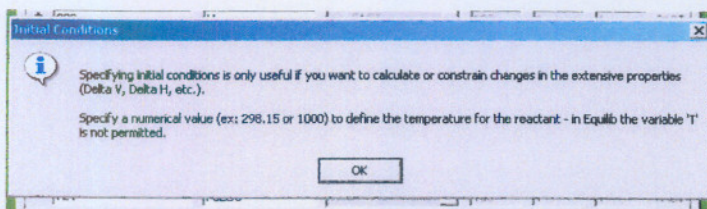
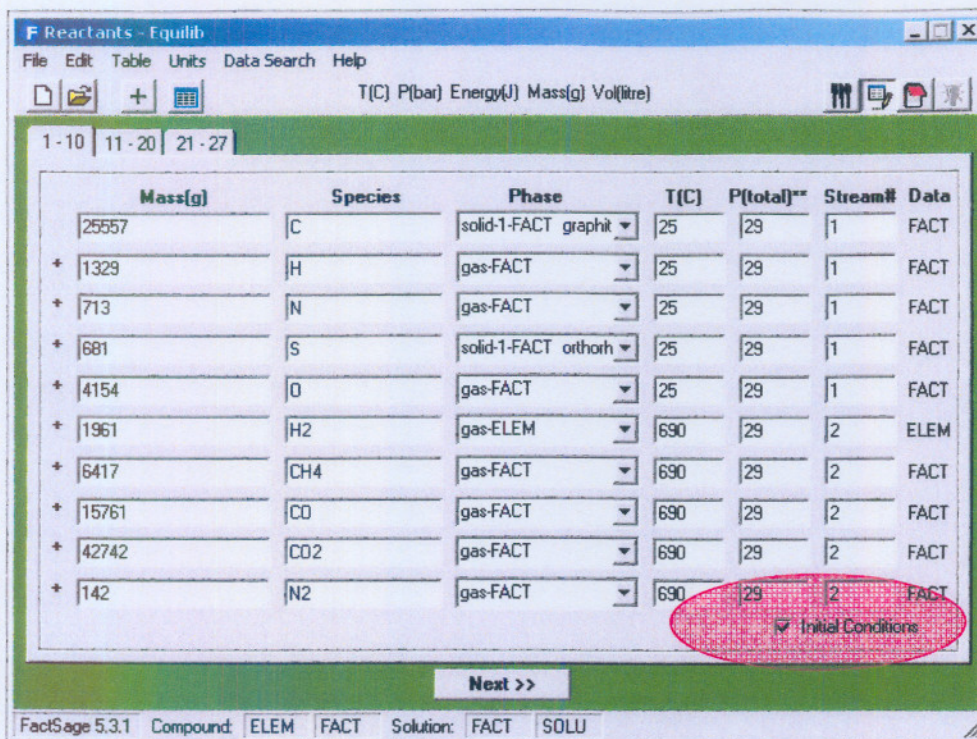
Middle Window (Reactants - Equilib):

Mass(g)	Species	Phase	T(C)	P[total]**	Stream#	Data
429	FeS2	solid-1-FACT pyrite	25	29	1	FACT
2117	SiO2	solid-1-FACT quartz	25	29	1	FACT
198	KAlSi3O8					
310	KAlSi3O10					
5558	Al2Si2O9(OH)					
28	TiO2					
706	CaCO3					
1069	CaMg(CO3)2					
116	CaSO4(H2O)					
0	CaO					

Bottom Window (Reactants - Equilib):

Mass(g)	Species	Phase	T(C)	P[total]**	Stream#	Data
0	Al2O3	solid-1-FACT gamm	25	29	1	FACT
0	Fe2O3	solid-1-FACT hemat	25	29	1	FACT
0	MgO	solid-FACT periclase	25	29	1	FACT
0	K2O	solid-FACT	25	29	1	FACT
0	Na2O	solid-1-FACT solid-o	25	29	1	FACT
27159	H2O	gas-FACT steam	690	29	2	FACT
2550	H2O	liquid-FACT	25	29	1	FACT

Initial conditions are selected when the constraints in the extensive properties are to be calculated or when more than one stream with different properties are specified, which is the case in the gasification process.



The coal was selected as stream 1 with an initial temperature of 25° and the pressure at 29 bar. Stream 2 was the up-flowing gas from the gasification zone and specified as 690°C and also at 29 bar.

Reactants - Equilib

File Edit Table Units Data Search Help

T(C) P(bar) Energy(J) Mass(g) Vol(litre)

1 - 10 | 11 - 20 | 21 - 27

Mass(g)	Species	Phase	T(C)	P(total)	Stream#	Data
25557	C	solid-1-FACT graphit	25	29	1	FACT
+ 1329	H	gas-FACT	25	29	1	FACT
+ 713	N	gas-FACT	25	29	1	FACT
+ 681	S	solid-1-FACT orthorh	25	29	1	FACT
+ 4154	O	gas-FACT	25	29	1	FACT
+ 1961	H2	gas-ELEM	690	29	2	ELEM
+ 6417	CH4	gas-FACT	690	29	2	FACT
+ 15761	CO	gas-FACT	690	29	2	FACT
+ 42742	CO2	gas-FACT	690	29	2	FACT
+ 142	N2	gas-FACT	690	29	2	FACT

Initial Conditions

Next >>

FactSage 5.3.1 Compound: ELEM FACT Solution: FACT SOLU

Menu - Equilib

File Units Parameters Help

T(C) P(bar) Energy(J) Mass(g) Vol(litre)

Reactants (27)

(gram) 25557 C + 1329 H + 713 N + 681 S +
 [25C,29bar,s1-FACT,#1] [25C,29bar,g-FACT,#1] [25C,29bar,g-FACT,#1] [25C,29bar,s1-FACT,#1] [25C,29bar,g-FACT,#1]

Products

Compound species
 gas ideal real 0
 aqueous 0
 pure liquids 0
 pure solids 0
 suppress duplicates apply
 species: 0

Solution species

* +	Base-Phase	Full Name
<input type="checkbox"/>	FACT-FeS	FeS- <i>sq</i>
<input type="checkbox"/>	FACT-ILME	Ilmenite
<input type="checkbox"/>	FACT-CaTi	Ca3Ti2O7-Ca3Ti2O6
<input type="checkbox"/>	FACT-PERO	Perovskite
<input type="checkbox"/>	FACT-PSEU	Pseudobrookite
<input type="checkbox"/>	FACT-TSP	MTi2O4-spinel
<input type="checkbox"/>	FACT-TiO2	Rutile

Legend
 - selected Show all selected
 species: 2 Clear
 solutions: 1

Custom Solutions
 fixed activities
 ideal solutions
 activity coefficients
 Details...

Pseudonyms
 apply List...

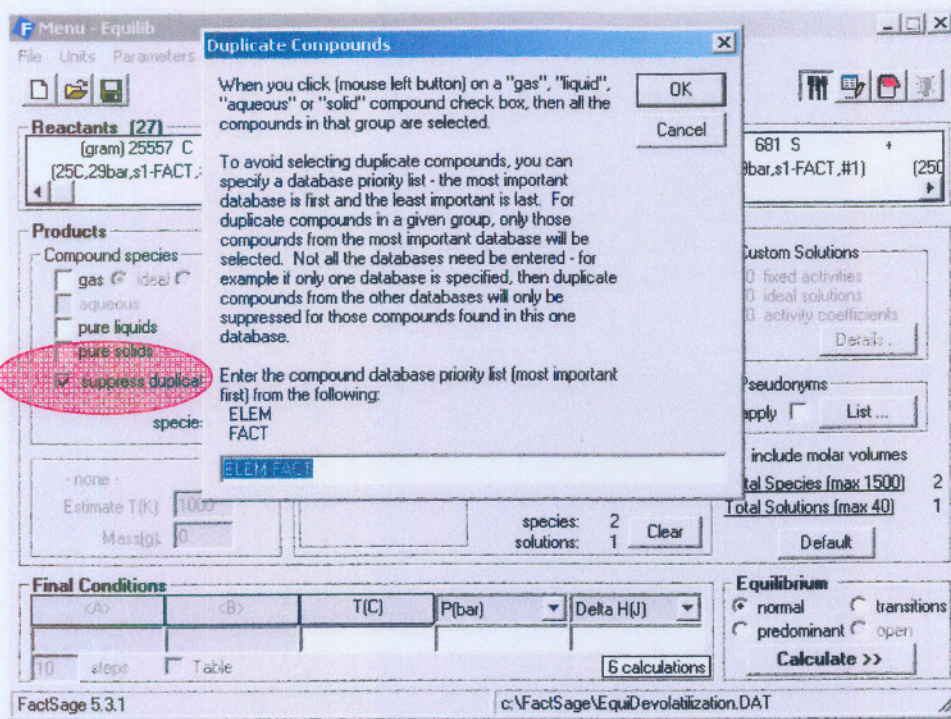
include molar volumes
 Total Species (max 1500) 2
 Total Solutions (max 40) 1
 Default

Final Conditions
 <A> T(C) P(bar) Delta H(J)
 10 steps Table 6 calculations

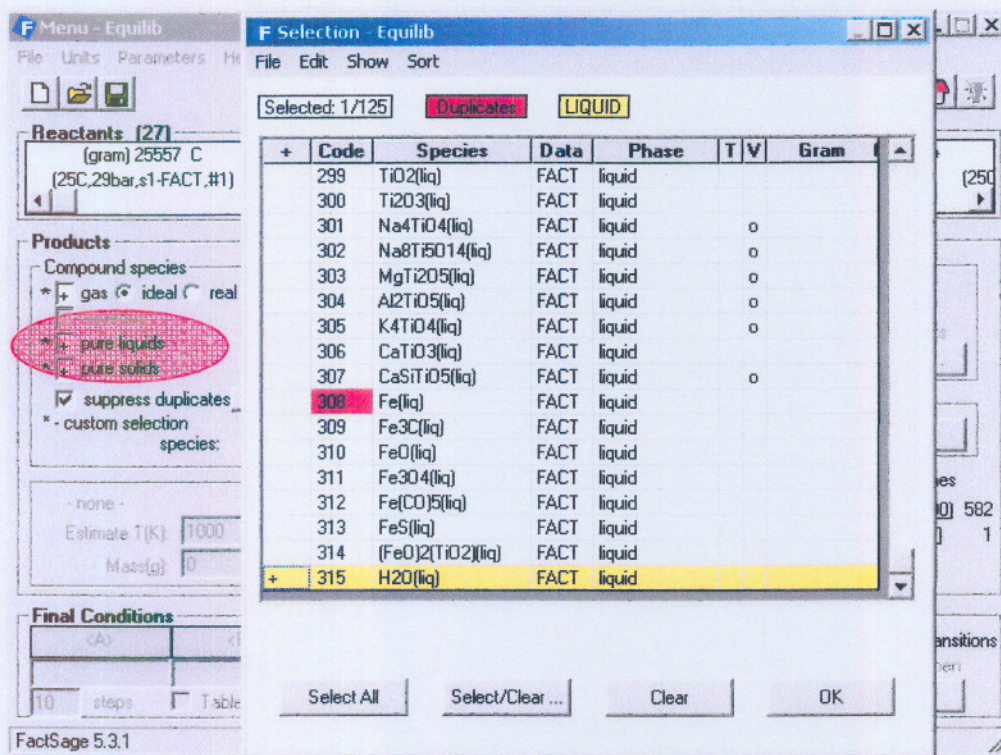
Equilibrium
 normal transitions
 predominant open
 Calculate >>

FactSage 5.3.1 c:\FactSage\EquiDevolatilization.DAT

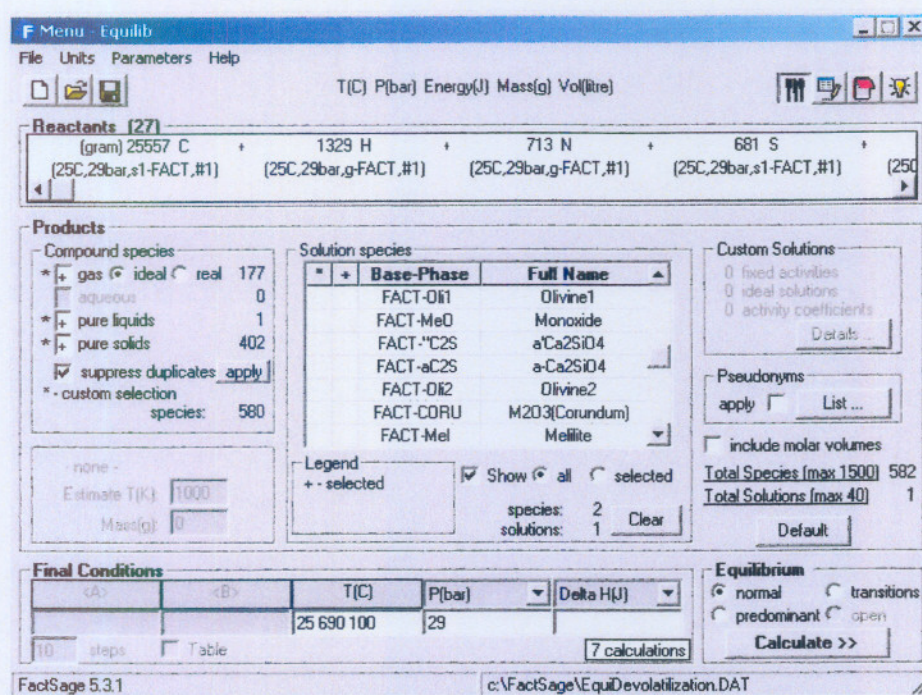
Under Products the first box selected was the suppress duplicates box. It is important to select this box first as it will only be active for the other selections ones this box is marked. Thereafter, the boxes of gas and pure solids were selected. If the suppress duplicates box is not selected first the total number of Species exceeded the maximum number of species.



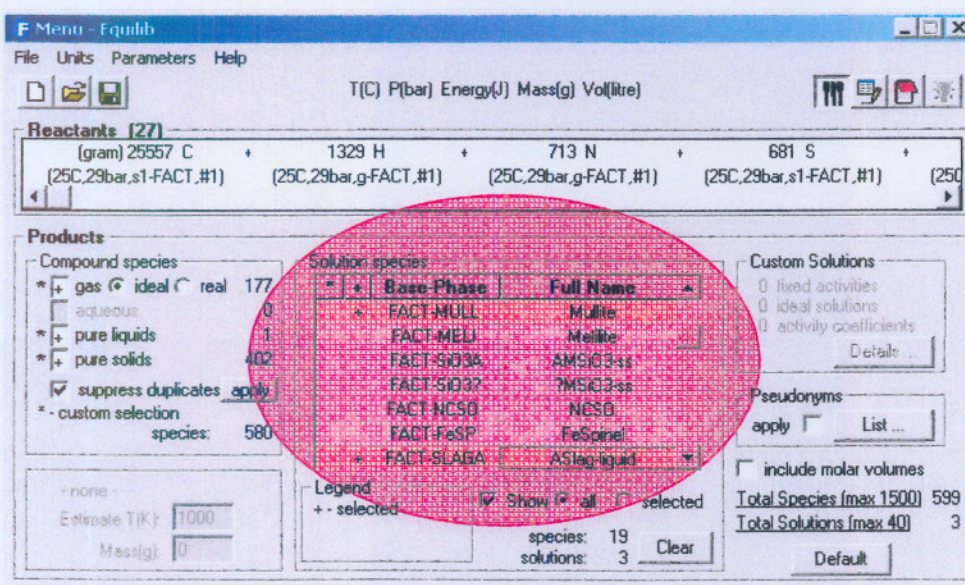
The products compound species gas, pure liquids and pure solids were thereafter selected. However, with the pure liquids it is known that from the gasification process only H₂O is formed as liquid that can be treated and modelled with the FactSage package. Other liquids such as tar and oils, alcohols, etc. will not be modelled and have to be deselected. Right-click on the pure liquid box and only select H₂O.



T(C) was entered as a range from 25°C to 690°C (temperature specified by ASPEN as end of zone) with intervals of 100°C. The P(bar) was entered as 29.



Under Solution species the following groups were selected as importance to this study: Aslag-liquid, Feldspar and Mullite. All other settings were left as default.



Gasification zone

A similar approach and procedure as for the drying and devolatilization zone was followed in order to model the gasification and combustion zone respectively. The differences in the models were mainly in the temperature ranges and reactants as

input. The results with regards to the mineral matter from the drying and devolatilization zone as per the FactSage model were used as input for the FactSage gasification zone model.

The temperature range for the gasification zone was specified as 690°C when the coal enters the zone (stream 2) and reacted with the up-flowing gas from the combustion zone (stream 1) with a temperature of 1200°C.

The screenshot shows the 'Reactants - Equilib' window in FactSage 5.3.1. The table below represents the data shown in the interface. Two rows are circled in red in the original image.

Mass(g)	Species	Phase	T(C)	P(total)**	Stream#	Data
13089	C	solid-1-FACT graphit	690	29	1	FACT
+ 681	H	gas-FACT	690	29	1	FACT
+ 365	N	gas-FACT	690	29	1	FACT
+ 348	S	solid-1-FACT orthorh	690	29	1	FACT
+ 2159	O	gas-FACT	690	29	1	FACT
+ 0	H2	gas-FACT	1200	29	2	FACT
+ 0	CH4	gas-FACT	1200	29	2	FACT
+ 0	CO	gas-FACT	1200	29	2	FACT
+ 16110	CO2	gas-FACT	1200	29	2	FACT
+ 142	N2	gas-FACT	1200	29	2	FACT

Initial Conditions

Next >>

FactSage 5.3.1 Compound: ELEM FACT Solution: FACT SOLU

The reactants in the model for the gasification zone were that of the results from the drying and devolatilization zone as output from the FactSage model for the coal flow, together with the up-flowing gas from the combustion zone as from the Aspen model.

Freeze/Unfreeze - Equilib

File Edit Table Units Data Search Help

TIC (Pb) Energy(M) Mass(g) Volume

1.10 | 11.20 | 21.30 | 31.36

Mass(g)	Species	Phase	TIC	Pb(mol)	Stream	Data	
13089	C	solid:FACT graphite	690	29	1	FACT	
+	691	H	gas:FACT	29	1	FACT	
+	365	N	gas:FACT	29	1	FACT	
+	348	S	solid:FACT sulfon	29	1	FACT	
+	2189	O	gas:FACT	690	29	1	FACT
+	0	H2	gas:FACT	1200	29	2	FACT
+	0	CH4	gas:FACT	1200	29	2	FACT
+	0	CO	gas:FACT				
+	16110	CO2	gas:FACT				
+	142	N2	gas:FACT				

Package 5.31 Compound ELEM FACT Solution FACT SOLU

Next >>

Freeze/Unfreeze - Equilib

File Edit Table Units Data Search Help

TIC (Pb) Energy(M) Mass(g) Volume

1.10 | 11.20 | 21.30 | 31.36

Mass(g)	Species	Phase	TIC	Pb(mol)	Stream	Data	
+	0	FeS2	solid:FACT pyrite	690	29	1	FACT
+	781	SO2	solid:FACT quartz	690	29	1	FACT
+	0	KAlSi3O8	solid:FACT microcl	690	29	1	FACT
+	0	KAlSi3O10(OH)2	solid:FACT muscovit	690	29	1	FACT
+	0	K2Si2O9(OH)4	solid:FACT kaolinit	690	29	1	FACT
+	0	TiO2	solid:FACT rutile	690	29	1	FACT
+	0	CaCO3	solid:FACT aragon	690	29	1	FACT
+	0	CaMgCO3	solid:FACT dolomite	690	29	1	FACT
+	0	CaSO4(H2O)2	solid:FACT gypsum	690	29	1	FACT
+	0	CaO	solid:FACT lime	690	29	1	FACT

Package 5.31 Compound ELEM FACT Solution FACT SOLU

Next >>

Initial Conditions

Freeze/Unfreeze - Equilib

File Edit Table Units Data Search Help

TIC (Pb) Energy(M) Mass(g) Volume

1.10 | 11.20 | 21.30 | 31.36

Mass(g)	Species	Phase	TIC	Pb(mol)	Stream	Data	
+	0	AD03	solid:FACT garn	690	29	1	FACT
+	0	Fe2O3	solid:FACT hemat	690	29	1	FACT
+	0	MgO	solid:FACT periclase	690	29	1	FACT
+	0	K2O	solid:FACT	690	29	1	FACT
+	0	Na2O	solid:FACT sodic-s	690	29	1	FACT
+	19099	H2O	gas:FACT steam	1200	29	2	FACT
+	0	H2O	solid:FACT	690	29	1	FACT
+	1696	Mg2MSiO18	solid:FACT cordier				
+	325	KAlSi2O6	solid:FACT leucite				
+	3762	CaAl2Si2O8	solid:FACT anorth				

Package 5.31 Compound ELEM FACT Solution FACT SOLU

Next >>

Freeze/Unfreeze - Equilib

File Edit Table Units Data Search Help

TIC (Pb) Energy(M) Mass(g) Volume

1.10 | 11.20 | 21.30 | 31.36

Mass(g)	Species	Phase	TIC	Pb(mol)	Stream	Data	
+	464	Fe2MSi2O18	solid:FACT hornrod	690	29	1	FACT
+	63	FeO(TiO2)	solid:FACT ilmenite	690	29	1	FACT
+	3463	K2SiO5	solid:FACT silliman	690	29	1	FACT
+	147	FeS	solid:FACT	690	29	1	FACT
+	0	AlSi2O13	solid:FACT mullite	690	29	1	FACT
+	0	FeAl2O4	solid:FACT hercynit	690	29	1	FACT

Package 5.31 Compound ELEM FACT Solution FACT SOLU

Next >>

Initial Conditions

Combustion zone

A similar approach and procedure as for the drying and devolatilization and gasification zone was followed in order to model the combustion zone. The differences in the models were mainly in the temperature ranges and reactants as input. The results with regards to the mineral matter from the gasification zone as per the FactSage model were used as input for the FactSage combustion zone model.

The temperature range for the gasification zone was specified as 1200°C when the coal and minerals enters the zone (stream 2) and reacted with the up-flowing agent into the gasifier (stream 1) with a temperature of 344°C.

FactSage 5.3.1 Compound: ELEM FACT Solution: FACT SOLU

Mass(g)	Species	Phase	T(C)	P(total)**	Stream#	Data
4451	C	solid-1-FACT graphit	1200	29	1	FACT
+ 231	H	gas-FACT	1200	29	1	FACT
+ 124	N	gas-FACT	1200	29	1	FACT
+ 118	S	solid-1-FACT orthorh	1200	29	1	FACT
+ 734	O	gas-FACT	1200	29	1	FACT
+ 0	H2	gas-FACT	344	29	2	FACT
+ 0	CH4	gas-FACT	344	29	2	FACT
+ 0	CO	gas-FACT	344	29	2	FACT
+ 0	CO2	gas-FACT	344	29	2	FACT
+ 142	N2	gas-FACT	344	29	2	FACT

Initial Conditions

Next >>

The reactants in the model for the combustion zone were that of the results from the gasification zone as output from the FactSage model for the coal flow, together with the up-flowing agent into the gasifier as from the Aspen model.

Reactants - Equib

File Edit Table Units Data Search Help

T(C) P(bar) Energy(J) Mass(g) Vol(lite)

1-10 | 11-20 | 21-28

Mass(g)	Species	Phase	T(C)	P(total)**	Stream#	Data
4451	C	solid-1-FACT graphite	1200	29	1	FACT
+ 231	H	gas-FACT	1200	29	1	FACT
+ 124	N	gas-FACT	1200	29	1	FACT
+ 118	S					
+ 734	O					
+ 0	H2					
+ 0	CH4					
+ 0	CO					
+ 0	CO2					
+ 142	N2					

FactSage 5.3.1 Compound: ELEM FACT Solu

Reactants - Equib

File Edit Table Units Data Search Help

T(C) P(bar) Energy(J) Mass(g) Vol(lite)

1-10 | 11-20 | 21-28

Mass(g)	Species	Phase	T(C)	P(total)**	Stream#	Data
+ 50900	H2O	gas-FACT steam	344	29	2	FACT
+ 0	H2O	liquid-FACT	1200	29	1	FACT
+ 823	AlSi2O13					
+ 234	MgO					
+ 249	FeO					
+ 4498	SiO2					
+ 29	TiO2					
+ 0.07	Ti2O3					
+ 697	CaO					
+ 1599	Al2O3					

FactSage 5.3.1 Compound: ELEM FACT

Reactants - Equib

File Edit Table Units Data Search Help

T(C) P(bar) Energy(J) Mass(g) Vol(lite)

1-10 | 11-20 | 21-28

Mass(g)	Species	Phase	T(C)	P(total)**	Stream#	Data
+ 29	K2O	liquid-FACT	1200	29	1	FACT
+ 0.07	MgS	gas-FACT	1200	29	1	FACT
+ 0.07	CaS	gas-FACT	1200	29	1	FACT
+ 0.07	FeS	liquid-FACT	1200	29	1	FACT
+ 0.07	K2S	liquid-FACT	1200	29	1	FACT
+ 319	CaAlSi2O8	solid-2-FACT anorthite	1200	29	1	FACT
+ 180	KAlSi2O6	solid-1-FACT leucite	1200	29	1	FACT
+ 11856	O2	gas-FACT	344	29	2	FACT

Initial Conditions

Next >>

FactSage 5.3.1 Compound: ELEM FACT Solution: FACT SOLU

REFERENCES

ALPERN, B., Nahuys, J. and Martinez, L., *Mineral matter in ashy and non-washable coals – its influence on chemical properties*, **Symposium on Gondwana Coals, Lisbon – proceedings and papers**, 1984, 70, (2), p. 299-317.

ALLIBERT, M., et. al., **Slag Atlas**, 2nd Edition, 1995.

ASTM D 3682-01, *Standard test method for major and minor elements in combustion residues from coal utilization processes*, **ASTM International**, 2002, p. 1-7.

ATTAR, A. and Hendrickson, G., *Functional groups and hetero-atoms in coal*, *Coal Structure*, New York, **Academic Press**, 1982, p. 131-199.

AYAT, M.G., *Composition of coal relative to its functionality and processability*, **Mining science and technology**, 1987, p. 105-112.

BACKMAN, R., Skrifvars, B., Hupa, M., Siiskonen, P. and Mantyniemi, J., *Flue gas chemistry in recovery boilers with high levels of chlorine and potassium*, **International Chemical Recovery Conference**, 1995, p. A95-A103.

BALE, C.W., Chartrand, P., Degterov, S.A., Eriksson, G., Hack, K., Manfoud, R. B., Melancon, J., Pelton, A.D. and Peterson, S., *FactSage Thermochemical Software and Databases*, GTT-Technologies, Germany, **Calphad**, 2002, **26**, p. 189-228.

BAXTER, L., *Coal characterisation techniques for slagging and fouling*, **Brigham Young University**, Provo, UT, 84601, Personal information received by email, larry_baxter@byu.edu, 2003.

BENSON, S.A., *Laboratory studies of ash deposit formation during the combustion of Western U.S. coals*, PhD Thesis, **Pennsylvania State University**, May 1987, p.3-243.

BENSON, S. A. and Laumb, M.L., *SEM analysis of ash, slag, and coal samples*, **Microbeam Technologies, Inc. (MTI)**, Grand Forks, USA, 9 July 2004, p. 1-29.

BIGGS, D.I. and Lindsay, C.G., *High-temperature interactions among minerals occurring in coal*, American Chemical Society, 1986, p. 128-137.

BORREGO, A.G., Alvorez, D. and Menendez, R., *Effects of inertinite content in coal on char structure and combustion*, **Instituto Nacional del Carbon, Energy and Fuels**, 1997, 702.

BOZIC, O., Leithner, R. and Muller, H., *Mineral matter transformation in coal fired furnaces to simulate slagging*, **Proc. Int. Tech. Conf. Coal Util. Fuel syst.**, 2000, p. 515-516.

CARPENTER, A.M., *Coal quality assessment – the validity of empirical tests*, **IEA Clean Coal Centre**, 2002, p.1-100, CCC/63.

COLLOT, A.G., *Matching gasifiers to coal*, **IEA Clean Coal Centre**, 2002, p.1-64, CCC/65.

CORNELL, J.A., *Experiments with mixtures. Designs, Models and the analysis of mixture data*, John Wiley & Sons, Inc., New York, 1981.

COUCH, G., *Understanding slagging and fouling in pf combustion*, **IEA Clean Coal Centre**, 1994, p.1-109.

DAKIC, D., Van der Honing, G. and Valk, M., *Fragmentation and swelling of various coals during devolatilization in a fluidized bed*, **Fuel**, 1989, 68, 911.

Deer, W.A., Howie, R.A. and Zussman, J., *An introduction to the rock forming minerals*, **Longmans**, 1966.

DU CANN, V.M., *Specialist, Coal and Organic Petrology*, Fully accredited Member of the International Committee for Coal and Organic Petrology (ICCP), Accreditation Certificate Number: ICCP/RA/2.2/0083 AB, 2004.

EPRI, *Electric utility use of fireside additive*, **EPRI Final Report**, CS-1318, Project 1035-1, 1980, p. III4.3-III4.5.

ERICKSON, T.A., Allan, S.E., McCollor, D.P., Hurley, J.P., Srinivasachar, S., Kang, S.G., Baker, J.E., Morgan, M.E., Johnson, S.A. and Borio, R., *Modelling of fouling and slagging in coal-fired utility boilers*, **Fuel Processing Technology**, 1995, 44, p. 155.

FALCON, R.M.S. and Snyman, C.P., *An introduction to coal petrography: atlas of petrographic constituents in the bituminous coals of Southern Africa*, 1986.

FALCON, R.M.S., *The characteristics of Southern African coals*, **J.S. Afr. Inst. Min. Metall.**, 1988, 88, (5), 145.

FRANCIS, W., *Coal - its formation and composition*, 1961, p. 324-328.

GALBREATH, K., Zygarlicke, C, et. al., *Collaborative study of quantitative coal mineral analysis using computer-controlled scanning electron microscopy*, **Fuel**, 1996, 75 (4), p. 424-430.

GIBB, *The UK collaborative research programme on slagging pulverised coal-fired boilers: summary of findings*, **Applications of advanced technology to ash-related problems in boilers**, www.bl.uk, 1996.

GIVEN, P.H., Poever, M.E., Wyss, W.F., *Chemical properties of coal macerals - introductory survey and some properties of exinites*, **Fuel**, 1960, p. 323-341.

GONI, C., Helle, S., Garcia, X., Gordon, A., Parra, R., Kelm, U., Jimenez, R. and Alfaro, G., *Coal blend combustion: fusibility ranking from mineral matter composition*, **Fuel**, 2003, 82, p. 2087-2095.

GRAY, V.R., *Prediction of ash fusion temperature from ash composition for some New Zealand coals*, **Fuel**, 1987, 66, p. 1230-1239.

GRAINGER, L., Gibson, J., *Coal utilization: technology, economics and policy*, 1981, p. 1-30.

GREEN, T.K., *The macromolecular structure of coal*, Department of Chemistry and centre for Coal Science, Western Kentucky University, **Journal of Coal Quality**, 1987, p. 90-93.

GIBB, W.H., *The UK collaborative research programme on slagging pulverised coal-fired boilers: summary and findings*, PowerGen, Power Technology, Nottingham NG11 OEE, England, **Applications to Advanced Technology to Ash-related problems in boilers**, 1996, p.41-65.

GOVENDER, A., *Determination and statistical evaluation of the effect of minerals and mineral associations in specific dense medium fractions on ash fusion temperature*, M.Sc., North-West University, 2005.

GRUBER, G.P. and Kalmanovitch, D., *Great Plains Gasification Plant Lignite Gasification Study*, 15th Biennial Low-Rank Fuels Symposium, St. Paul, Minnesota, 1989, p. 1-8.

GUPTA, S., Wall, T.F., Creelman, R.A. and Gupta, R., *Ash fusion temperatures and the transformations of coal ash particles to slag*, Department of Chemical Engineering, University of Newcastle, Australia, **Fuel Processing Technology**, 1998, 56, p. 33-43.

HATT, R., *Correlating the slagging of a utility boiler with coal characteristics*, **Commercial Testing and Engineering Co.**, Lexington, USA, 1980.

Hirschfelder, H., Buttke, B., Steiner, G., *Concept and realisation of the Schwarze Pumpe*, FRG 'Waste to Energy and chemicals centre', IChemE Conference 'Gasification in Practice', Assolombarda, Milan, Italy, 26-27 February 1997.

Howard, J.B., Peters, W.A. and Seiro, M.A., *Coal devolatilization information for reactor modelling – assessment of data and apparatus availability with recommendations for research*, **Department of Chemical Engineering**, Cambridge, Massachusetts, 1981.

Huffman, G.P. and Huggins, F.E., *Investigation of partial ash melting by phase analysis of quenched samples*, Proceedings of the 1981 conference on fouling and slagging, 1981, p.259 – 279.

JAK, E., Degterov, S., Hayes, P.C. and Pelton, A., *Thermodynamic modelling of the system Al_2O_3 --- SiO_2 --- CaO --- FeO --- Fe_2O_3 to predict the flux requirements for coal ash slags*, **Fuel**, 1998, 77 (1-2), p. 77-84.

JAK, E., *Prediction of coal ash fusion temperatures with the F*A*C*T thermodynamic computer package*, **Fuel**, 2002, 81 (13), p. 1655-1668.

JAK, E. and Hayes, P.C., *Applications of the new F*A*C*T database to the prediction of melting behaviour of coal mineral matter*, Cooperative Research Centre for Black Coal

Utilisation, Pyrometallurgy Research Group, **The University of Queensland**, Australia, p.1-9, 2005.

JUCKS, W., Sandhoff, A.G., *Theory of coal pyrolysis*, **The Pennsylvania State College**, State College, Penna, 1980, p. 567-569.

JUNIPER, L., *Ash deposition indices revisited*, Ultra-systems Technology Pty Ltd, **Coal Utilization Brisbane**, 1996, p. 1-5.

KALMANOVITCH, D.P. and Williamson, J., *Crystallization of coal ash melts*, **ACS Symposium Series**, 1986, 234.

KALMANOVITCH, D.P. and Frank, M., *An effective model of viscosity for ash deposition phenomena*, University of North Dakota, Energy and Mineral Research Center, Grand Forks, **Energy Foundation Conferences**, 1988, p.89-101.

KALMANOVITCH, D.P., Reactions in coal ash melts, PhD Thesis, Imperial College of Science and Technology, 1983.

KAMER, F. R., Zygarlicke, C.J. and Brekke, **Energy and Environmental Research Center, University of North Dakota**; D.W Steadman, E.N. and Benson, S.A., Microbeam Technologies, *New analysis techniques help control boiler fouling*, Power Engineering, 1994, p. 35-38.

KONDRATIEV, A. and Jak, E., *Predicting coal ash slag flow characteristics (viscosity model for the Al_2O_3 -CaO-FeO-SiO₂ system)*, **Fuel**, 2001, 80 (14), 1989.

LAUMB, J., McCollor, D.P. and Schwalbe, R., *Coal Quality and boiler operations: viscosity predictions*, **Internal EERC report**, jlaumb@undeerc.org, 2004.

MELZER, S., *Investigations of 3 different source materials for gasification using HT-XRD*, **Corus Research, Development and Technology**, 2003, p. 1-11.

MELZER, S., *Personal email communication*, stefan.melzer@corusgroup.com, 2005.

MICROBEAM TECHNOLOGIES, INC., www.microbeam.com, 2003.

NEAVEL, R.C., *Coal structure and coal science: overview and recommendations*,

Coal Structure ACS, 1981, p. 1-13.

Nowacki, P., *Coal gasification processes*, **Energy Technology review** No. 70, 1981.

RAASK, E., *Flame vitrification and sintering characteristics of silicate ash*, **American Chemical Society**, 1986, p. 138-155.

REIFENSTEIN, A.P., Kahraman, H., Coin, C.D.A., Calos, N.J., Miller, G. and Uwins, P., *Behaviour of selected minerals in an improved ash fusion test: quartz, potassium feldspar, sodium feldspar, kaolonite, illite, calcite, dolomite, siderite, pyrite and apatite*, **Fuel**, 1999, 78, p. 1449-1461.

ROSS, D.P., Kosminski, A. and Agnew, J.B., *Reactions between sodium and silicon minerals during gasification of low-rank coal*, **12th International Conference on Coal Science**, 2003, Australia, p. 1-9.

RUSSELL, N.V., Mendez, L.B., Wigley, F. and Williamson, J., *Ash deposition of a Spanish anthracite: effects of included and excluded mineral matter*, **Fuel**, 2002, 81, p. 657-663.

SAKORAFI, V., Michailidis, K. and Burrigato, F., *Mineralogy, geochemistry and physical properties of fly ash from the Megalopolis lignite fields, Peloponnese, Southern Greece*, **Fuel**, 1996, 75 (4), p. 423-419.

SABS, *A techno-economic and historical review of the South African coal industry in the 19th and 20th centuries and analyses of coal product samples of South African collieries 1998-1999*, **Bulletin 113**, 1999.

Sasol Annual Report, 2002, p. 23, www.sasol.com.

SASOL-LURGI Technology Company (Pty) Ltd., *Company Profile and Reference List*, November 2005.

SCHEFFE, H. *Experiments with mixtures*, **Journal of the Royal Statistical Society**, B, Vol. 20, pp. 344-360, 1958.

Schilling, H.D., Bonn, B. and Krauss, U., *Coal gasification – existing processes and new developments*, 1979.

SEGGIANI, M., *Empirical correlations of the ash fusion temperatures and temperature of critical viscosity for coal and biomass ashes*, **Fuel**, 1999, 78, p. 1121-1125.

SFA Pacific report prepared by for the U.S. Department of Energy, Office of Fossil Energy, National Energy Technology Laboratory and the Gasification Technologies Council, *Gasification: Worldwide use and acceptance*, Contract DE-AM01-98FE65271, January 2000.

SKORUPSKA, N.M. and CARPENTER, A.M., *Computer-controlled scanning electron microscopy of minerals in coal*, **IEA Coal Research**, 1993, p. 1-21.

SLAGHUIS, J.H., *Volatile material in coal and the role of inherent mineral matter*, 1989, (Dip. Tech. UNISA).

SLAGHUIS, J.H., *COAL GASIFICATION, A study guide for the national diploma in Fuel Technology*, **Coal Processing III**, Part A, 1993, p. 1-81.

SLEGEIR, W.A., Singletary, J.H. and Kohut, J.F., *Application of a microcomputer to the determination of coal ash fusibility characteristics*, **Journal of Coal Quality**, 1988, 7 (2), p. 48-54.

SOBIECKI, A., *Investigation of the high temperature transformations of coal minerals in the SCS Coal (base) by HT X-ray diffraction*, **Sasol Technology**, R&D, Materials Characterisation, 2004, Internal Sasol Report.

STACH, E., Mackowsky, M.T.H., Teichmuller, M., Taylor, G.H., Chandra, D. and Teichmuller, R., **Stach's textbook of coal petrology**, Third revised and enlarged edition, Berlin Gebruder Borntraeger, 1982.

STAT-EASE, Inc. Design-Expert® Software, *Design-Expert 6 User's Guide*, Stat-Ease, Inc., Minneapolis, MN, 2000.

http://www.timedomaincvd.com/CVD_Fundamentals/films/SiO2_properties.html

TOMEKZEK, J. and Palugniok, H., *Kinetics of mineral matter transformation during coal combustion*, **Fuel**, 2002, 81, p. 1251-1258.

UTILIS ENERGY, *Coal Gasification 2005 – roadmap to commercialization*, <http://www.utilisenergy.com>, February 2005.

US Department of Energy Report, *Gasification Technologies – an industry perspective*, **NETL**, 2002.

US Department of Energy, *Major environmental aspects of gasification – based power generation technologies*, **NETL**, 2002.

VAN ALPHEN, C., *AFT modification – CCSEM characterisation of coal feed and gasifier ash*, **Van Alphen Consultancy**, South Africa, cncc@mweb.co.za, October 2004, p. 1-24.

VAN DER WALT, L., *ADAMS & ADAMS*, Physical Address: 1140 Prospect Street, Hatfield, Pretoria, 0083, South Africa, Postal Address: PO Box 1014, Pretoria, 0001, South Africa, Tel (Local): 012 481 1500, Tel (International): +27 12 481 1500, Fax (Local): 012 362 6440, Fax (International): +27 12 362 6440, E-mail: lvdw@adamsadams.co.za, URL: <http://www.adamsadams.co.za>.

VAN DYK, J.C., Thermal friability of coal sources used by Sasol Chemical Industries (SCI) for gasification – Quantification and statistical evaluation, **M.Sc. Thesis**, University of the Witwatersrand, Johannesburg, 1999.

VAN DYK, J.C., Keyser, M.J., van Zyl, J.W., *Suitability of feedstocks for the Sasol-Lurgi Fixed Bed Dry Bottom Gasification Process*, **GTC Conference**, San Francisco, USA, October 2001.

VAN DYK, J.C., *Development of an alternative laboratory method to determine thermal fragmentation of coal sources during pyrolysis in the gasification process*, **Fuel**, 2001, 80, p. 245.

VAN DYK, J.C. AND KEYSER, M.J., *Characterisation of inorganic material in Secunda and the effect of washing on coal properties*, Mineral Processing Conference 2002, Cape Town.

VAN DYK, J.C., Baxter, L.L. and Van Heerden, J.H.P., *Chemical fractionation tests on South African coal sources to obtain species-specific information on ash fusion temperatures (AFT)*, **Sasol Internal report**, 2004.

VAN DYK, J.C. and Melzer, S., *Interpretation of mineral matter transformation during*

Sasol-Lurgi fixed bed gasification by means of high temperature x-ray diffraction, **21st International Annual Pittsburgh Coal Conference**, Osaka, Japan, September 2004.

VAN DYK, J.C. and Keyser, M.J., *Characterization of inorganic material in Secunda coal and the effect of washing on coal properties*, SAIMM, Journal of the South African Institute of Mining and Metallurgy, Volume 105, No. 1, January 2005, p. 1-6.

VAN DYK, J.C., Baxter, L.L. and Van Heerden, J.H.P., Coetzer, R.L.J., *Chemical fractionation tests on South African coal sources to obtain species-specific information on ash fusion temperatures (AFT)*, **Fuel**, Vol. 84, October 2005, p. 1768-1777.

VASSILEV, S.V., Kitano, K., Takeda, S. and Tsurue, T., *Influence of mineral matter and chemical composition of coal ashes on their fusibility*, **Fuel Processing Technology**, 1995, 45, p. 27-51.

VASSILEV, S.V. and Vassileva, C.G., *Mineralogy of combustion wastes from coal-fired power stations*, **Fuel Processing Technology**, 1996, 47, p. 261-280.

VASSILEV, S.V. and Vassileva, C.G., *Occurrence, abundance and origin of minerals in coals and coal ashes*, **Fuel Processing Technology**, 1996, 48, p. 85-106.

VASSILEVA, Ch.G. and Vassilev, S.V., *General observations on the phase-mineral transformations in inorganic matter of some Bulgarian coals during heating*, *Comptes rendus del'Academie bulgare des Sciences*, Tome 55, No. 7, 2002, p. 47-50.

VASSILEVA, Ch.G., *Phase-mineral transformations in inorganic matter of Bulgarian lignites during heating*, *Comptes rendus del'Academie bulgare des Sciences*, Tome 56, No. 9, 2003, p. 19-26.

VISSER, P., **Coal and Minerals**, Secunda, South Africa, Tel: +27 (0) 17-631 0320, Fax: +27 (0) 17-631 2390, Email: piet.visser@coalandminerals.com, 2004.

WALL, T.F., Creelman, R.A., Gupta, R.P., Coin, C. and Love, A., *Coal ash fusion temperatures – new characterisation techniques, and associations with phase equilibria*, **Applications of advanced technology to ash related problems in boilers**, 1996, p. 541-556.

WARD, C.R., Taylor, J.C., Matulis, C.E. and Dale, L.S., *Quantification of mineral matter in the Argonne Premium Coals using interactive Rietveld-based X-ray diffraction*, **International Journal of Coal Geology**, 2001, 46, p. 67-82.

WARD, *Analysis and significance of mineral matter in coal seams*, **International Journal of Coal Geology**, 2002, 50, p. 135-168.

WARD, C.R. and Taylor, J.C., *Quantitative mineralogical analysis of coals from the Callide Basin, Queensland, Australia using X-ray diffractometry and normative interpretation*, **International Journal of Coal Geology**, 1996, 30, p. 211-229.

WATT, J.D. and Fereday, F., *The flow properties of slags formed from the ashes of British coals: Part 1. Viscosity of homogeneous liquid slags in relation to slag composition*, **Journal of the Institute of Fuel**, 1969, p. 99-103.

WILLIAMSON, J., *Personal email communication*, jim.williamson@ic.ac.uk, 2005.

YAN, L., Gupta, R.P. and Wall, T.F., *A mathematical model of ash formation during pulverised coal combustion*, **Fuel**, 2002, 81, p. 337-344.

YOON, H., Wei, J. and Denn, M. M., *A model for moving-bed coal gasification reactors*, **AIChE Journal**, 1978, Vol. 24, No.5, p. 885.

ZEVENHOVEN-ONDERWATER, M., Backman, R., Skrifvars, B. and Hupa, M., *The ash chemistry in fluidised bed gasification of biomass fuels. Part I: predicting the chemistry of melting ashes and ash-bed material interaction*, **Fuel**, 2001, 80 (10), p. 1489-1502.

www.factsage.com